IFAC

INTERNATIONAL FEDERATION OF AUTOMATIC CONTROL

WARSZAWA 1969

Direct Control Problems

Design Tools and Methods

Fourth Congress of the International Federation of Automatic Control
Warszawa 16–21 June 1969

TECHNICAL SESSION 11

NOT

Organized by
Naczelna Organizacja Techniczna w Polsce

INTERNATIONAL FEDERATION OF AUTOMATIC CONTROL

Direct Control Problems
Design Tools and Methods

TECHNICAL SESSION No 11

FOURTH CONGRESS OF THE INTERNATIONAL
FEDERATION OF AUTOMATIC CONTROL
WARSZAWA 16 – 21 JUNE 1969

Organized by
Naczelna Organizacja Techniczna w Polsce

Contents

Wydawnictwa Czasopism Technicznych NOT - Polska

Zakład Poligraficzny WCT NOT. Zam. 118/69.

A GENERAL METHOD FOR THE DESIGN OF LINEAR AND NONLINEAR CONTROL SYSTEMS

P.M. Frank, Universität Karlsruhe, Germany

1. Introduction.

Conventional design of feedback control significantly concentrates on a few prototypes of easily realizable controllers, the parameters of which have to be adjusted in such a way that optimal results within the predetermined limits may be obtained. The modern practice of direct computer application in control loops, however, makes it possible to realize even the most complicated controller structures. Consequently, the restriction on the conventional controllers can fall away and the request for optimal control structure becomes of real practical importance. From this point of view, the essential two questions are:

i.) Which is the best possible control of a given plant, at all, i.e. what are the inevitable control errors?

ii.) Which is the simplest way to find out such a controller as to come nearest to the ultimate physical limitations?

A lot of mathematical expence and many complicated studies of stability are necessary to answer these questions on the basis of the single control loop, because the problem of manipulating the plant has to be solved concerted with the stabilization problem of the closed loop in one single unit, the controller.

This paper deals with a new concept of feedback control, by which the manipulating problem and the problem of stabilization can be solved separately. This concept makes it possible to determine the inevitable control error and conclusively leads to optimal realizable controllers for linear plants as well as for nonlinear ones without particular mathematical expence. In order to find suitable technical solutions, approximations with regard to the special technical circumstances will be necessary.

2. Specification of the Design Method.

2.1 Basic Control Concept.

Fig.1a shows the block diagram of the control loop, on which the design method is based, for linear conditions. A dynamic plant model S' is connected in parallel with the disturbed plant (transfer function S(s)). If no disturbances enter S' and if S' simulates the plant perfectly (S' = S), the output signal of S' represents the manipulated response x_y of the plant. By substracting this signal from the controlled variable x, the signal x_y is compensated and only the disturbed response z is left over. From -z and the reference input w the manipulated signal y is generated by means of the two units N_z resp. N_w. In the following we will call them manipulating systems.

Since x_y has no longerany influence upon the input of N_z, the closed-loop system (fig.1a) can be replaced by an open-loop system as shown in fig. 1b.[1] The controlled variable in the frequency domain becomes

$$X(s) = N_w(s)S(s)W(s) + \left[1 - N_z(s)S(s)\right] Z(s). \qquad (1)$$

If no noise is superposed on the reference variable w, it follows from equ.(1) that, in order to obtain ideal control ($x \equiv w$), the transfer functions $N_z(s)$ and $N_w(s)$ must exactly equal 1/S(s). Generally, 1/S(s) is not realizable and must, therefore, be approximated sufficiently. It is important now that the quality of this approximation has no influence on the stability of the closed loop.

By a simple block diagram transformation, the feedback arrangement considered can be converted into the classical single control loop as shown in fig. 1c. The corresponding feedback controller consists of the manipulating systems N_w and N_z, the latter being fed back positively by a model of the plant. If $N_w = N_z = N$, the equivalent controller transfer function becomes

$$R(s) = \frac{N(s)}{1-N(s)S(s)} . \qquad (2)$$

Note that for the performance of ideal control, i.e. for $N(s) \rightarrow 1/S(s)$, equ.(2) yields $R(s) \rightarrow R_\infty/S_1(s)$ with $R_\infty \rightarrow \infty$. This is the same result as in the case of single feedback control loop.

From the control configuration outlined above, a simple controller design can be developed. Let us assume for the first that the dynamics of the plant are known and constant in time and that the plant is stable. Poles of arbitrary order may, however, occur in the origin of the s-plane. Unstable plants should be stabilized first by an auxiliary feedback loop which later on can be combined with the controller. The essential steps in controller design are now:

i.) Simulation of the plant
ii.) Approximation of the inverse plant model 1/S by the two manipulating systems N_w and N_z. (Spoken more generally: Performance of an optimal open-loop control of the plant).

This method of design has an important advantage over the direct method based on the single control loop: That part of the controller, which is responsible for the stability of the closed loop, is known from the very beginning. The problem left over is a pure open-loop problem which can be solved without regarding the stabilization problem. Besides this, since now w as well as z are available separately, the control loop can be simultaneously optimized both for reference inputs w and disturbances z even if the characters of z and w are different.

2.2 Evaluation of the Inevitable Control Errors.

For the determination of $N_w(s)$ and $N_z(s)$ we have to note that both the reference input w(t) and the dominant disturbance z(t), which has to be compensated, are usually superposed by additional small disturbances $w_1(t)$ resp. $z_1(t)$. From the practical point of view it is convenient to require that in the ideal case no reaction to $w_1(t)$ and $z_1(t)$ is startet in the controller. $w_1(t)$ resp. $z_1(t)$ may, for example, be noise of small intensity being present in any physical system.

If the plant is simulated exactly, we get for the controlled variable in the frequency domain:

$$X = N_w S\left[W + W_1\right] + \left[1 - N_z S\right]\left[Z + Z_1\right]$$

The control error must now be defined as

$$X_w = W - X + Z_1.$$

So we have

$$X_w = \underbrace{\left[1 - N_w S\right] W - N_w S W_1}_{X_{wF}} - \underbrace{\left[1 - N_z S\right] Z + N_z S Z_1}_{X_{wZ}}. \qquad (3)$$

On the other hand, the errors of manipulation caused by nonideal realization of N_w and N_z are

$$E_w = \left[\frac{1}{S} - N_w\right] W - N_w W_1; \qquad E_z = \left[\frac{1}{S} - N_z\right] Z - N_z Z_1. \qquad (4)$$

Combining equation (3) and (4), we find

$$X_{wF}(s) = S(s)E_w(s); \qquad X_{wZ}(s) = S(s)E_z(s). \qquad (5)$$

If $N_w(s)$ and $N_z(s)$ are determined in such a way, that any prescribed performance criteria

$$Q_w\left\{x_{wF}(t)\right\} = Q_w\left\{e_w(t) * s(t)\right\}$$

$$Q_z\left\{x_{wz}(t)\right\} = Q_z\left\{e_z(t) * s(t)\right\}$$

are minimized (see next paragraph), the resulting control error can be explained as to be the inevitable error. Thus, the inevitable error can be calculated immediately from equ.(3).

2.3 Determination of $N_w(s)$ and $N_z(s)$ for Continuously Acting Control.

Actually, the disturbances $w_1(t)$ and $z_1(t)$ are to be filtered out as well as possible by $N_w(s)$ resp. $N_z(s)$ according to a certain performance criterion Q_w resp. Q_z. In respect to $w(t)$ and $z(t)$, however, $N_w(s)$ and $N_z(s)$ has to approximate optimally $1/S(s)$ (problem of optimal filtering). In any case, the optimal manipulating system must be physically realizable. Therefore, the impuls responses $n_w(t)$ and $n_z(t)$ must disappear for $t < 0$. The Fouriertransformability $\int_{-\infty}^{\infty}|n(t)|\,dt < \infty$ is often requested as a further condition. As a basis for the determination of $N_w(s)$ may serve the block diagram shown in fig.2. This block diagram results from a change of the sequence of N_w and S in fig. 1b. $N_z(s)$ may be calculated just in a similar way; therefore we concentrate in the following on the determination of $N_w(s)$.

The above problem is well known and solutions exist for many applications. For stationary <u>statistical inputs</u> $w(t)$ and stationary statistical disturbances $w_1(t)$ and minimizing the mean square error $\overline{x^2_{wF}}$, the WIENER-HOPF-equation yields the following frequency characteristic[1,2]

$$N_w(j\omega) = \frac{1}{\Psi_u^+(j\omega)} \, \mathrm{RO} \left\{ \frac{\Psi_{vw}(\omega) S(-j\omega)}{\Psi_u^-(j\omega)} \right\}. \tag{6}$$

$\Psi_u^+(j\omega)$ and $\Psi_u^-(j\omega)$ are those terms of the power spectral density $\Psi_{uu}(\omega)$ whose roots occur only in the upper, resp. lower $j\omega$-plane. These terms can be found out by factorizing the power spectral density, $\Psi_{uu}(\omega) = \Psi_u^+(j\omega) \cdot \Psi_u^-(j\omega)$, where $\Psi_{uu}(\omega) = S(j\omega)S(-j\omega)\Psi_{vv}(\omega)$ and $\Psi_{vv}(\omega)$ is the power spectral density of the complete input signal $v(t) = w(t) + w_1(t)$.

$\Psi_{vw}(\omega)$ is the cross-power spectral density between the input $v(t)$ and the desired output $w(t)$.

RO $\{ \}$ symbolizes the operator of realizability. Its application demands: transform the term in parantheses by means of the two-sided $\mathcal{L}^{-1}$-transform and afterwards transform the result back again by means of the right-sided $\mathcal{L}$-transform. It is convenient to develop the term in parantheses into partial fractions and to omit those terms, whose poles occur in the lower $j\omega$-half-plane.

If the reference signal $w(t)$ is an <u>aperiodic(al) deterministic(al)</u> one and the disturbance $w_1(t)$ is of stationary statistical nature, - the other conditions being the same as above - LEE finds [2]

$$N_w(j\ ) = \frac{\varrho^2}{\Psi_u^+(j\omega)} \, \mathrm{RO} \left\{ \frac{|W(j\omega)|^2 \cdot S(-j\omega)}{\Psi_u^-(j\omega)} \right\}. \tag{7}$$

$W(j\omega)$ is the amplitude spectrum of the deterministic(al) input component $w(t)$

$\Psi_{uu}(\omega) = \Psi_u^+(j\omega)\Psi_u^-(j\omega) = S(j\omega)S(-j\omega)\left[\Psi_{w_1w_1}(\omega) + \varrho^2|W(j\omega)|^2\right]$;
where $\Psi_{w_1w_1}(\omega)$ is the power spectral density of $w_1(t)$ and ϱ is a constant.

For determination of $N_z(j\omega)$, we have to replace $w(t)$ by $z(t)$ and $w_1(t)$ by $z_1(t)$ in equ.(6) and (7). By this means it is possible, e.g., to optimize the control loop for step characteristics of the reference input $w(t)$ as well as for statistical distur-

bances $z(t)$ simultaneously.
We can also ignore $w_1(t)$ and $z_1(t)$ for the first. Then we have instead of equ.(6)

$$N_w(j\omega) = \frac{1}{\Psi^+_u(j\omega)} \, RO \left\{ \frac{\Psi^+_u(j\omega)}{S(j\omega)} \right\} \qquad (8)$$

and instead of equ.(7)

$$N_w(j\omega) = \frac{1}{U^+(j\omega)} \, RO \left\{ \frac{U^+(j\omega)}{S\,(j\omega)} \right\}, \qquad (9)$$

where $U^+(j\omega)$ contains roots only in the upper $j\omega$-half-plane, and can be found out by factorizing $|U(j\omega)|^2 = |S(j\omega)|^2 |W(j\omega)|^2$. Since, usually, the degree of nominator of $N_w(j\omega)$ exceeds that of the denominator, realization poles have to be provided additionally. By choise of suitable locations of that poles, additional performance criteria, for example time domain criteria, can be minimized.
Naturally, any other performance criterion can be applied to instead of the mean square error. The arrangement considered above can also be used for the design of time optimal control systems. In this case, N_w resp. N_z symbolize digital systems which generate the optimal step series for manipulation of the plant. We will not enter into this problem.

2.4 Realization.

The feedback configuration considered may serve as a first step for finding out the optimal structure of the controller. There are three possible modes of realization:

i.) Continuously acting control (CC)
ii.) Direct digital control (DDC)
iii.) Hybrid control (HC)

It is an essential disadvantage of the direct realization of the controller according to fig. 1b, that the manipulated signals generated in N_z resp. N_w are not supervised. Mistakes as, e.g., caused by parameter variations of N_w resp. N_z, can yield steady state control errors. For CC and DDC, this effect can be avoided by determining the resulting controller transfer function and realizing it as a unity according to the single feedback device. Frequently, simplifications of the technical realization can be achieved by such an operation. As for plants with distributed parameters, however, it seems that the transcendental terms of R(s) must be approximated by rational terms.

The direct application of the feedback configuration (fig.1b) using a plant model, is signalized by considerable clearness. Besides this, it allows a new mode of controller realization, which we call hybrid control: The plant model is realized in an analog way, the manipulating systems are realized discretely, e.g. by means of a digital computer (fig.3). The only purpose of the computer is to perform optimal open loop control. Its algorithm gets therefore, rather simplified compared with its use in DDC. Even more important is, that in case of failure of the computer, the control loop can never get instable.

In many practical cases, either the reference variable is zero (constant-value control) or the disturbance variable and the reference variable have the same character. Then only one manipulating system N is required, which has to be designed with reference to w-z.(see equ.(2)). For the following, this simplification is assumed. The results can be transfered without difficulty to the more general problem $N_w(s) \neq N_z(s)$.

3. Applications to some linear Plants.

3.1 Plants with Rational Transfer Functions with Minimal Phase.

At first, let us consider plants with transfer functions of the type

$$S(s) = \frac{a_o+a_1s+\dots+a_ms^m}{s^p(b_o+b_1s+\dots+b_ns^n)}, \tag{10}$$

where m, n, p $\geq$ o and integer and m $\leq$ p + n. Moreover, no poles and zeros may occur in the right half of the s-plane. The physically realizable solution for N(s) follows from equ.(8) as N(s) = 1/S(s). Substituting this into equ.(3), yields x_w = O, i.e. no inevitable control error appears in this case.

In respect to the <u>technical</u> realizability, additional realization poles must be provided in N(s). Let us, generally, put up the following expression for the technically realizable approximation of N(s):

$$N_r(s) = \frac{U(s)}{S(s)\cdot V(s)}\ , \tag{11}$$

where U(s) and V(s) are polynomials in s, whose difference of order must at least equalize the resulting order m-p-n of the plant. By substitution into equ.(2) follows the controller transfer function

$$R(s) = \frac{1}{S(s)}\ \frac{1}{\frac{V(s)}{U(s)}-1}. \tag{12}$$

The control error is

$$X_w(s) = \left[1 - \frac{U(s)}{V(s)}\right] W(s) - \left[1 - \frac{U(s)}{V(s)}\right] Z(s). \tag{13}$$

As can be improved, U(s)/V(s) represents the transfer function of the closed loop. The resulting order of U(s)/V(s) is prescribed by S(s). The only problem still to be solved is to find aconvenient expression U/V with the above mentioned limitation, so that a certain performance criterion will be satisfied. In practice, prepared catalogs can be used.[3,4]

If optimal control for disturbances as well as for reference inputs is desired (fig.1c), U/V refering to W(s) in equ.(13) must be different from U/V refering to Z(s).

If $p > o$ and disturbances are to be compensated, which enter the control loop at the input of the plant, V(s) becomes $1+c_1s+\dots+c_qs^q$ with $q = n + p - m$. U(s) must now be a polynomial of the order p, whose first (p+1) terms equal those of V(s). It can be improved that the disturbance response diappears for $t\to\infty$.

3.2 Plants with Nonminimum Phase.

Let us now consider plants with transfer functions of the type $S(s) = S_1(s)\cdot A(s)$, where

$$S_1(s) = \frac{\sum\limits_{\nu=o}^{m} a_\nu s^\nu}{\sum\limits_{\mu=o}^{n} b_\mu s^\mu}$$

represents a minimum phase term and

$$A(s) = \frac{\sum_{\nu=0}^{l} (-1)^{\nu} c_{\nu} s^{\nu}}{\sum_{\nu=0}^{l} c_{\nu} s^{\nu}}$$

an all-pass term. The physically realizable approximation of $1/S(s)$ follows from equ.(8) as

$$N(s) = \frac{1}{S_1(s)} A_k^{-1}(s), \tag{14}$$

where $A_k^{-1}(s)$ symbolizes the best physically realizable approximation of $1/A(s)$. Since $A_k^{-1}(s) \neq 1/A(s)$, an inevitable control error appears:

$$X_{wu}(s) = \left[1-A_k^{-1}(s)A(s)\right]W(s) - \left[1-A_k^{-1}(s)A(s)\right]Z(s). \tag{15}$$

A technically realizable approximation of $N(s)$ is

$$N_r(s) = \frac{A_k^{-1}(s)}{S_1(s)V(s)} . \tag{16}$$

In the simplest case, $V(s)$ symbolizes a polynomial in s, whose order equals the difference of the orders of $A_k^{-1}(s)$ and $S_1(s)$. More generally, $V(s)$ is a rational fraction. The transfer function of the controller becomes

$$R(s) = \frac{1}{S_1(s)} \frac{A_k^{-1}(s)}{V(s)-A_k^{-1}(s)A(s)} . \tag{17}$$

Equ.(17) represents the optimal linear controller structure technically realizable and equ.(15) the corresponding inevitable control error. If, in the case of step inputs, ISE is the performance criterion, then $A_k^{-1}(s) = 1$. For plants with pure all-pass character ($S_1(s) = 1$) we then find $V(s) = 1$. The transfer functions of controllers for pure all-pass plants up to the order 4 are the following:

All-pass $A(s)$	Controller $R(s)$	
$\frac{c_o-s}{c_o+s}$	$\frac{1}{2} + \frac{c_o}{2}\frac{1}{s}$ (PI)	(18)
$\frac{c_o-c_1s+s^2}{c_o+c_1s+s^2}$	$\frac{1}{2} + \frac{c_o}{2c_1}\frac{1}{s} + \frac{1}{2c_1}s$ (PID)	

$$\frac{c_o-c_1s+c_2s^2-s^3}{c_o+c_1s+c_2s^2+s^3} \qquad \frac{1}{2}+\frac{c_o/c_1}{2s}+\frac{(c_2c_o/c_1)s}{2(s^2+c_1)} \quad \text{(PIS)}$$

$$(18)$$

$$\frac{c_o-c_1s+\ldots+s^4}{c_o+c_1s+\ldots+s^4} \qquad \frac{1}{2}+\frac{1}{2c_3}\,s+\frac{c_o}{c_1s}+\frac{\left(\frac{c_2}{c_3}-\frac{c_1}{c_3^2}-\frac{c_o}{c_1}\right)s}{s^2+\frac{c_1}{c_3}} \quad \text{(PIDS)}$$

For all-passes of higher order, additional S-terms (undamped oszillating systems) appear in the controller transfer function.

3.3 Plants with Distributed Parameters.

Let us first consider plants whose transfer function consists of a dead-time and a rational minimum phase component:

$$S(s) = S_1(s)e^{-T_ts} \quad ; \quad S_1(s) = \frac{a_o+a_1s+\ldots+a_ms^m}{b_o+b_1s+\ldots+b_ns^n} . \qquad (19)$$

The physically realizable approximation of $1/S(s)$ is

$$N(s) = \frac{1}{S_1(s)}\,N_T(s), \qquad (20)$$

where $N_T(s)$ means the optimal, physically realizable approximation of

$$e^{+T_ts} .$$

The unavoidable control error becomes

$$X_{wu}(s) = \left[1-N_T(s)e^{-T_ts}\right]W(s) - \left[1-N_T(s)e^{-T_ts}\right]Z(s). \qquad (21)$$

By inserting realization poles, we get for the controller transfer function

$$R(s) = \frac{1}{S_1(s)}\,\frac{N_T(s)}{V(s)-N_T(s)e^{-T_ts}} . \qquad (22)$$

The controller consists of the manipulating system $N_T/(S_1V)$, which is positively fed back trough the plant model S; the order of the polynomial V(s) results from the difference between the orders of $N_T(s)$ and $S_1(s)$. By finding out suitable coefficients of V(s) the control loop can be optimized. Since the control loop is extremely sensitive to dead-time variations, it is convenient to consider such variations by the determination of V(s): The smaller the bandwidth of V(s) is chosen, the less sensitive is the control loop against parameter variations. More in detail this design method is treated in another publication.[5]

As for plants with distributed lag, whose transfer functions are of the type

$$S(s) = S_1(s)e^{-\sqrt{Ts}}$$

($S_1(s)$ as above), this method succeeds as well, but the mathematical expense in-creases on account of the bad $\mathcal{L}$-transformability of $e^{-\sqrt{Ts}}$. Additionally, the technical realization becomes more expensive, because even the controller contains distributed lag. In this case, the hybrid arrangement of the controller seems to be advantageous.

4. Application to Nonlinear Plants.

4.1 Basic Control Concept and Design Technique.

The method described may be even more advantageous in case of nonlinear plants. Here the stabilization by means of plant simulation yields a remarkable simplification of the controller design.

Fig.4 shows the block diagram of the control loop for nonlinear plants, when the disturbances z(t) enter the control loop at the output of the plant. Let us assume that the plant can be represented by a nonlinear characteristic NL and a linear transfer function S(s). The essential steps of design are:

i.) Simulation of the plant in the positive feedback path of the controller (for purpose of stabilization of the control loop and extracting the disturbed response).

ii.) Cascade compensation of the plant (for the purpose of optimal control).

According to ii.) a manipulating system must be found which completes the dynamics of the whole cascade to a transfer function 1. The system to be determined may consist of a linear component N(s) and a nonlinear characteristic NL .

As in the linear case, the transfer function N(s) can be found by an approximation of 1/S(s).

Additionally, a realizable nonlinearity NL^* is to be determined, which has to accomplish the following condition (see fig.5): In the ideal case, it is desired that the cascade of NL^* and NL is a linear system with the transfer function 1. If NL symbolizes a statical characteristic, NL^* represents the inverse characteristic of NL.

In many cases, this postulation is physically realizable, as e.g. for quadratic characteristics etc. There are, however, a lot of characteristics, whose inverse characteristic is not realizable exactly, as e.g. those, whose slope is zero within finite regions (saturation, dead zone etc.). The more general formulation of the problem is, therefore, to find out that realizable nonlinearity NL^* , which minimizes a given performance criterion $Q\{x_w\}$(see fig.5b). NL^* is not any longer restricted to be a statical characteristic.

4.2 An Example of Application.

To demonstrate this method, let us consider the design of a continuously acting controller for a first order plant with saturation on the following terms: When the reference input is a step function $W_0\sigma(t)$, the control error x_w may go to zero (with a tolerance of $\pm\varepsilon$) with-in the shortest time possible T_A (time-optimal continuous control).

Fig.6 shows the arrangement of the control loop. At first, the plant has to be simulated in the positive feedback path of the controller. The linear component of the manipulating system is a phase lead system $(1 + T_1 s)$ with a realizing pole at $1/\tau$. The value of τ/T_1 should be taken as great as possible.

The nonlinear component NL^* can be found by the following consideration: If there is no saturation or if NL can be perfectly compensated, the optimal shape of the manipulated variable $y_1(=y_0)$

is an impuls function with the amplitude W_oT_1/τ (see fig.7a). The resulting step response of the control loop (see fig.7b, curve 1) is an exponential function with the time constant τ. By the effect of saturation, the term of y_1, exceeding the limitations y_m, is cut off. Consequently, the step response is retarded as shown in fig. 7b, curve 2.

The inverse characteristic of saturation is on principle not realizable. The best what can be done in view of a short transient time, is to retain the manipulated signal at the limitation y_m for a longer time. The extension time $T_B' - T_B$ must be nearly proportional to the intensity of the overshoot. Fig.8 shows a circuit for realizing this.[6]

The corresponding step response of the closed loop is shown in fig.7b, curve 3. x follows the time-optimal curve with the time constant T_1 by T_B'. At the point T_B', y_1 steps back to the shape of y_o and x follows, therefore, curve 1. Fig.9 shows the corresponding analog circuit of the controller.

The transient times T_A/T_1 (without use of NL^* as well as for use of NL^*) are plotted in fig.10 for $\tau = 0{,}1\ T_t$ as a function of the tolerance $|\varepsilon|$. Parameter is W_o/y_m. When the steps of w(t) and the tolerances ε are small, considerable diminutions of T_A can be obtained by use of NL^*. The curve in broken lines represents the linear border line, where the amplitude of the impuls just touches the limitations y_m. In the region above the border line, the control loop effects like a discrete time optimal control and in the lower region like a linear control.

In this way we obtain a nearly time optimal continuous control, which, in practice, does not differ considerably from the ideal time optimal control, but which actuates linear in the case of small inputs. This is a real advantage, since no oszillations around the rest position appear.

References.

1 NEWTON, G.L.; GOULD, L.A.; KAISER, J.F.: Analytical Design of Linear Feedback Controls, John Wiley, New York, 1961.

2 SCHLITT, H.: Anwendung statistischer Verfahren in der Regelungstechnik. Beiheft zur Regelungstechnik, Oldenburg - München (1962), S. 42 ff.

3 REINISCH, R.: Beitrag zur Strukturoptimierung linearer stetiger Regelkreise. Z. msr., H.4 (1959), S.154-165 und NT 9 H.4 (1959), S. 149-158.

4 WEBER, W.: Ein systematisches Verfahren zum Entwurf linearer und adaptiver Regelungssysteme. ETZ-A, Bd.88 (1967), H.6, S.138-144.

5 FRANK, P.M.: Zur Theorie und Realisierung der vollständigen Prädiktorregelung von Totzeitstrecken. Z. msr. (1969).

6 THALER, G.J.; PASTEL, M.P.: Analysis and Design of Nonlinear Feedback Control Systems, Mc Graw-Hill, New York (1962).

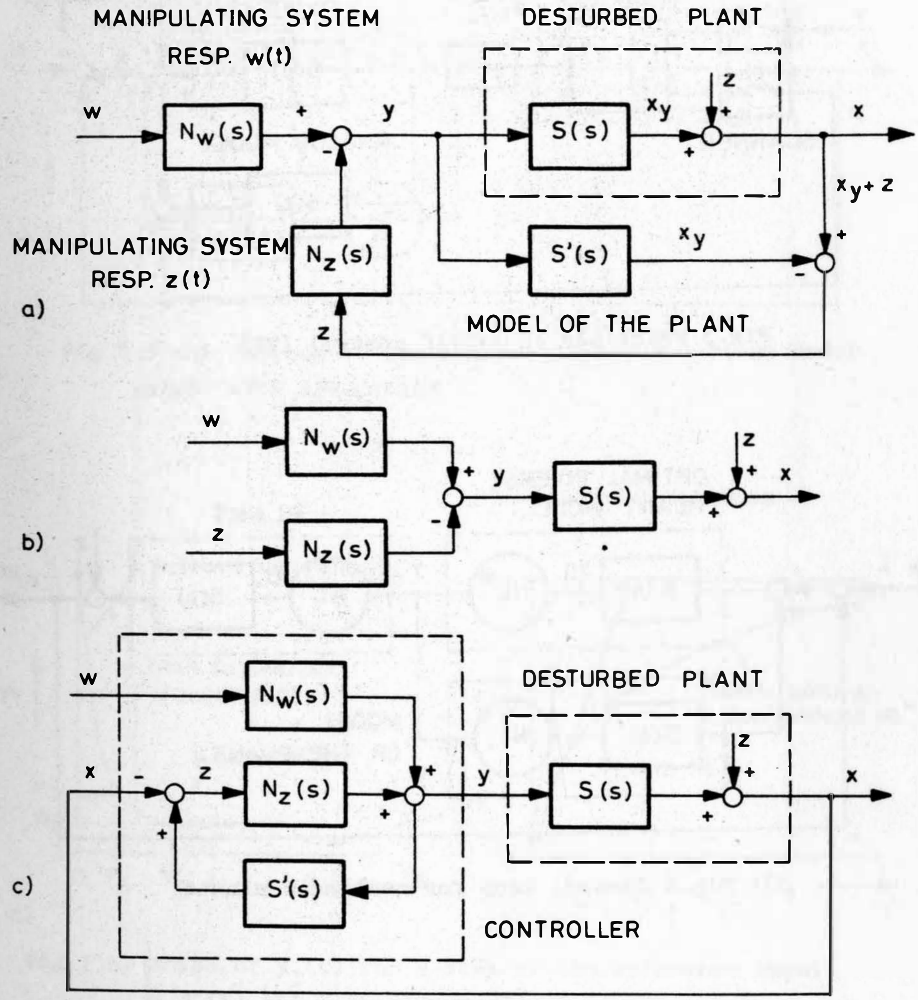

Fig.1 a) basic configuration of the control loop
b) equivalent block diagram of the closed loop for $S'=S$
c) equivalent configuration of single feedback control

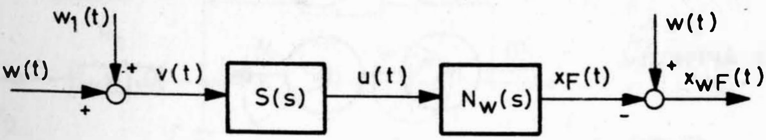

Fig.2 Block diagram for determination of $N_w(s)$

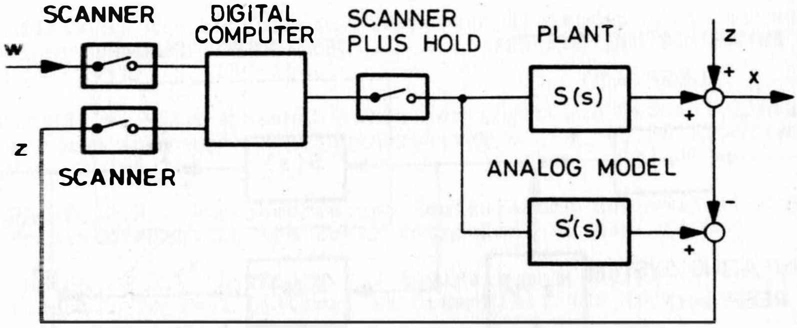

Fig.3 Prinziple of hybrid control (HC)

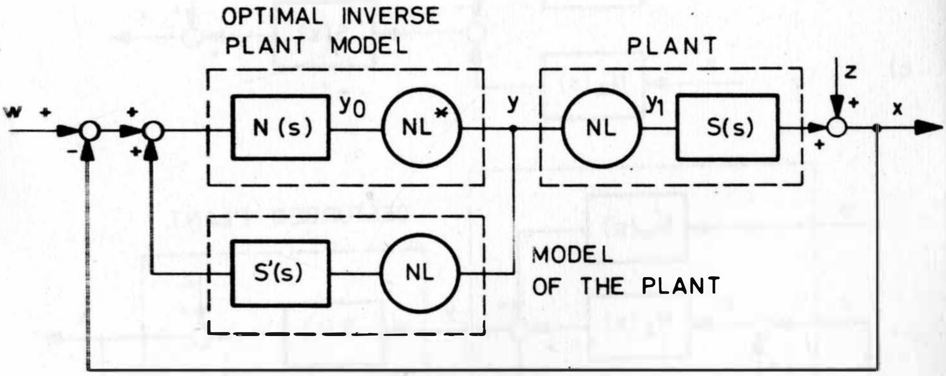

Fig.4 Control loop for nonlinear plants

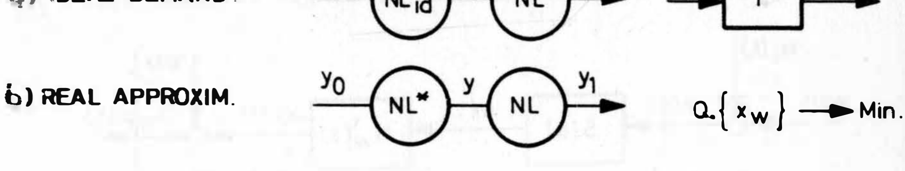

Fig.5 On the definition of NL*

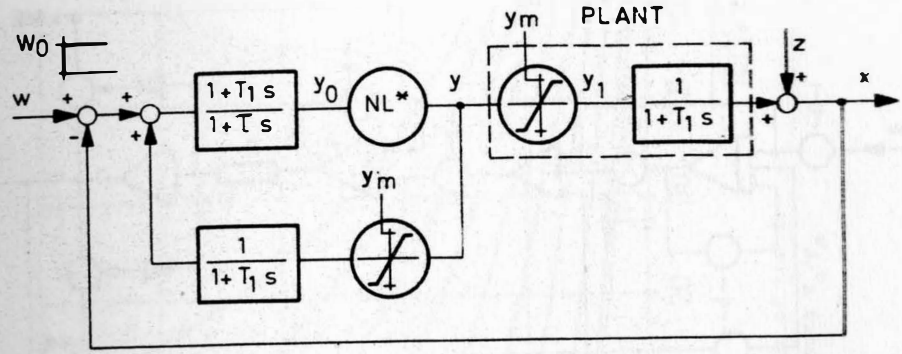

Fig.6 Block diagram of the control loop for a first order plant with saturation

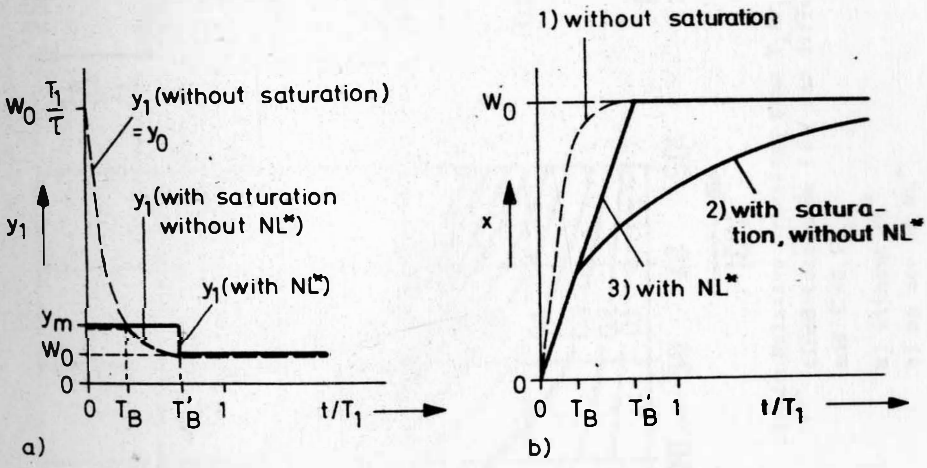

Fig.7 a) Shape of $y_1(t)$ for a step of the reference input $W_o \sigma(t)$ and $T_1/\tau = 10$; $y_m/W_o = 2$
b) corresponding shapes of the controlled variable x

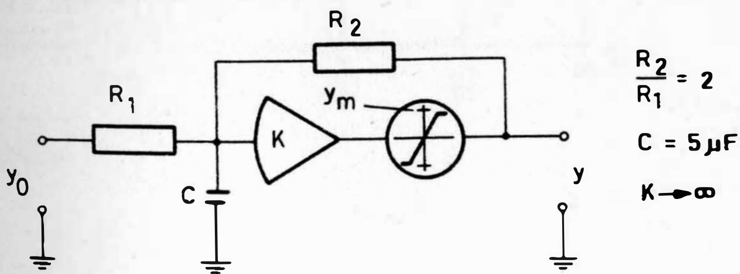

Fig.8 Electrical network for NL^* (example)

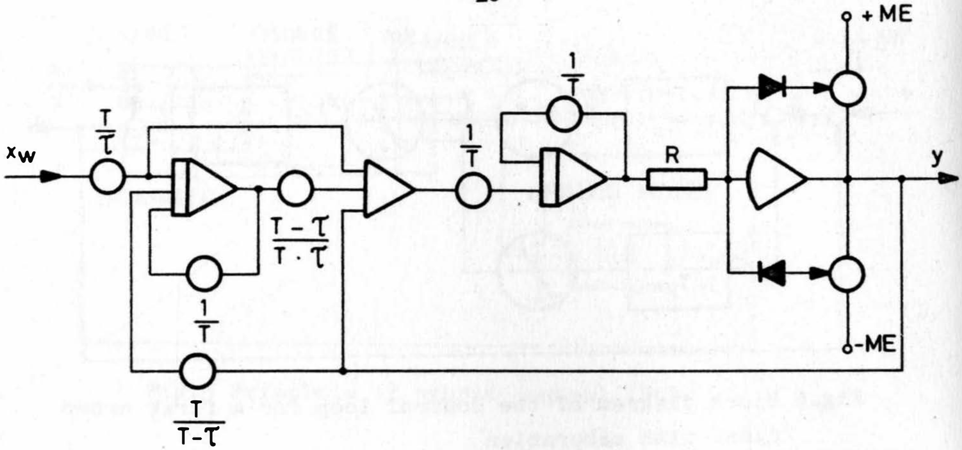

Fig.9 Analog diagram of the controller

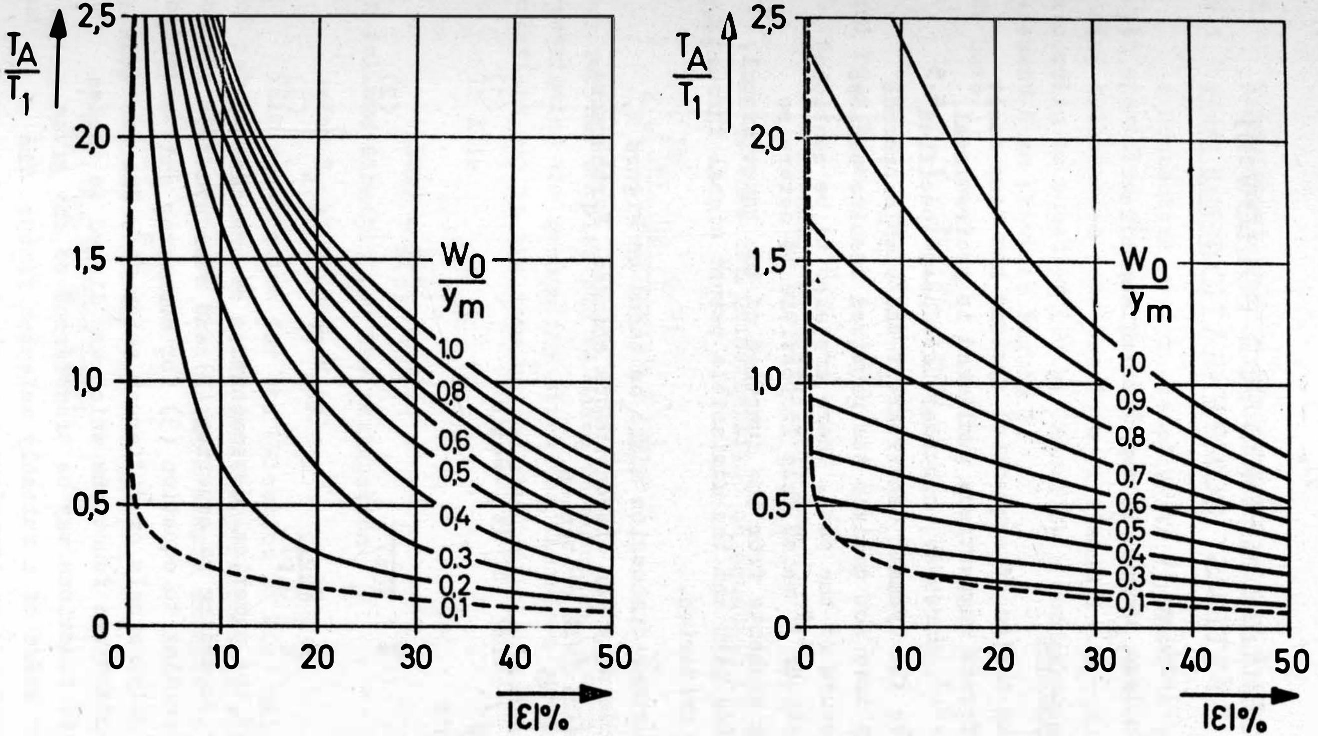

Fig.10 Relative transient time T_A/T_1 as a function of the desired tolerance $/\varepsilon/$ for different step inputs W_o/y_m and $\tau = 0,1T_1$

a) without NL^*

b) by use of NL^*

AN ALGEBRAIC METHOD FOR FOLLOW-UP SYSTEMS' COMPENSATION

by Klaus W. Pleßmann
Technical College Aachen, German Federal Republic

1. Introduction

Optimum design of sequential systems has been dealt with by different suggestions published in professional literature[1,2,3]. Moreover, cascades have been specified[4,5] which improve the dynamic behaviour if the simple cascade control loop does not deliver the required results because of the structure of the path. There are also to be mentioned those suggestions[6,7] which make it possible to determine compensating elements from the function of the input signal, the given line path and the admissible output signal through a quadratic criterion.

Our further discussion shall be based on Figure 1, where w stands only for discontinuous changes. Furthermore, F(p) is linear. ITAE criterion

$$\int_0^{\infty} /w-x/\ t.\ dt \longrightarrow \min \tag{1}$$

and statements

$$\frac{x}{w} = \frac{1}{N(p)} \tag{2}$$

and

$$\frac{x}{w} = \frac{P(p)}{Q(p)} \tag{3}$$

make possible the numerical determination of standard polynominals according to equation (2) and standard functions according to equation (3) for numerator and denominator polynominals of different order [8,9]. The result are standardised functions which are listed in tables 1 and 2. These functions may be transferred to any given time range by means of a suitably selected factor. The following shows how to transform sequential systems to the form of equations (2) and (3), respectively, by means of compensating elements.

2. Transformation into Standard Polynomial Form

2.1 First Method

A sequential system according to Figure 2 is given with specified frequency responses F_{S1} and F_{S2}. x/w is being transformed into the form of standard polynomial according to equation (2) by inserting a compensating element K as shown in Figure 3.

We have

$$x = F_{S1} F_{S2} (w-x) \tag{4}$$

$$x_1 = F_{S1} K (w-x_1) + x \tag{5}$$

and from this

$$K = \left\langle F_{S1} F_{S2} (N-1) - 1 \right\rangle \frac{1}{F_{S1}} \tag{6}$$

If we base the transformation on equation (3), we obtain

$$K = \left\langle \frac{F_{S1} F_{S2} (Q-P)}{P} - 1 \right\rangle \frac{1}{F_{S1}} \tag{7}$$

Our further studies can be based on equation (6) without restricting the generality since the therefrom resulting relations may in the same way be applied to equation (7).

If K is

$$K(p) = \frac{Z(p)}{N(p)} \tag{8}$$

it follows directly for the realisation:

$$\text{order } Z_K(p) = \text{order } N_K(p)$$

This restriction for the selection of N(p) which has not yet been discussed is of great importance. We shall give you the statements on this using a simple example in the following:

We have

$$F_{S1} \cdot F_{S2} = \frac{C_R}{p(1 + pT)} \tag{9}$$

and

$$N-1 = a_1 p + \ldots\ldots + a_{n-1} p^{n-1} + a_n p^n \qquad (10)$$

and, thus, we obtain from equation (6) by the simplifying assumption

$$F_{S1} = \frac{1}{1 + pT}$$

for the compensating element

$$K = \left\langle \frac{C_R\ (a_1 p + \ldots + p^n)}{p\ (1+pT)^{m-1}} - 1 \right\rangle (1+pT)$$

$$= \frac{C_R(a_1 + \ldots + p^{n-1}) - (1+pT)^{m-1}}{(1+pT)^{m-2}}$$

Finally we get for n=m

$$K = \frac{C_R a_1 - 1 + (c_R a_2 - (m-1)T)p + \ldots + (c_R a_{m-1} - \binom{m-1}{m-2} T^{m-2})p^{m-2} + }{(1 + pT)^{m-2}}$$

$$\frac{+ (c_R - T^{m-1})p^{m-1}}{} \qquad (11)$$

by applying the binominal theorem.

The above-mentioned realisation condition is valid if we conclude

$$c_R - T^{m-1} = 0 \qquad (12)$$

If we take line paths according to equation (9), we get

1. Order $Z_K(p)$ = Order $N_K(p)$
2. Order $N(p)$ = Order $F_{S1}(p) \cdot F_{S2}(p)$
3. Order $Z_K(p)$ = Order $N(p) - 2$

The realisation condition is to be tested correspondingly and a set of secondary conditions is to be derived (as in this case according to equation (12)) if the compensating method discussed so far is to be used, but where the frequency response of the line paths is different.

On the basis of the given frequency response of the line path, the total line path should be divisible into two paths, it is possible to derive the frequency response of a compensating element by simple algebraic means, whereby the frequency response transforms the overall transient response of the closed circuit into the form of standard polynomial. In most cases there will occur secondary conditions because of the realisability of $K(p)$.

If the frequency response is not given, but loci x/w and x_2/w are given according to Figure 4, the derived method may still be applied, only that the compensating element is determined graphically. Outgoing from describing equation (6) for $K(p)$, the locus therefore may be determined point by point. The starting point must be equation (6), just the same as in the algebraic method.

We have

$$\frac{x}{w} = F = F_{S1} \cdot F_{S2}$$

and

$$\frac{x_1}{w} = F_{S1}$$

and, subsequently,

$$K = \langle F(N-1)-1 \rangle \frac{1}{F_{S1}} \tag{13}$$

It must be considered that F and F_{S1} are given only point by point. Thus, the construction requires one inversion, one subtraction and two multiplications. Graphical multiplication of two complex magnitudes is indicated in Figure 5.

The known characteristics $N(j\omega) - 1$ are taken as basis, $F_{S1}(j\omega)$ is inverted and, thus, equation (13) can be constructively processed.

Figure 6 shows the construction for one point of K. The following points are given:

$N\,(\omega_1)^{-1}$ Point on the chosen standard locus

$F_1\,(\omega_1)$ · Point on the inverted characteristic $F_{S1}(j\omega)$

$F\,(\omega_1)$ Point on locus $\frac{x}{w}$

By multiplication of $N\,(\omega_1)^{-1}$ with $F_2\,(\omega_1)$ we get point $A\,(\omega_1)$, then

$B\,(\omega_1) = A\,(\omega_1)^{-1}$

and, finally, wanted point $K\,(\omega_1)$ by multiplication of $B\,(\omega_1)$ with $F_1\,(\omega_1)$.

Naturally, with this construction only approximate values can be found which mainly depend on the accuracy of the drawing. Another difficulty is due to the fact that $N(j\omega)^{-1}$ must be selected before carrying out the design. A close relationship exists between the selection of this value and the realisability of the compensating element as has already been described above. It must, furthermore, be considered that the frequency response required for realisation must be determined from the point-by-point acquired locus of $K(j\omega)$. Thus, it seems advisable to start with an approximation for $K\,(j\omega)$, for instance by assuming

$$K\,(j\omega) = V_1\,\frac{1 + j\omega a_1}{1 + j\omega b_1} \tag{14}$$

or

$$K\,(j\omega) = \frac{V_2}{1 + j\omega a_2 + (j\omega)^2 b_2} \tag{15}$$

Studies have shown that quite good results can be obtained with these approximations, for which three points each are required in the design, without too much expenditure (see Section 3 on this).

2.2 Second Method

We have mentioned already at the beginning that special compensating methods for sequential systems have been suggested. With reference to these methods[6,7] let us examine a system as shown in Figure 7.

We have, with line segment $F_S(p)$ being known:

$$\frac{x}{w} = \frac{1}{1 + 1/F} = \frac{1}{N} \tag{16}$$

and

$$F = \frac{F\,K}{1 - KF} \tag{17}$$

Equation (16) and (17) give

$$K_1 = \frac{1}{F_s N} \tag{18}$$

Since in real systems the linear loop of the circuit has only one single point which is stable, this part is changed into a compensating element K(p).

We have

$$K = \frac{1}{F(N-1)} \tag{19}$$

or according to equation (3)

$$K = \frac{P}{F_S\ (Q-P)} \tag{20}$$

It is out of question that this method can also be dealt with and evaluated graphically. The resulting construction may be regarded as a special case of the first method. In contrast to the above-mentioned method no secondary conditions are required for the realisation of the element to be constructed according to equation (20). The order of the standard polynomial or the standard function is only a function of the order of $F_S(p)$.

2.3 Numerical Application

Especially the second method can be applied in connection with a DDC. Thereby, two items are of importance:

1. Optimum adjustment of the circuit is obtained by irregular changing of w for x(t) according to

equation (1). The computer co-operates with a multitude of circuits, except some special cases. Therefore, w may be regarded as step function for each computing cycle with good approximation.

2. An algorithm can be derived from the describing equations for K(p) by means of the methods of Z transformation or special methods[10]. This algorithm can directly be programmed. In this conjunction, the algorithm for K(p) may be regarded as digital filter.

It should also be mentioned that this optimisation method delivers not only the approximate (by means of graphical design as above-mentioned) but the optimum guide action (with the parameters of the line path being known) with regard to the ITAE criterion.

3. Example

Let us assume we have the following frequency responses

$$F_{S1} = \frac{1}{1 + p}$$

$$F_{S2} = \frac{1}{p(1+p)^3}$$

Then we have

$$K = 2{,}261 \frac{1 + 0{,}3047p - 0{,}6634p^2 - 0{,}8513p^3}{1 + 3p + 3p^2 + p^3}$$

taking, thereby, into account the realisation condition and equation (7).

N(p) resulted from line 5 of table 1 on the basis of the above-mentioned considerations. x(t) is plotted in figure 8. Let us take the loci of the discussed example and make the following statement for the compensation

$$K = \frac{V_2}{1 + a_2p + b_2p^2}.$$

The following pairs of values result from the construction of K - 3 points -

$$\omega_1 = 0{,}2 \, \frac{1}{\text{sec}} \; : \; P_1 = 1{,}9 - j\,1{,}12$$

$$\omega_2 = 0{,}6 \, \frac{1}{\text{sec}} \; : \; P_2 = 0{,}41 - j\,1{,}76$$

$$\omega_3 = 0{,}9 \, \frac{1}{\text{sec}} \; : \; P_3 = -\,0{,}19 - j\,1{,}61$$

and, subsequently,

$$K = \frac{2{,}31}{1 + 2{,}25p + 0{,}69\,p^2}$$

If K is applied in the sequential system according to Figure 3, we have a time behaviour of x(t) as plotted in Figure 9.

4. Summary

Two methods have been described which - on the basis of standard polynomials or standard functions, make it possible to determine compensating elements by means of simple algebraic transformations. Secondary conditions result from the line segment to be given with regard to the selection of polynomials or functions taking, thereby, into account realisation conditions.

It has, furthermore, been demonstrated that the suggested methods may also be applied if the loci are given. In this case it is possible to evaluate the compensating element to be determined by approximation. This has been proved by experience and means a simplification of the resulting construction. The results of calculation and construction have been demonstrated by means of a simple example.

Order	N(p)
1	$1+p$
2	$1+1,497p+p^2$
3	$1+2,171p+1,778p^2+p^3$
4	$1+2,645p+3,337p^2+1,951p^3+p^4$
5	$1+3,261p+4,689p^2+4,5p^3+2,075p^4+p^5$
6	$1+3,777p+6,866p^2+7,118p^3+5,687p^4+2,24p^5+p^6$

Table 1 Standard Polynomials

Order	
2.1	$P(p) = 1+2,595p$ $Q(p) = 1+2,98p+p^2$
3.1	$P(p) = 1+3,512p$ $Q(p) = 1+4,226p+2,791p^2+p^3$
3.2	$P(p) = 1+1,375p+2,069p^2$ $Q(p) = 1+1,857p+2,733p^2+p^3$
4.1	$P(p) = 1+4,764p$ $Q(p) = 1+6,069p+6,892p^2+3,425p^3+p^4$
4.2	$P(p) = 1+2,06p+3,36p^2$ $Q(p) = 1+2,841p+5,268p^2+3,238p^3+p^4$
4.3	$P(p) = 1+2,075p+2,159p^2+1,833p^3$ $Q(p) = 1+2,602p+3,276p^2+2,987p^3+p^4$
5.1	$P(p) = 1+9,213p$ $Q(p) = 1+10,696p+14,736p^2+10,273p^3+3,304p^4+p^5$
5.2	$P(p) = 1+1,25p+3,199p^2$ $Q(p) = 1+2,719+5,818p^2+5,99p^3+2,894p^4+p^5$

Order	
5.3	$P(p) = 1+2{,}462p+2{,}313p^2+2{,}926p^3$ $Q(p) = 1+3{,}337p+4{,}801p^2+5{,}788p^3+3{,}339p^4+p^5$
5.4	$P(p) = 1+2{,}738p+3{,}505p^2+3{,}339p^3+1{,}186p^4$ $Q(p) = 1+3{,}365+5{,}292p^2+5{,}771p^3+3{,}478p^4+p^5$
6.1	$P(p) = 1+6{,}806p$ $Q(p) = 1+8{,}989p+16{,}975p^2+15{,}609p^3+9{,}905p^4+2{,}992p^5+p^6$
6.2	$P(p) = 1+0{,}594p+3{,}818p^2$ $Q(p) = 1+2{,}475p+6{,}638p^2+8{,}926p^3+7{,}192p^4+2{,}949p^5+p^6$
6.3	$P(p) = 1+1{,}267p+3{,}142p^2+2{,}52p^3$ $Q(p) = 1+2{,}621p+5{,}861p^2+8{,}08p^3+6{,}935p^4+2{,}76p^5+p^6$
6.4	$P(p) = 1+2{,}862p+4{,}266p^2+3{,}816p^3+2{,}772p^4$ $Q(p) = 1+3{,}752p+7{,}144p^2+8{,}513p^3+7{,}634p^4+3{,}692p^5+p^6$
6.5	$P(p) = 1+4{,}092p+5{,}951p^2+8{,}466p^3+4{,}469p^4+p^5$ $Q(p) = 1+4{,}521p+7{,}729p^2+11{,}061p^3+8{,}183p^4+4{,}201p^5+p^6$

Table 2 Standard Functions

Literature

1 Truxal: Entwurf automatischer Regelsysteme.
R. Oldenbourg, Wien u. München 1960

2 Nixon: Principles of Automatic Controls.
Prentice-Hall, Englewood Cliffs 1958

3 Savant: Basic Feedback Control System Design.
McGraw-Hill, New York 1958

4 Gille, Pelegrin, Decaulne:
Lehrgang der Regelungstechnik.
R. Oldenbourg, München 1960

5 Pestel, Kollmann:
Grundlagen der Regelungstechnik.
Friedr. Vieweg u. Sohn, Braunschweig

6 Newton, Gould, Kaiser:
Analytical Design of Linear Feedback Controls.
John Wiley, 1957

7 Frank: Beitrag zum Entwurf von Reglern durch Nachbildung der Regelstrecke.
unveröffentlicht

8 Dustan, Graham, Lathrop:
Synthesis of Optimum Transient Response.
Trans. AIEE, 72(1953) PtII, pp 273

9 Pleßmann: Normpolynome und Normfunktionen.
unveröffentlicht

10 Boxer, Thaler:
A Simplified Method of Solving Linear and Nonlinear Systems.
Proc. IRE (1956), pp 89

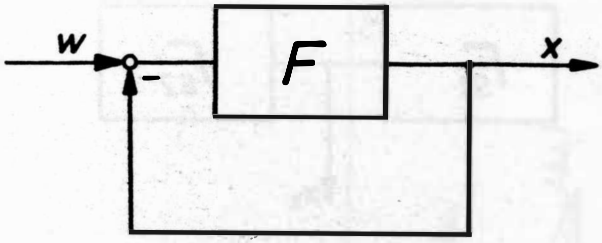

Figure 1   Sequential System

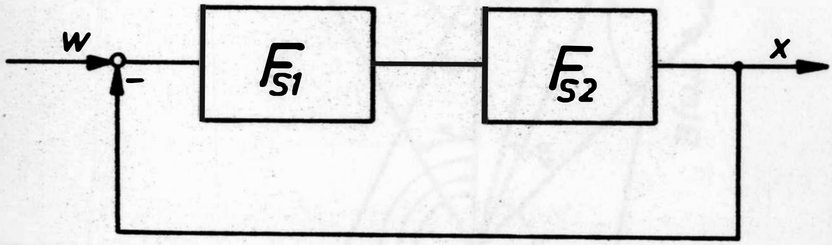

Figure 2   Tested Cascade Control Loop

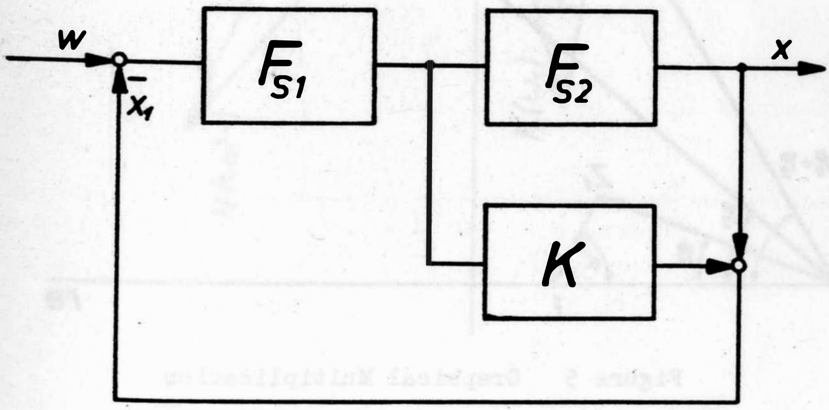

Figure 3   Sequential System with Compensation

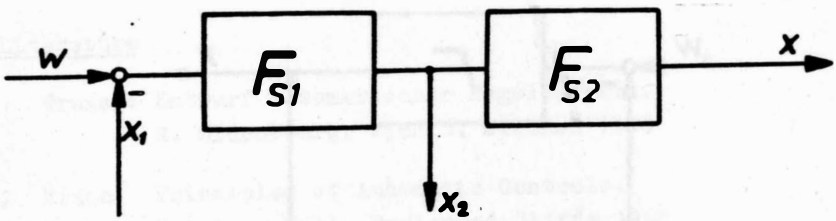

Figure 4 Division of Line Segment

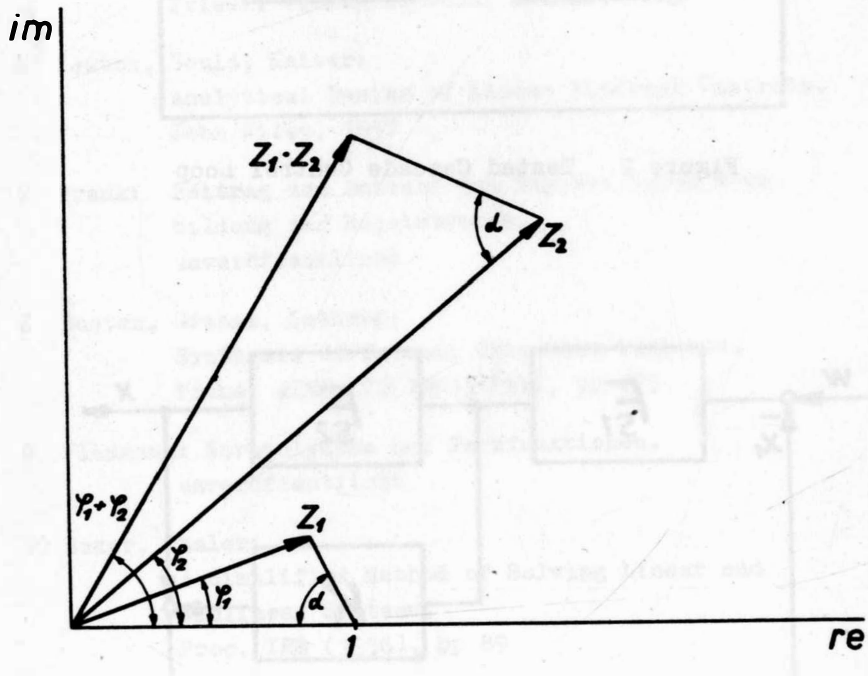

Figure 5 Graphical Multiplication

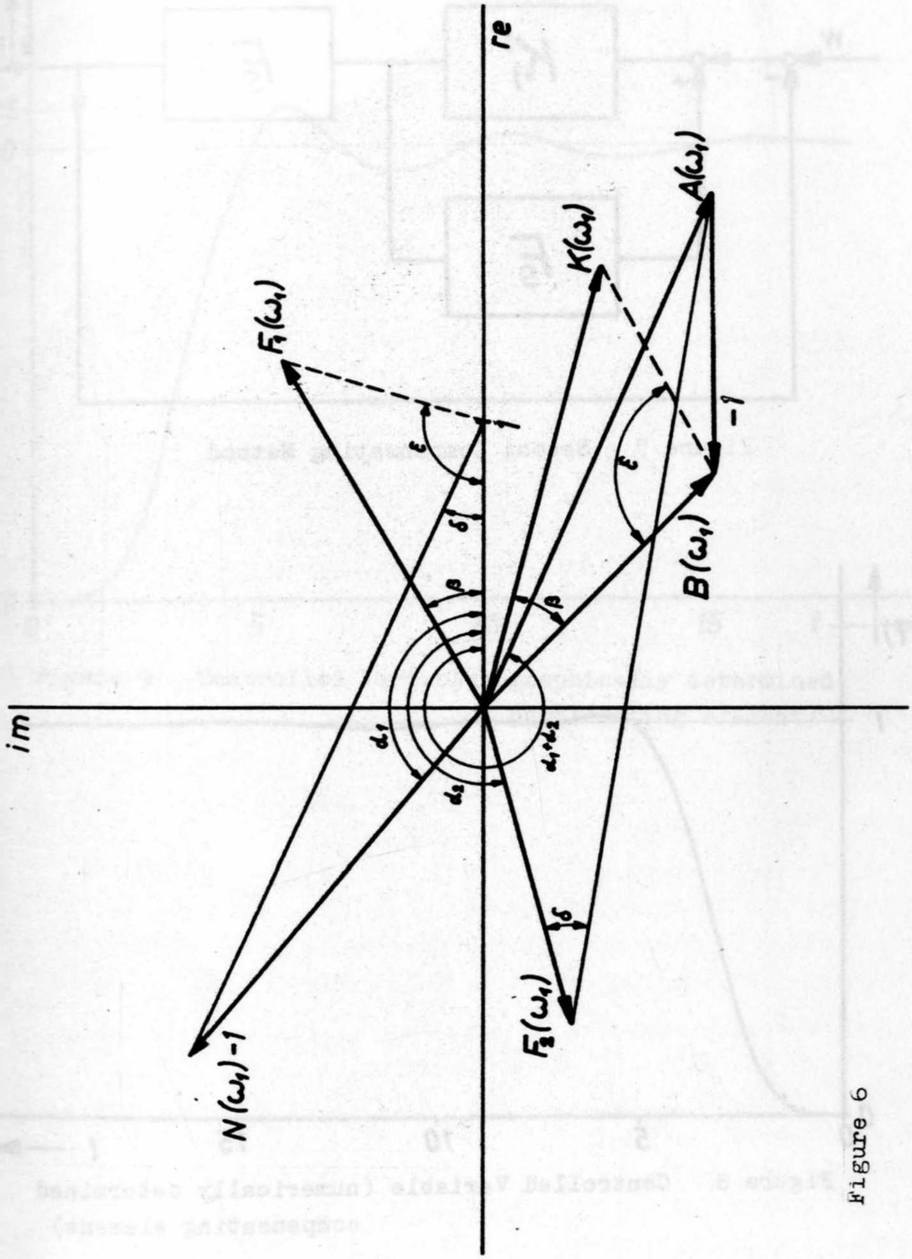
re
im
$A(\omega_1)$
$K(\omega_1)$
$F_1(\omega_1)$
$F_2(\omega_1)$
$B(\omega_1)$
$N(\omega_1)-1$
-1
1
ε
δ
β
α_1
α_2
$\alpha_1+\alpha_2$

Figure 6

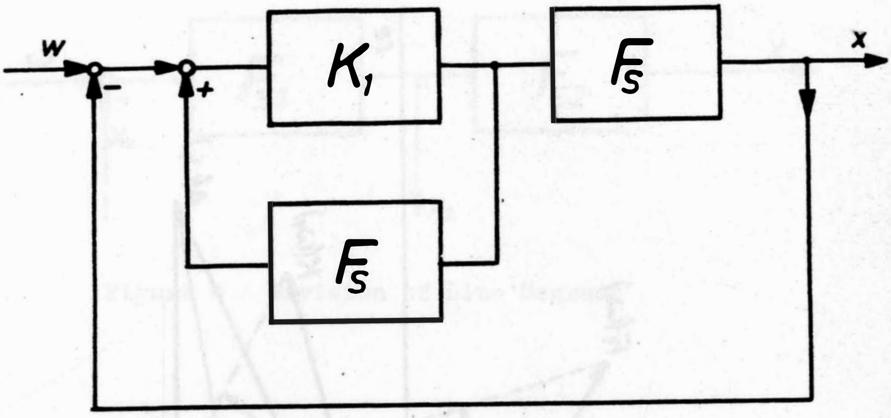

Figure 7 Second Compensating Method

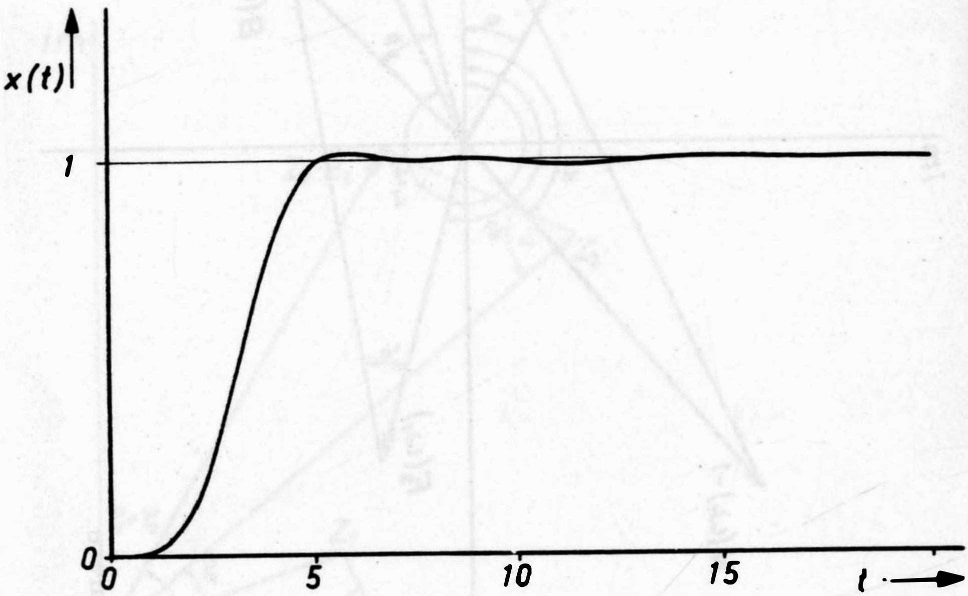

Figure 8 Controlled Variable (numerically determined compensating element)

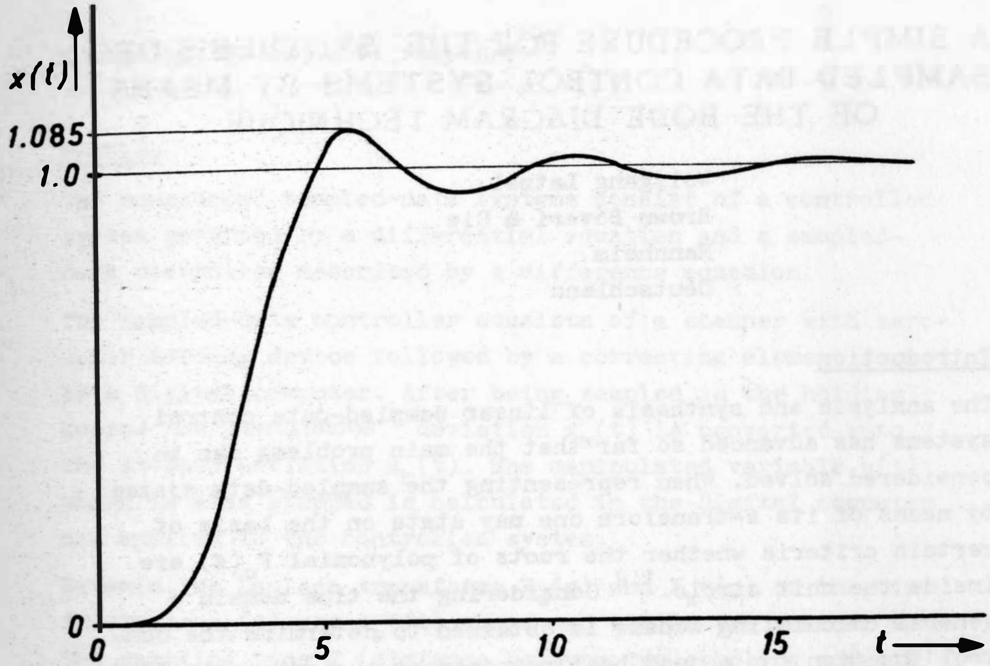

Figure 9 Controlled Variable (graphically determined compensating element)

A SIMPLE PROCEDURE FOR THE SYNTHESIS OF SAMPLED-DATA CONTROL SYSTEMS BY MEANS OF THE BODE-DIAGRAM TECHNIQUE

Wolfgang Latzel
Brown Boveri & Cie
Mannheim
Deutschland

Introduction

The analysis and synthesis of linear sampled-data control systems has advanced so far that the main problems can be considered solved. When representing the sampled-data system by means of its z-transform one may state on the basis of certain criteria whether the roots of polynomial $F_o(z)$ are inside the unit circle.[1,2] Considering the time domain a general calculating scheme is obtained to determine the control function for a dead beat response at a given controlled system of class N and a discrete controller of class N.[3,4] To reduce the equipment it is advisable to choose class n of the controller smaller than class N of the controlled system thereby increasing the calculating operations to determine the control function.[5,6]

Up to now there exists, however, no convenient procedure to calculate the coefficients of the controller from the representation of the controlled system by means of the Bode diagram as this is the case with continuous control systems.

Such a procedure would be of advantage as its mode of representation will be based on the description of continuous systems where the sampling effect will be considered by an adequate correcting function. In addition, the relation between cutoff frequencies and gains in the Bode diagram and the controller coefficients remains clear, whereas it will be lost in the computational procedures. It will be shown that with the below mentioned procedure only an approximate dead beat response will be obtained which does not have the high parameter sensitivity caused by a setting according to dead beat response.

Problem

The considered sampled-data systems consist of a controlled system governed by a differential equation and a sampled-data controller described by a difference equation.

The sampled-data controller consists of a scanner with zero-order holding device followed by a correcting element formed in a digital computer. After being sampled in the holding device the continuous deviation $x_w(t)$ is converted into the stepped deviation $x_h(t)$. The manipulated variable $y(t)$ which is also stepped is calculated in the digital computer and applied to the controlled system.

Between the Laplace transforms $X_w(p)$ and $X_w{*}(p)$ of the time functions $x_w(t)$ and $x_w{*}(t)$ ahead and behind the scanner with the sampling time T (distance between two sampling moments) there is the relation:

$$X_w{*}(p) = \frac{1}{T} \sum_{k=-\infty}^{\infty} X_w(p+j\,k\Omega) \qquad \Omega = \frac{2\pi}{T} \tag{1}$$

The holding device with the correcting element of class n (see Fig. 1) has the transfer function:

$$\frac{Y(p)}{X_w{*}(p)} = \frac{1-e^{-pT}}{p} \cdot \frac{d_o+d_1.e^{-pT}+\ ...\ +d_n.e^{-npT}}{1-c_1.e^{-pT}-\ ...\ -c_n.e^{-npT}} \tag{2}$$

The calculation of this correcting element is to be performed directly by means of the Bode diagram. It is advisable to start with the transfer function in the basic strip with k=0. The influence of the suppressed harmonic oscillations of Eq. (1) will be investigated later. The transfer function of the complete sampled-data controller in the basic strip is:

$$F_{Ro}(p) = \frac{Y(p)}{X_w(p)} = \frac{1-e^{-pT}}{pT} \cdot \frac{d_o+d_1.e^{-pT}+\ ...\ +d_n.e^{-npT}}{1-c_1.e^{-pT}-\ ...\ -c_n.e^{-npT}} \tag{3}$$

The coefficients c_i, d_i of the sampled-data controller should be calculated in such a way that with controlled systems of higher order ($N \geq 2$) an approximate dead beat response with a correction time of 3 to 4 sampling periods will be obtained. It will be shown that the cases n = 1,2,3 are sufficient.

The procedure for the synthesis described below applies to any sampling time T compatible with the stability of the system. The max. value of T permissible for the stability and for the desired time response can be determined by means of this procedure.

1) The description of the first-order sampled-data controller by means of the Bode diagram

For the case n=1 the socalled PD-sampled-data controller is obtained with the transfer function in the basic strip:

$$F_{Ro}(p) = \frac{1-e^{-pT}}{pT} \cdot \frac{d_o+d_1 . e^{-pT}}{1-c_1 . e^{-pT}} \tag{4}$$

In order to find the frequency response pertaining to this transfer function the known transformation $z^{-1} = \frac{1-w}{1+w}$ of the z-plane is applied to the w-plane. To obtain the same dimension for the frequencies p and w, it is advisable to express this transformation as follows:

$$e^{-pT} = \frac{1-w\frac{T}{2}}{1+w\frac{T}{2}} \qquad p = \sigma + j\omega \qquad w = u + jv \tag{5}$$

After this transformation has been applied to the z-dependent portion the transfer function is:

$$F_{Ro} = V.\frac{1}{pT} \cdot \frac{wT}{1+w\frac{T}{2}} \cdot \frac{1+wT_a}{1+w\frac{T}{2} . \frac{1+c_1}{1-c_1}} \tag{6}$$

with the abbreviations

$$V = \frac{d_o+d_1}{1-c_1} \tag{7}$$

$$T_a = \frac{T}{2} \cdot \frac{d_o-d_1}{d_o+d_1} \tag{8}$$

From the w-dependent portion the following statements on the coefficients can be derived:

In order to have a rate action it is necessary that $T_a > \frac{T}{2}$ which yields:

$d_o > 0, \quad d_1 < 0.$

It is necessary that $c_1 < 0$, should the feedback by c_1 result in an improvement as against the case $c_1 = 0$.

An explicit form in p which can be used for the direct description in the Bode diagram, is obtained by the retransformation of Eq. (6) for the range of small and high values of /w/.

On account of Eq. (5) w = p holds for $\left|w\frac{T}{2}\right| \ll 1$, and thus we obtain from Eq. (6):

$$F_1' = V \cdot (1+pT_a) \tag{9}$$

For $|wT_a| \gg 1$ we extend Eq. (6) by $1+w\frac{T}{2}$ and transform, at first, the following term:

$$\frac{1+w\frac{T}{2}}{1+w\frac{T}{2}\cdot\frac{1+c_1}{1-c_1}} = \frac{1-c_1}{1-c_1 \cdot e^{-pT}} \tag{10}$$

After adequate extensions we obtain for the remaining term:

$$F_1'' = V\frac{wT}{pT} \cdot \frac{wT_a}{(1+w\frac{T}{2})^2} = V.pT_a.\left[\frac{wT}{pT.(1+w\frac{T}{2})}\right]^2 \tag{11}$$

The term in brackets is the transfer function of scanner and holding device in the basic strip so that Eq. (11) is written:

$$F_1'' = V.pT_a . \left[F_{Ho}(p)\right]^2 \tag{12}$$

Since $T_a > \frac{T}{2}$, the validity ranges for Eq. (9) and Eq. (12) are overlapping sufficiently so as to allow a combining of the two equations. With the function according to Eq. (10) one finally obtains

$$\underline{F_{Ro}(p) = V\,(1+pT_a) . \left[F_{Ho}(p)\right]^2 . \frac{1-c_1}{1-c_1 . e^{-pT}}} \tag{13}$$

Thus, we have succeeded in representing the PD-sampled-data controller by a product of two transfer functions where the first one describes the ideal continuous PD-controller and the second one the effect of sampling and of the feedback element c_1. The frequency responses pertaining to the correcting transfer function

$$F_{kl}\,(pT,\, c) = \left[\frac{1-e^{-pT}}{pT}\right]^2 . \frac{1+c}{1+c\;.e^{-pT}} \tag{14}$$

are shown in Fig. 2. An increase in c reduces the phase angle in the range $\omega = 0 \ldots \frac{\Omega}{2}$ and results in a growing increase close to half the sampling frequency $\frac{\Omega}{2} = \frac{\pi}{T}$. At c = 1 the correcting fuction has a singular point.

An improvement of the control action by the feedback variable $c_1 = -c$ is to be expected if $c_1 = -0.6 \ldots -0.8$ is chosen. Then, the amplitude increase at $\frac{\Omega}{2}$ remains within reasonable limits, whereas the phase angle is considerably reduced compared with the case $c_1 = 0$.

After selecting c_1 we obtain for the coefficients d_o and d_1:

$$\underline{d_o = V.(1-c_1) . \left[\frac{T_a}{T} + \frac{1}{2}\right]} \quad . \tag{15}$$

$$d_1 = -V.(1-c_1).\left[\frac{T_a}{T} - \frac{1}{2}\right] \qquad (16)$$

The deviations between the frequency response representations according to Eqs. (4) and (13) are below 1 dB in the range $\omega = 0 \ldots \frac{\Omega}{2}$. At the ratio $T_a/T = 4,3,2,1$ and a frequency of $\frac{\Omega}{2}$ the phase error is only $5^o, 6^o, 9^o, 17^o$; at lower frequencies it is correspondingly lower.

2) Instructions for the adjustment of sampled-data controllers to continuous controlled systems

Generally the adjustment of sampled-data controllers to continuous controlled systems is based on the dead beat response where the controlled variable is approaching the value of the reference input within a given time. A controlled system of class N requires a sampled-data controller of class N where the time response has N+1 switch points.

If class n of the sampled-data controller is chosen smaller than class N of the controlled system, only an approximate dead beat response has to be expected. The dimensioning of the coefficients is based on the requirement that the quadratic deviation integral for $t > nT$ becomes minimum. For this case extensive calculating operations are required. [6,7]

For the representation by means of the Bode diagram we obtain relatively simple adjustment conditions provided the time response pertaining to the approximate dead beat response can be given.

Experience has shown that controlled systems of higher classes can be controlled without overshooting with a time response to be composed of three third-order parabolae with the relation:

$$y(t) = \dddot{x}(t) \qquad (17)$$

During the three sampling times with the length $T_m/3$ the manipulated variable is constant and assumes the values $y=y_m$, $-2y_m$, y_m (see Fig. 3)

By integrating three times, x can be described as a sum of four third-order parabolae (with $\sigma(t)$ for the step function):

$$x(t)=y_m\left[\frac{t^3}{6}\cdot\sigma(t)-\frac{1}{2}\left(t-\frac{T_m}{3}\right)^3\cdot\sigma\left(t-\frac{T_m}{3}\right)+\frac{1}{2}\left(t-\frac{2T_m}{3}\right)^3\cdot\sigma\left(t-\frac{2T_m}{3}\right)\right.$$
$$\left.-\frac{1}{6}(t-T_m)^3\cdot\sigma(t-T_m)\right] \qquad (18)$$

By means of the Laplace transformation we obtain for the desired transfer function of the closed control loop (to be denoted as F_{wopt}):

$$F_{w_{opt}}(p)=\left[\frac{1-e^{-pT_m/3}}{pT_m/3}\right]^3 \qquad (19)$$

This involves the following transfer function of the open control loop:

$$F_{o_{opt}}(p)=\frac{\left[1-e^{-pT_m/3}\right]^3}{\left[pT_m/3\right]^3-\left[1-e^{-pT_m/3}\right]^3} \qquad (20)$$

Its frequency response is shown in Fig. 4

At low frequencies $|F_{o_{opt}}|$ shows a decrease of 20 dB/decade for the integral action. The zero-decibel-frequency is $\omega_{d1} = \frac{2\pi}{Tm}$ at a phase margin of $\varphi_{Rd} = 65^o$. With the frequency $\omega_{d2} = \frac{2\pi}{Tm}$ there is $\varphi_{o_{opt}} = -180^o$ at a gain margin of $A_{Rd} = -9dB$.

The gain characteristic $|F_{o_{opt}}|$ rises in the range $\varphi_{o_{opt}} = -180^o ... -270^o$ at the maximum 1.5 dB over the straight line dropping with 20 dB/decade. With the frequency $\Omega = \frac{2\pi}{T} = \frac{6\pi}{Tm}$, there is $|F_{o_{opt}}| = 0$ at a phase angle $\varphi_{o_{opt}} = -540^o$. On account of the periodicity of $F_{w_{opt}}$ harmonic oscillations will also occur in $F_{o_{opt}}$ which are, however, negligible as they are below 1 per cent.

As example for the dimensioning of the PD sampled-data controller the controlled system given in[6] is used.

$$F_S(p) = \frac{1}{(1+pT_1)(1+pT_2)(1+pT_3)(1+pT_4).pT_5} \tag{21}$$

where T_1=2s, T_2=1.2s, T_3=1s, T_4=0.8s, T_5=1s.

As in Fig. 15 in[6] a sampling time of T = 4.5s is chosen. Fig. 5 shows the arithmetic operation to be performed in a few steps. After representing the exact gain characteristic $|F_S|$ the selected cutoff-frequency $1/T_a$ is that frequency at which $|F_S|$ has dropped by further 3 dB as against the constant drop of 20 dB/decade.

Coefficient c_1 has been selected so as to result in the desired gain characteristic. The gain is chosen dependent on the phase margin and the gain margin.

For a choise of V=0.1; c_1=-0.7, T_a=3.1s and T=4.5s we obtain for the controller coefficients:

$d_o = 0.20$

$d_1 = -0.03$ $\qquad$ $c_1 = -0.7$

In Fig. 6 the time response is shown obtained with these values. The correction time is 18s as against 12s in Fig. 15 in [6], the quadratic deviation integral is only 18 per cent greater.

As shown by the frequency response $F_{o_{opt}}$ in Fig. 4, the harmonic oscillations in Eq. (1) are negligible if the time response can be described by a course as in Fig. 3.

For the impulse frequency response $F_o^*(j\omega)$ required to describe the sampled-data control system we have to consider in Eq. (1) the terms with $k = 0$ and $k = -1$, then we obtain:

$$F_o^*(j\omega) = F_o(j\omega) + \overline{F_o}\,(j(\Omega-\omega)) \tag{22}$$

Assuming a frequency response $F_{o\,opt}(j\omega)$ according to Eq. (20) we have at a frequency $\frac{\Omega}{2}$ a phase angle of -260^o and thus a negative real component. When the sampling time decreases in proportion to the increasing sampling frequency the phase angle $\varphi_o\,(j\,\frac{\Omega}{2})$ increases. No loss of stability will have to be expected if $\varphi_o\,(j\frac{\Omega}{2}) = -270^o\ldots-450^o$ as positive real components are belonging thereto. If, however, $\varphi_o(j\frac{\Omega}{2}) = -450^o\ldots-630^o$ the stability may be endangered if the real component of $F_o(j\frac{\Omega}{2})$ becomes too large. In order to avoid this care should be taken that the gain characteristic of $F_o(j\omega)$ at high frequencies, especially at $\frac{\Omega}{2}$ will not exceed the straight line $1/p\frac{Tm}{2}$ dropping at 20 dB/decade.

3) The representation of the frequency response of the second-order sampled-data controller

With n = 2, we obtain from Eq. (3) after applying the transformation of Eq. (5) the following transfer function:

$$F_{Ro} = \frac{1}{pT} \cdot \frac{wT}{1+w\frac{T}{2}} \cdot \frac{d_o+d_1+d_2+wT(d_o-d_2)+(w\frac{T}{2})^2(d_o-d_1+d_2)}{1-c_1-c_2+wT(1+c_2)+(w\frac{T}{2})^2\,(1+c_1-c_2)} \tag{23}$$

<u>Case (a)</u> $\quad c_1+c_2 = 1 \qquad c_1 > 0, \quad c_2 > 0$ (24)

In the denominator of the last fraction the constant term is dropped so that by reducing the fraction by wT for $w \to 0$ term pT is maintained in the denominator and describes an I-action. Thus, case (a) describes an PID-sampled-data controller the transfer function of which is defined by:

$$F_{Ro}(p) = V \cdot \frac{(1+pT_a)(1+pT_b)}{pT} \cdot \left[F_{Ho}(p)\right]^2 \cdot \frac{1+c_2}{1+c_2 \cdot e^{-pT}} \quad (25)$$

The PID-sampled-data controller can be described by a product of two transfer functions where the first one describes the ideal, continuous PID controller and the second one the effect of sampling and of the feedback element c_2. The effect of the feedback element is again given by F_{kl} as per Fig. 2 with $c = c_2$. From c_2 we obtain c_1 according to Eq. (24).

For the coefficients d_o, d_1, d_2 we obtain:

$$d_o = V\,(1+c_2)\left[\frac{T_aT_b}{T^2} + \frac{T_a+T_b}{2T} + \frac{1}{4}\right] \quad (26)$$

$$d_1 = -2V(1+c_2)\left[\frac{T_aT_b}{T^2} - \frac{1}{4}\right] \quad (27)$$

$$d_2 = V\,(1+c_2)\left[\frac{T_aT_b}{T^2} - \frac{T_a+T_b}{2T} + \frac{1}{4}\right] \quad (28)$$

Fig. 7 shows the obtained time response on a fourth-order controlled system (as Eq. (21), however without I-element):

$$F_S(p) = \frac{1}{(1+pT_1)(1+pT_2)(1+pT_3)(1+pT_4)} \quad (29)$$

When adjusting the controller first T_a is selected equal to the max. delay time $T_1 = 2s$. As cutoff-frequency $1/T_b$ that frequency is chosen at which the gain characteristic $\left|F_S \frac{1+pT_a}{pT_a}\right|$ has dropped by further 3 dB as against the constant drop of 20 dB/decade: $1/T_b=0.48s^{-1}$.

The value required for V results from the phase margin. Curve a in Fig. 7 corresponds to a phase margin of 65^o at V=0.495 and T=3.3s.

Thus, we find:

$d_o = 1.01$

$d_1 = -0.24$ $\quad c_1 = 0.4$

$d_2 = 0.02$ $\quad c_2 = 0.6$

Curve b corresponds to $V=0.53$ at a phase margin of 62^{o}.

Case (b). With certain values of c_1, c_2 we obtain a second-order sampled-data controller with PD_2- action permitting to govern controlled systems with double-integral action[4].

From Eq. (23) we obtain for the transfer function of the PD_2- sampled-data controller:

$$F_{Ro} = V \cdot \frac{1}{pT} \cdot \frac{wT}{1+w\frac{T}{2}} \cdot \frac{(1+wT_a)(1+wT_b)}{(1+wT_c)(1+wT_d)} \tag{30}$$

$$\text{with } V = \frac{d_o+d_1+d_2}{1-c_1-c_2} \tag{31}$$

The rate times T_a, T_b are defined by adjustment to the given controlled system and are set by selecting the d_i. Depending on c_1, c_2 the delay times T_c, T_d have a certain range. The limit value of the w-dependent term of Eq. (30) for $w \rightarrow \infty$ remains unchanged if instead of the two separate roots T_c and T_d a double root at $T_o = \sqrt{T_c T_d}$ is chosen. Thus, the design of the controller is considerably simplified and a relation between c_1 and c_2 obtained:

$$c_2 = -\left(\frac{c_1}{2}\right)^2 \qquad c_1 < 0, \qquad c_2 < 0 \tag{32}$$

Hence, the transfer function of the PD_2- sampled-data controller is:

$$F_{Ro}(p) = V(1+pT_a)(1+pT_b)\left[F_{Ho}(p)\right]^3 \left[\frac{1-\frac{c_1}{2}}{1-\frac{c_1}{2}\cdot e^{-pT}}\right]^2 \tag{33}$$

Fig. 8 shows the frequency responses of the correcting transfer function

$$F_{k2}(pT, c) = \left[\frac{1-e^{-pT}}{pT}\right]^3 \cdot \left[\frac{1+c}{1+c\cdot e^{-pT}}\right]^2 \tag{34}$$

which is to be added to the transfer function of the ideal PD_2- controller (with $c=-\frac{c_1}{2}$). For the coefficients d_o, d_1, d_2 we find:

$$d_o = V(1-\frac{c_1}{2})^2 \cdot \left[\frac{T_aT_b}{T^2} + \frac{T_a+T_b}{2T} + \frac{1}{4}\right] \tag{35}$$

$$d_1 = -2V\,(1-\frac{c_1}{2})^2 \cdot \left[\frac{T_aT_b}{T^2} - \frac{1}{4}\right] \tag{36}$$

$$d_2 = V\,(1-\frac{c_1}{2})^2 \left[\frac{T_aT_b}{T^2} - \frac{T_a+T_b}{2T} + \frac{1}{4}\right] \tag{37}$$

Fig. 9 shows the time response on a controlled system

$$F_S(p) = \frac{1}{(1+pT_1)(1+pT_2)(1+pT_3)(1+pT_4).pT_5.pT_6} \tag{38}$$

which we find from Eq. (21) by adding one I-element with T_6=10s. As with the first example the adjustment yielded T_a=3.1s, whereas T_b=310s was assumed to be two powers of ten higher in order to get the maximum possible phase lead within the range of the zero-decibel frequency. With T=4.5s, we obtained with $-\frac{c_1}{2}$ = o.5 an admissible proportional gain of $V=2.5.10^{-3}$ and hence:

d_o = 0.372
d_1 = -0.425 $\quad$ c_1 = -1
d_2 = 0.058 $\quad$ c_2 = -0.25

The time response is satisfactory, however not the steady-state error on account of the very small admissible value of V. A disturbance $z = 10^{-3}$ will result in a deviation x_w=40 per cent.

4) <u>The representation of the third-order sampled-data controller with integral action</u>

By means of a suitable programming a third-order sampled-data controller can be realized with a PID_2- time response. From its transfer function

$$F_{Ro} = \frac{1}{pT} \cdot \frac{wT}{1+w\frac{T}{2}} \cdot$$

$$\frac{d_o+d_1+d_2+d_3+\frac{wT}{2}(3d_o+d_1-d_2-3d_3)+(\frac{wT}{2})^2(3d_o-d_1-d_2+3d_3)+(\frac{wT}{2})^3(d_o-d_1+d_2-d_3)}{1-c_1-c_2-c_3+\frac{wT}{2}(3-c_1+c_2+3c_3)+(\frac{wT}{2})^2(3+c_1+c_2-3c_3)+(\frac{wT}{2})^3(1+c_1-c_2+c_3)} \quad (39)$$

follows as condition for the integral action:

$$c_1+c_2+c_3 = 1 \quad (40)$$

Hence, the transfer function is written:

$$F_{Ro} = V.\frac{1}{pT} \cdot \frac{(1+wT_a)(1+wT_b)(1+wT_c)}{(1+w\frac{T}{2})(1+wT_d)(1+wT_e)} \quad (41)$$

The numerator polynomial with the d_i is defined by the adjustment to the controlled system, whereas the denominator polynomial will be chosen so that a double root at $T_o = \sqrt{T_dT_e}$ exists. Hence, we find:

$$c_1 = 1 - 2.\sqrt{c_3} \qquad c_1 > 0 \quad (42)$$

$$c_2 = 2.\sqrt{c_3}-c_3 \qquad c_2 > 0, \quad c_3 > 0 \quad (43)$$

and for the transfer function:

$$F_{Ro}(p) = V.\frac{(1+pT_a)(1+pT_b)(1+pT_c)}{pT} \cdot \left[F_{Ho}(p)\right]^3 \cdot \left[\frac{1+\sqrt{c_3}}{1+\sqrt{c_3}.e^{-pT}}\right]^2 \quad (44)$$

In the correcting function $F_{k2}(pT,c)$ it is necessary to have.

$c = \sqrt{c_3}$.

For the coefficients d_i we have:

$$d_o = V\,(1+\sqrt{c_3})^2 \cdot \left[\frac{T_aT_bT_c}{T^3} + \frac{T_aT_b+T_aT_c+T_bT_c}{2T^2} + \frac{T_a+T_b+T_c}{4T} + \frac{1}{8}\right] \tag{45}$$

$$d_1 = -3V.(1+\sqrt{c_3})^2 \cdot \left[\frac{T_aT_bT_c}{T^3} + \frac{T_aT_b+T_aT_c+T_bT_c}{6T^2} - \frac{T_a+T_b+T_c}{12T} - \frac{1}{8}\right] \tag{46}$$

$$d_2 = 3V\,(1+\sqrt{c_3})^2 \cdot \left[\frac{T_aT_bT_c}{T^3} - \frac{T_aT_b+T_aT_c+T_bT_c}{6T^2} - \frac{T_a+T_b+T_c}{12T} + \frac{1}{8}\right] \tag{47}$$

$$d_3 = -V\,(1+\sqrt{c_3})^2 \cdot \left[\frac{T_aT_bT_c}{T^3} - \frac{T_aT_b+T_aT_c+T_bT_c}{2T^2} + \frac{T_a+T_b+T_c}{4T} - \frac{1}{8}\right] \tag{48}$$

When applied to the controlled system of Eq. (38), $T_b=T_c$ $=500s$ was selected, whereas $T_a=3.1s$. At a sampling time $T=3s$ and with $c_3=0.4$ we obtained an admissible gain of $V=1.1\ .10^{-5}$ and for the coefficients:

$d_o = 0.92381$

$d_1 = -2.15790$ $\qquad c_1 = 0.2$

$d_2 = 1.55160$ $\qquad c_2 = 0.64$

$d_3 = -0.31749$ $\qquad c_3 = 0.16$

with

$$V = \frac{d_o+d_1+d_2+d_3}{(1+\sqrt{c_3})^2} \tag{49}$$

there results from the coefficients $V= 1.02\ .10^{-5}$; thus, it is shown that with the d_i no further tens places are required. The time response (Fig. 10) shows a satisfactory result.

For reasons of stability there should only be a very small effect of the integral action. A variable disturbance z will result in a rate error x_w. Should the disturbance z change during the period T_z by the value 1, there results a steady-state error with the value $x_w = \frac{1}{V} \cdot \frac{T}{T_z}$.

Summary

The proposed procedure for the synthesis of sampled-data control systems on the basis of the Bode diagram technique features a relatively simple and clear calculation of sampled-data control controllers uses the well-proven method for continuous systems. It is mainly applied to controlled systems of the order $N \geq 2$ and sampled-data controllers of the order $n \leq 3$, where it is necessary that $n \leq N$.

Controllers with I-action are defined by $\sum c_i = 1$. The results obtained with this procedure are shown on controlled systems of higher orders than three.

Reference:

1) Jury, E.J.: On the Roots of a Real Polynomial Inside the Unit Circle and a Stability Criterion for Linear Discrete Systems. IFAC London 1963, Butterworth, pp. 142 to 153

2) Thoma, M.: Über die Wurzelverteilung von linearen Abtastsystemen (On the Root Distribution of Linear Sampled-Data Control Systems)
Regelungstechnik 1963, Heft 2, pp. 70 to 74

3) Föllinger, O.: Synthese von Abtastsystemen im Zeitbereich (Synthesis of Sampled-data Control Systems within the Time Domain)
Regelungstechnik 1965, Heft 6, pp. 269 to 275

4) Föllinger, O.: Realisierung eines Abtastreglers durch Netzwerke (Realization of a Sampled-data Controller by

networks)
Nachrichtentechnische Zeitschrift 1966, Heft 5,
pp. 273 to 279

5) Haberstock, F.: Über die Synthese von Abtastreglern für Regelkreise beliebiger Ordnung (On the Synthesis of Sampled-data Controllers for Control Systems of any Order)
Regelungstechnik 1965, Heft 5, pp. 235 to 239
and Heft 6, pp. 281 to 286

6) Hofmann, R.: Ein Beitrag zur Theorie der Abtastsysteme für Regelkreise beliebiger Ordnung. (Comment on the Theory of Sampled-data Systems of any Order)
Regelungstechnik 1967, Heft 7, pp. 309 to 315

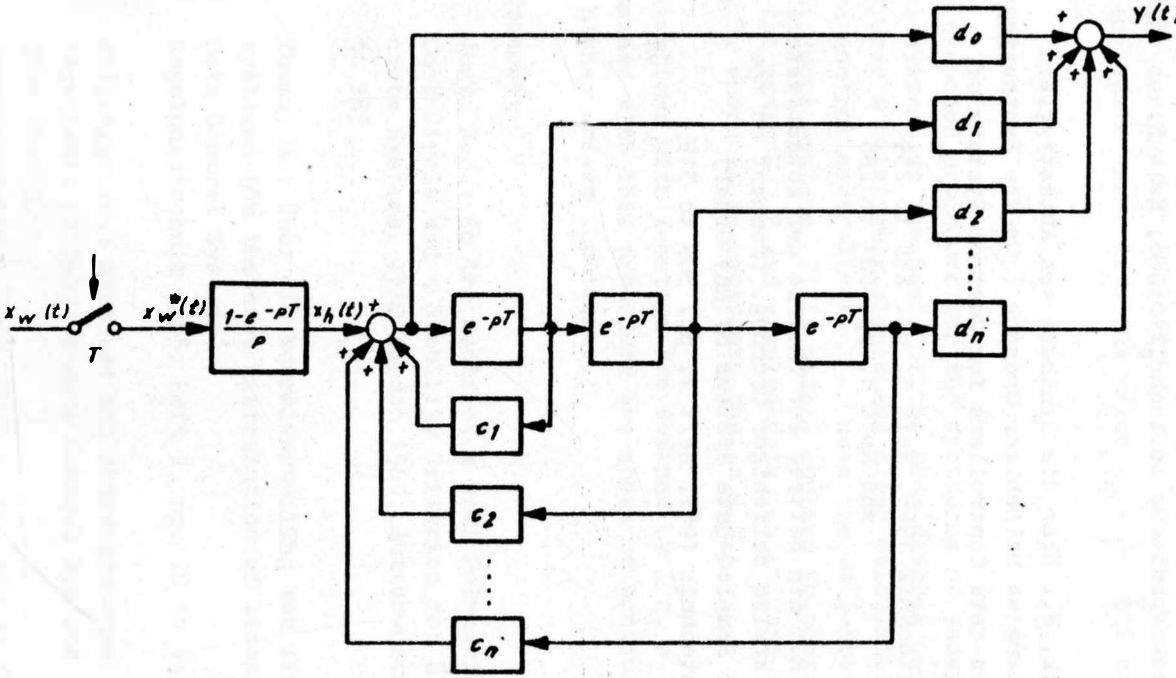

Fig. 1 Signal flow diagram of a sampled-data controller of class n

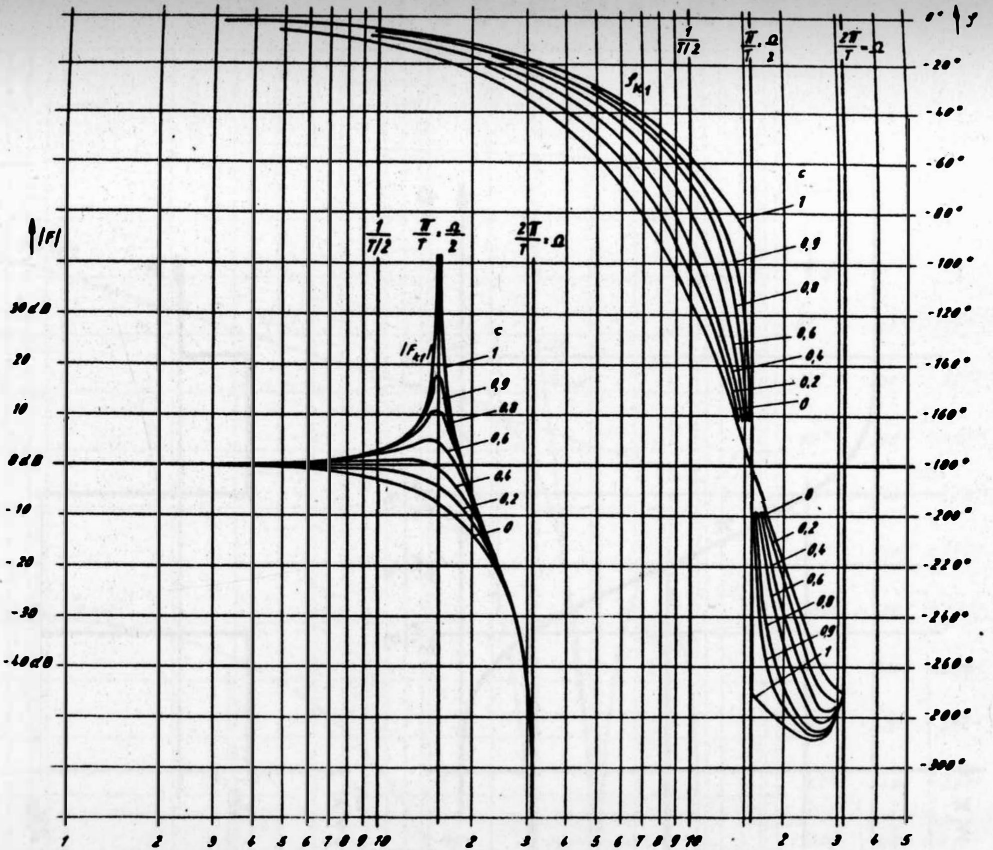

Fig. Frequency responses of the correcting transfer function F_{kl} according to Eq. (14)

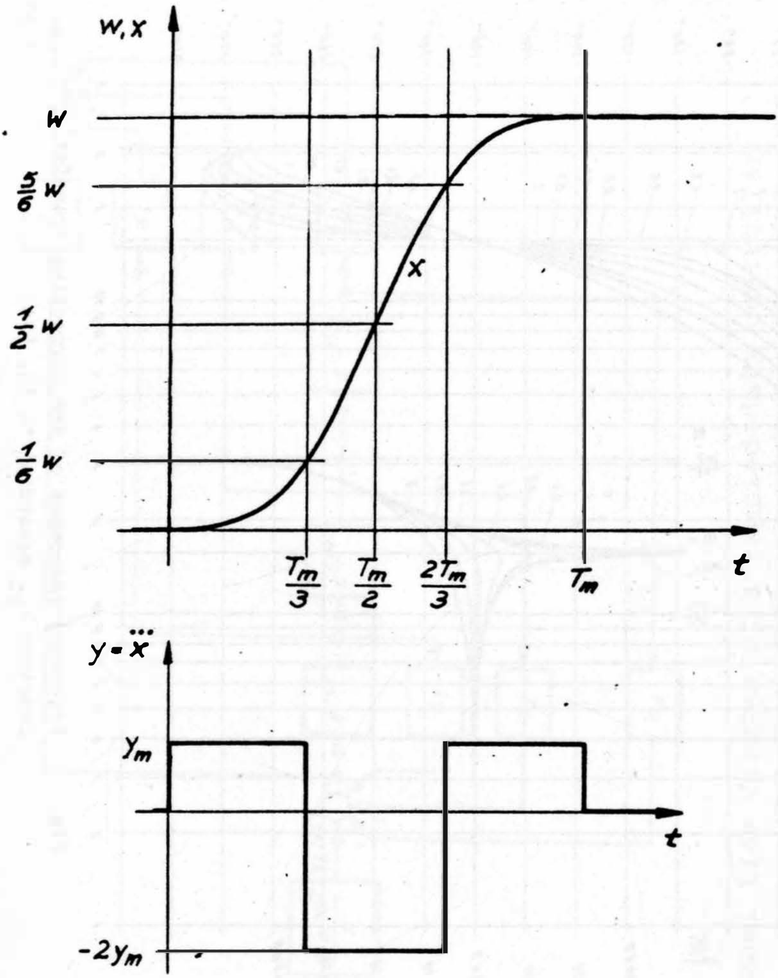

Fig. 3 Desired optimal third-order time response

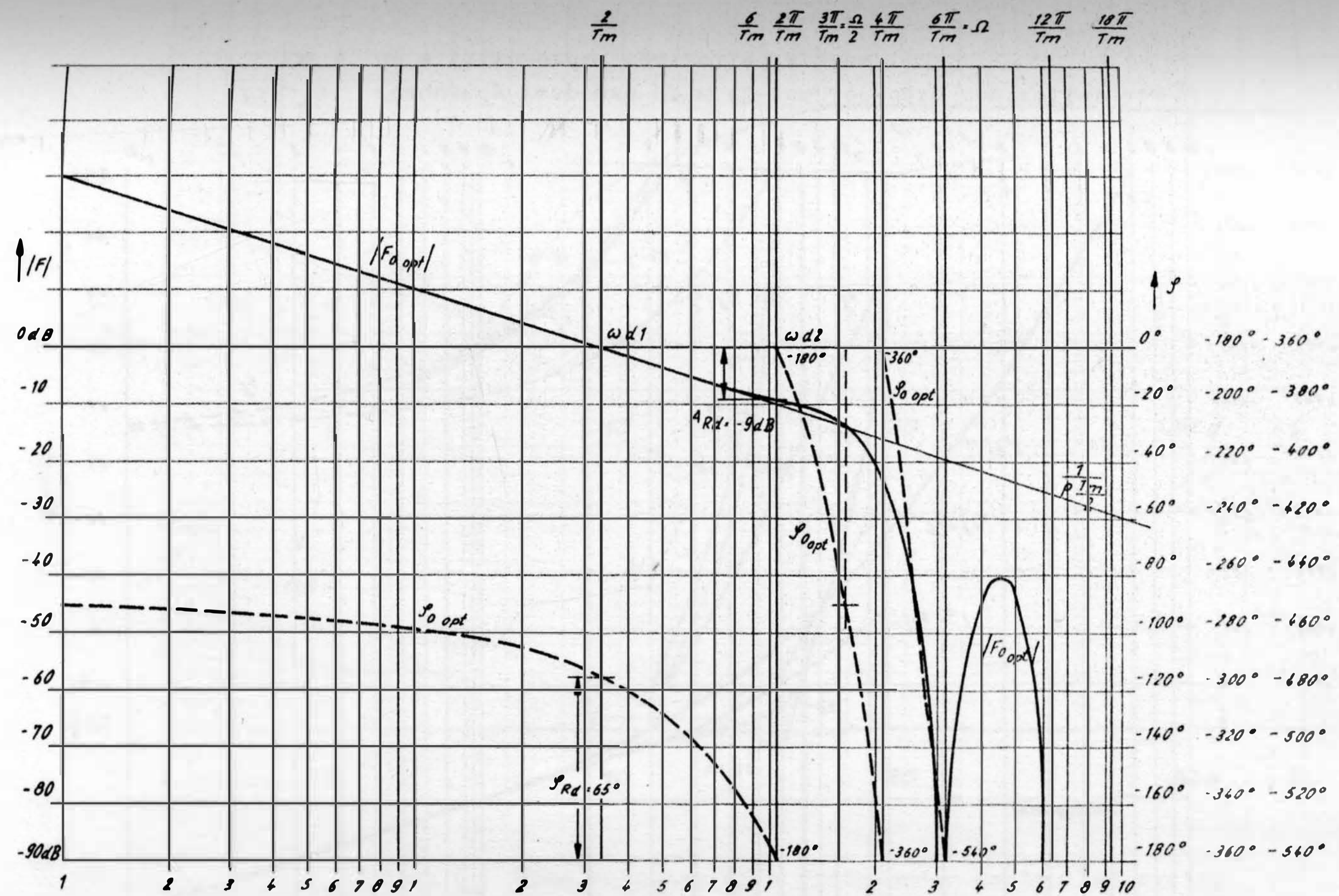

Fig. 4 Frequency response $F_{o_{opt}}$ to the time response in Fig. 3

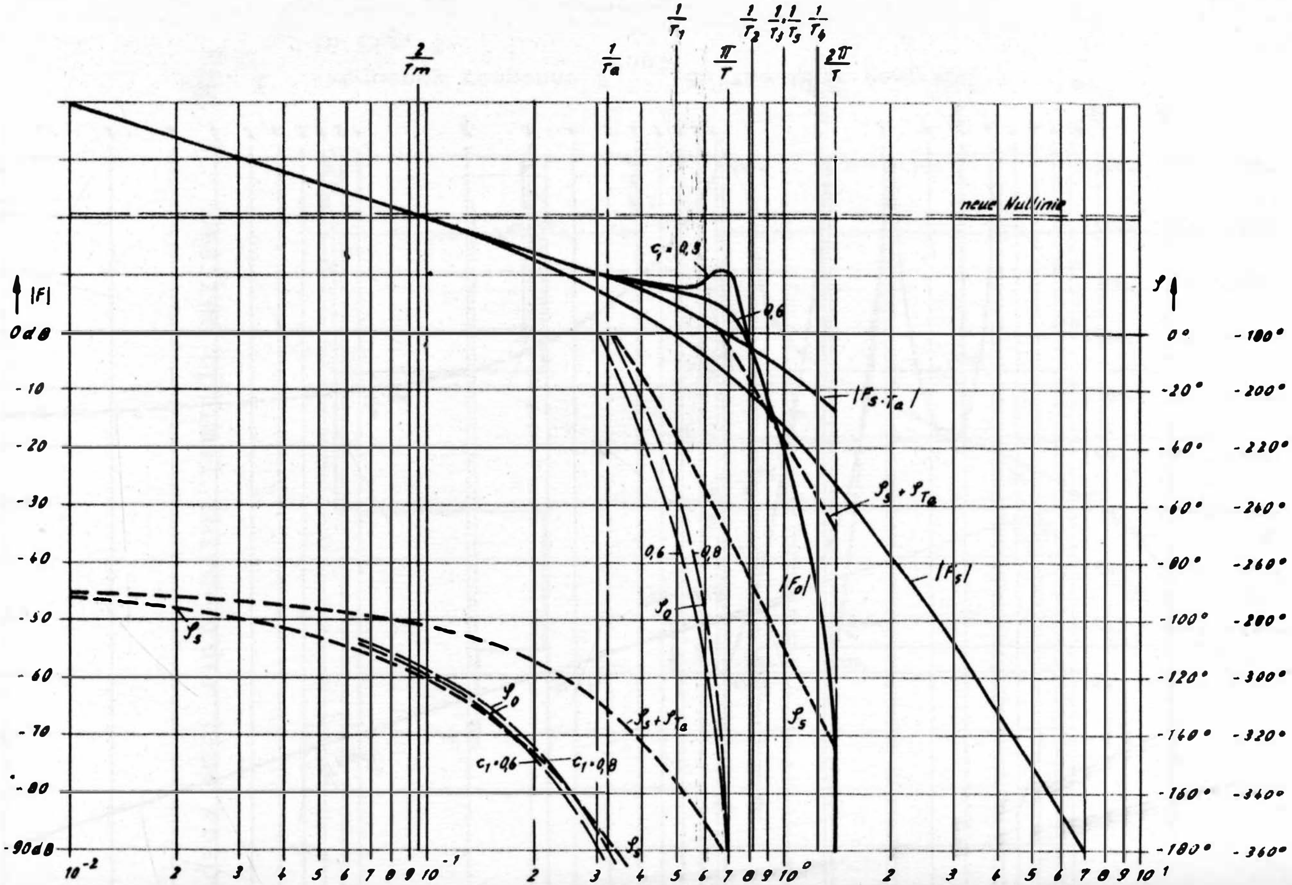

Fig. 5 Frequency response of a PD-sampled-data controller on a fifth-order controlled system

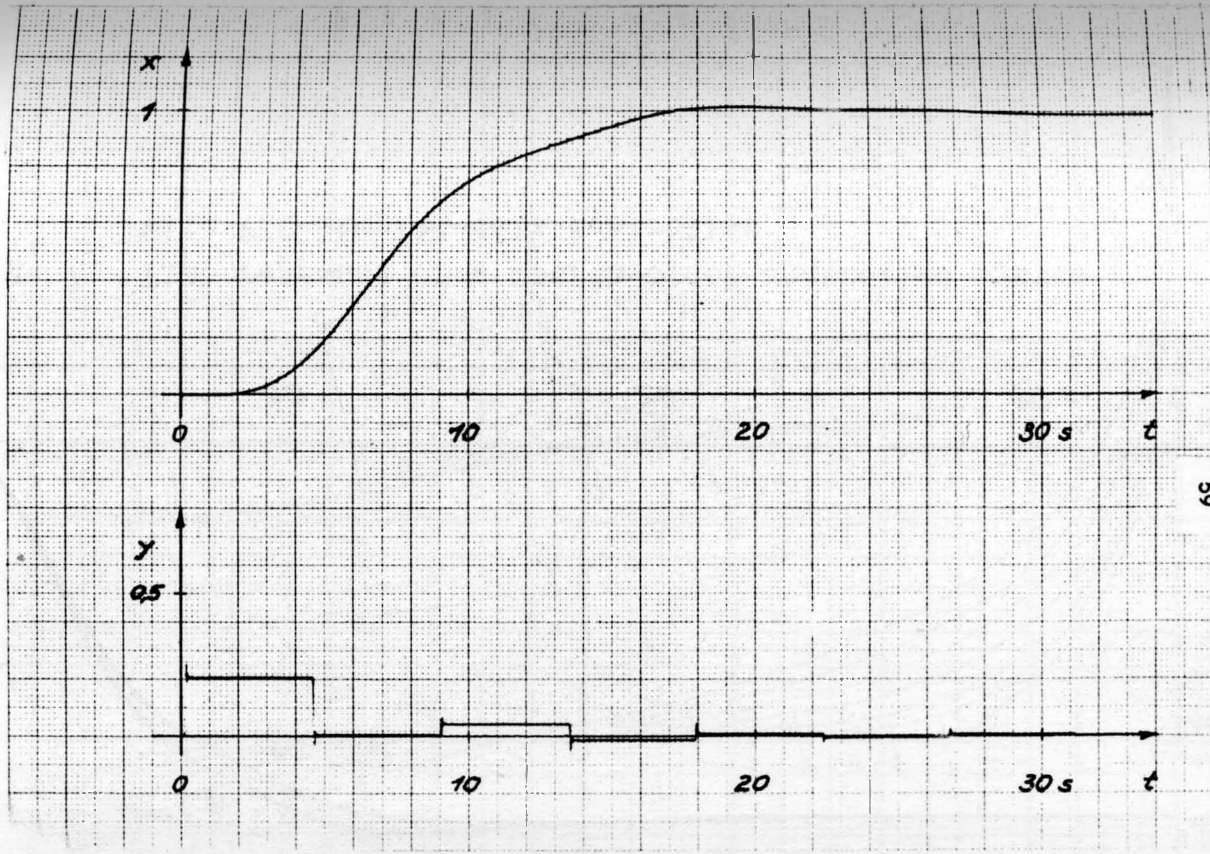

Fig. 6   Time response of a fifth-order controlled system
with a PD-sampled data controller

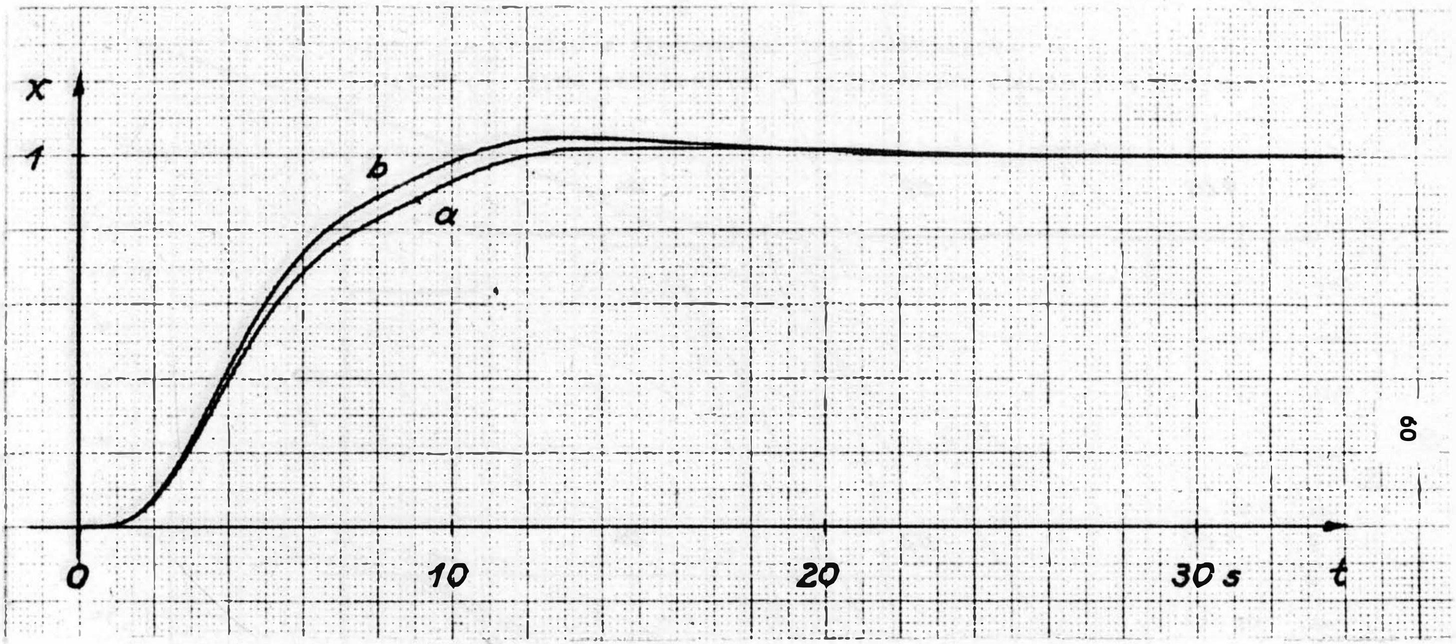

Fig. 7 Time response of a fourth-order controlled system with PID-sampled-data controller

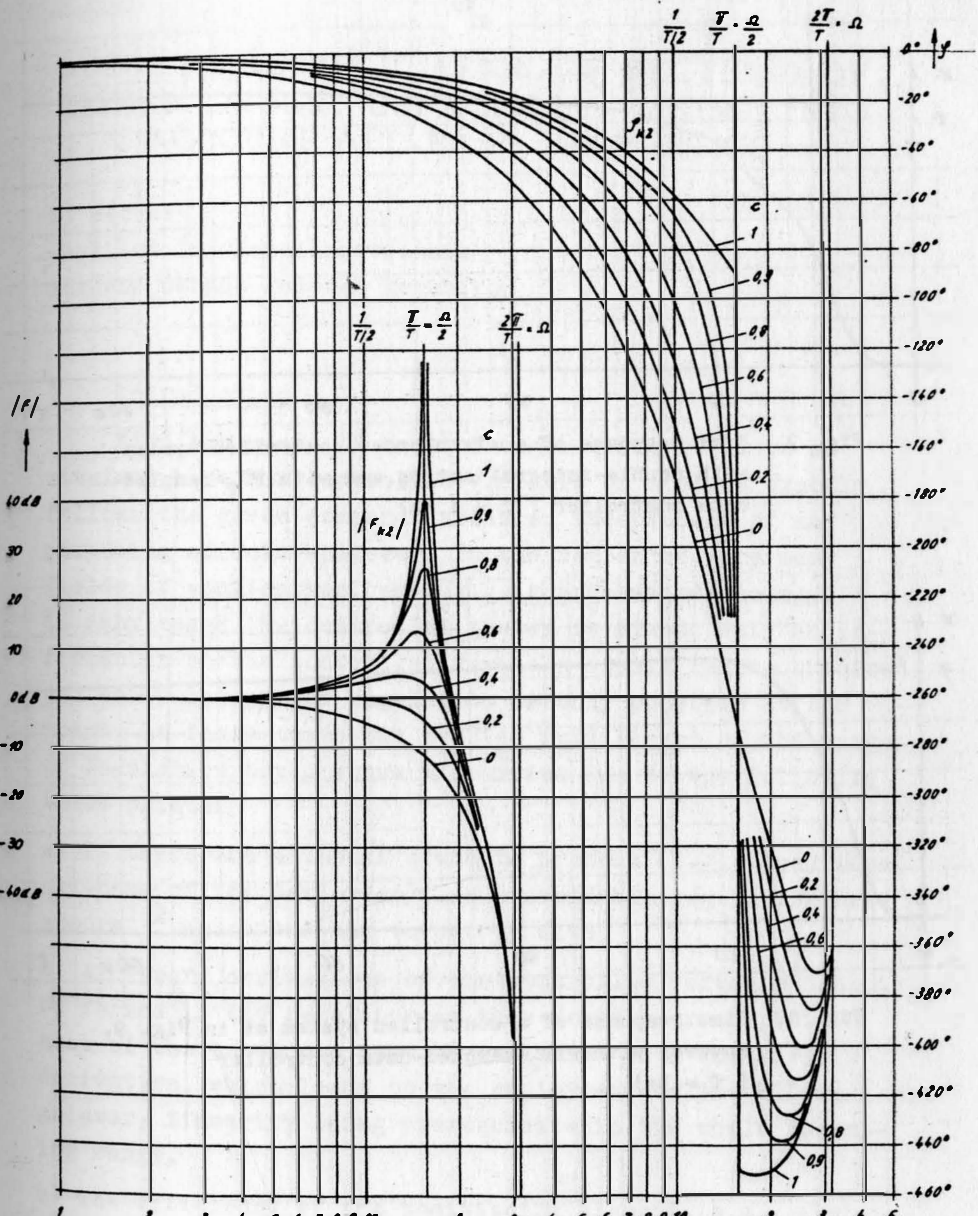

Fig. 8 Frequency responses of the correcting transfer function F_{k2} according to Eq. (34)

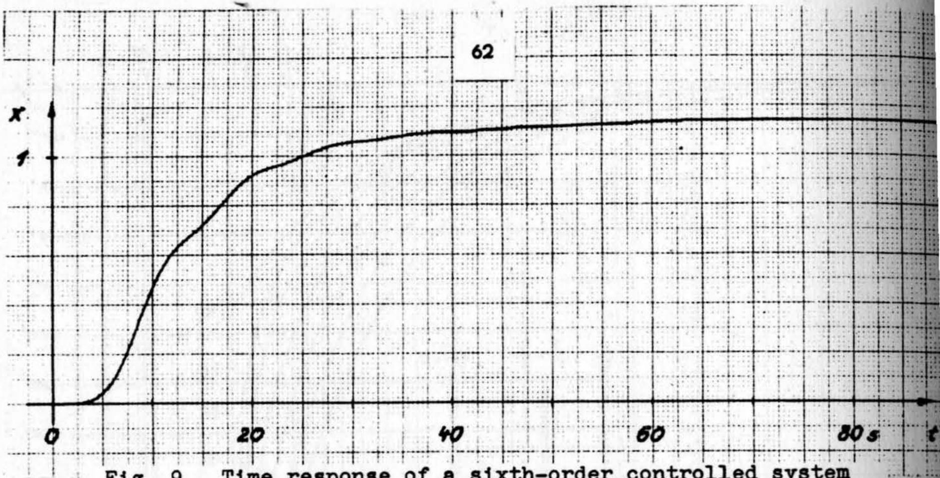

Fig. 9 Time response of a sixth-order controlled system with double-integral action and with PD_2-sampled-data controller (T = 4.5s)

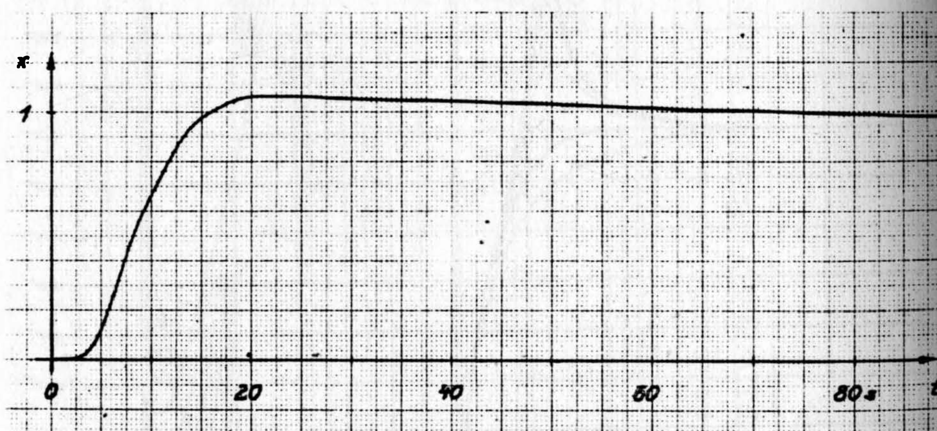

Fig. 10 Time response of a controlled system as in Fig. 9, however with PID_2-sampled-data controller (T = 3s)

SUBOPTIMAL REGULATION OF SECTIONS OF HIGHER ORDER, ESPECIALLY TAKING INTO ACCOUNT ALL-PASS PROPERTIES

W. Becker
Institut für Regelungstechnik
Aachen/ German Federal Republic

1. Introduction

With the means of control engineering it is to be attained that the controlled variable of a plant exactly follows the given command variable, independent of any pertubing effects whatever. In the region of very many fields of application, as e.g., in process technology, in many cases the controlled system is fixed, only an information on the controlled variable itself can be obtained and manipulation for regulation is only possible at one point. In these cases the precise fulfillment of the task of regulation noted above miscarries due to the following three points:

a) If there are all-pass elements present (e.g., dead time, all-pass of the 1st order), an unavoidable regulating area occurs[1,2] which one has to put up with.

b) Arbitrary derivations of the controlled variable cannot be formed in the regulator as they would be required. In most of the cases one must be satisfied with the first derivation, which leads to the employment of the PID-regulator, linearity being prerequisite in the whole operating range.

c) The efficiency of the positioning element, e.g., its positioning speed, is limited. The optimum regulation in these cases, which nowadays is described with the aid of the maximum principle of Pontrjagin and co-workers[3], however again presupposes all derivations of the controlled variable.

In the following, a conception for regulation is developed, which takes all three restrictions stated into account for the case that the command variable changes suddenly.

In order to come to results which can be employed in practice, a controlled system is here assumed, which can be described by (n-2) series connected delay elements of the 1st order, as well as an all-pass element of the 1st order with the frequency response

$$F_a = \frac{1 - pT_o}{1 + pT_o} \tag{1}$$

and a dead-time element. The positioning element should have integral behaviour, which applies for many practical cases, at least approximately[4]. Taking the positioning speed to be restricted, the restriction is assumed to be symmetrical. A restriction of the positioning stroke can be disregarded for the time being. This controlled system including the positioning elements (see Figure 1) possesses the following frequency response ($T_{n-1} = T_o$)

$$F = \frac{\underline{x}}{\underline{y}_R} = V_S C_R \frac{(1-pT_o)e^{-pT_t}}{p(1+pT_1)\,(1+pT_2)\ldots(1+pT_{n-1})} \tag{2}$$

2. Criteria of Optimization

If, in the task set here, one selects the time until the rated value is attained as the criterion of optimization, then one obtains the so-called optimal time or rapidity regulation. But this criterion cannot be applied for a suboptimal regulation, as in these cases the rated value is only exactly attained for t --- ∞. In these cases the time is stated until drifting into a tolerance barrier. This, however, does not appear to be convenient, as then the optimal positioning possibly depends on the value of this barrier, and just as with criteria as the quadratic regulating area, the ITAE criterium etc., the optimal time process no longer appears to be the most favourable transition. As compared to this, the linear regulation area referred to the command jump W is a convenient criterion of optimization with the addition that no overshootings may occur.

$$I = \int_0^\infty \frac{x_W}{W}\,dt \qquad \left(\text{with } \frac{x_W}{W} \geq 0 \text{ für alle } t\right) \qquad (3)$$

Here this criterion leads to the most rapid aperiodic transition and contains the optimal time process as an absolute optimum.

3. Optimal Time Regulation

With the controlled system to (2) as is known one obtains the optimal time process, if the quantity y_R alternately assumes its upper and lower extreme value. The process consists of n-intervals if n is the degree of the denominator polynominal[3,5,6]. That also applies for the here existing dead-time element and the all-pass element of the 1st order[7]. The optimal switching times t_1 to t_n are only determined by the denominator polynominal and must, if all time constants are different, satisfy the following system of equations:

$$\begin{array}{llllll}
 & -2t_1 & +2t_2 & -+\ldots & \pm t_n & = -\dfrac{W}{Y_{Rmax}C_R V_S} \\
1 & -2e^{t_1/T_1} & +2e^{t_2/T_1} & -+\ldots & \pm e^{t_n/T_1} & = 0 \\
\cdot & \cdot & \cdot & \cdot & \cdot & \cdot \\
\cdot & \cdot & \cdot & \cdot & \cdot & \cdot \\
\cdot & \cdot & \cdot & \cdot & \cdot & \cdot \\
1 & -2e^{t_1/T_{n-1}} & +2e^{t_2/T_{n-1}} & -+\ldots & \pm e^{t_n/T_{n-1}} & = 0
\end{array} \qquad (4)$$

That means that besides the time constants of the controlled system, the switching times are only dependent on the expression

$$\frac{W}{Y_{Rmax} C_R V_S} = \tau_w \tag{5}$$

This value τ_w precisely states the time, after which the output quantity y_S of the integrator for the first time attains the final value.

~~As~~ example the course of y_R, y_S and x at an optimal transition is depicted in Figure 2 for a section, which consists of two delay elements.

4. Linear Regulating Area in the Case of Optimal Time and Suboptimal Process

The linear regulating area can simply be determined in the following manner: When passing through a delay unit of the 1st order with the time constant T and the amplification factor 1, the linear regulating area increases by T, in the case of an all-pass element to (1) by $2T_o$ and in the case of a dead-time element by T_t. Consequently, the regulating area is composed of the sum of all time constants, including T_o and T_t, and of the linear regulating area of the input function y_S, shaded in Figure 2, which is described by means of the switching times. At n switching intervals one thus obtains for the optimal regulating area

$$I_o = \underbrace{\sum_{\nu=0}^{n-1} T_\nu + T_t}_{\text{caused by the section}} \underbrace{- \frac{1}{2\tau_w}\left[\sum_{\nu=1}^{n-1} (-1)^\nu \, 2t_\nu^2 + (-1)^n t_n^2\right]}_{\text{caused by the input function}} \tag{6}$$

In principle the course is depicted in Figure 3.

If one forms the limiting value for $\tau_w \rightarrow 0$, i.e., no limitation is effective, then one obtains

$$\lim_{\tau_w \rightarrow 0} I = T_o + T_t \tag{7}$$

This represents the unavoidable regulating area, which is caused by the dynamics of the controlled system and which one must put up with. Here it should also be pointed out that when the zero occurs in the numerator of (2), although the optimal course is concluded at the same time as without this zero, the linear regulation area, however, is increased by T_o.

If one reduces the n switching intervals to a single one, i.e. if one only lets the integrator run up to its final value, in order to then switch off, then all $t_\nu = \tau_w$ and one obtains

$$I_1 = \sum_{\nu=0}^{n-1} T_\nu + T_t + \frac{1}{2}\tau_w \tag{8}$$

This straight line with the gradient 0.5 (see Figure 3) simultaneously represents the asymptote for (6), if τ_w strives towards the infinite.

If one combines all time constants of the denominator polynominal in (2) to a single time constant T, then, if one substitutes the relations for the switching times,

$$I_u = \sum_{\nu=0}^{n-1} T_\nu + T_t + \frac{1}{2}\tau_w - \frac{T^2}{\tau_w}\left[\ln(1+\sqrt{1-e^{-\tau_w/T}})\right]^2 \tag{9}$$

$$\text{with } T = \sum_{\nu=1}^{n-1} T_\nu$$

results. It turns out that the linear regulation area (6), which one obtains for the exact optimal time course, is always greater than the one specified by (9), which thus represents a lower bound. This relation is great advantage for coarse estimates.

For its realization a system with n switching intervals requires n free parameters, i.e., generally (n-1) derivations of the controlled variable. As normally, however, only the first derivation is available that means that only systems with two switching intervals can be built up with tolerable expenditure. On the basis of the system of equations (4) it can be shown that the process precisely takes place with minimal linear regulation area without overshooting, if both these switching intervals are attuned to the greatest time constant of the section. In this case the linear regulation area assumes an expression according to the relation (9), in which T is to be replaced by T_n, the greatest time constant of the system. This relation is plotted in Figure 3 with the designation I_2. The impairment in the case of this suboptimal process as against the strictly optimal one is expressed by the distance of the curve I_2 and I_0 in Figure 3. The difference is the greatest for $\tau_w = 0$ and then just amounts to

$$I = \sum_{\nu=1}^{n-1} T_\nu - T_m \tag{10}$$

For increasing values of τ_w the difference constantly becomes smaller. The deviations of this suboptimal process from the strictly optimal one can always then be disregarded, when the sum of dead time, all-pass time constant and of the greatest section time constant is very large in relation to the remaining time constants. Hereby, the difference is the smaller, the greater W is in relation to $Y_{Rmax}C_RV_S$. In every case the deviation can easily be determined by means of the relations given here. If no digital computer programme is available for the determination of the switching times in the case of sections of higher order, then these can be determined by means of approximations, or one just contents oneself with an estimation of the linear regulation area according to (9).

5. Realization of the Suboptimal Regulation System

The suboptimal regulation system suggested here starts from the fact that the part of the controlled system with the greatest time constant is strictly regulated according to optimal time, the rest of the section is not taken into account and is practically connected in series with the actual regulation circuit. That can be achieved without engagement in the controlled system by connecting a model parallel to the controlled system, which with simple means reproduces the controlled system as well as possible (see Figure 4). Then the difference u between the controlled variable x and the output of the model is approximately zero. In this case the optimal time regulator of 2nd order over the integrator only works together with the first part of the model, a delay element of the 1st order, whose time constant corresponds with the greatest section time constant. Thus y_S carries out the desired adjustment movement with 2 switching intervals. The compensation of the remainder of the section takes place by means of the second part of the model, an element with all-pass character and the frequency response

$$F = \frac{1 - pT_{R2}(V_{R2}-1)}{1 + pT_{R2}} \tag{11}$$

whose transient function is fully drawn out in Figure 5.

In general, for the determination of the coefficients, one proceeds in such a manner that the controlled system without positioning element is approximated by means of two time constants T_{S1}, T_{S2} and delay time T_u. Here attention must be paid to the fact that the approximation is mainly favourable for great values of t. Strong deviations in the initial part of the transient functions do not matter so much, as at that time the control deviation is generally still rather great and thus, at least during the greater part of the transition, no influencing of the switching condition exists. Then $T_{R1} = T_{S1}$ is to be set for the greater of the two equivalent time constants. The rest of the section, shaded in Figure 5, can be approximated by means of the term (11). With the equivalent characteristic values T_{S2} and T_u

$$V_1 = V_S \text{ , } T_{R1} = T_{S1}\text{, } V_2 = e^{T_u/T_{S2}}\text{, } T_{R2} = T_{S2} \qquad (12)$$

then results for all characteristic values of the model.

In the present form the system is not very suitable for practical employment. Under the assumption that compensation is ideal ($u=0$) and only stepped command signals occur, the block wiring diagram Figure 4 can be redrawn into Figure 6. One thus obtains a two-point switch with a twofold delayed feedback, which, however, is partially cascaded in non-linear manner. In this case the non-linear characteristic becomes independent of the characteristic values of the controlled system. For them the following equation applies

$$x_a = x_e - \operatorname{sgn} x_e \ln (1+|x_e|) \qquad (13)$$

Hereby, x_e can only move in the region from -1 to +1. The other regulator characteristic values in Figure 5 result from the characteristic values (12) by the inversion of the block wiring diagram to

$$V_{R1} = \frac{1}{Y_{Rmax}} \text{ , } T_{R1} = T_{S1}$$

$$V_{R2} = \frac{T_{s2}}{T_{S1}} e^{T_u/T_{S2}}\text{, } T_{R2} = T_{S2} \qquad (14)$$

$$V_R = \frac{1}{Y_{Rmax} V_S C_R T_{S1}}$$

As Y_{Rmax} generally is not variable, 4 free parameters remain, in order to adapt the regulator to the controlled system.

The regulator will always be able to enforce the desired behaviour of the controlled variable, if the difference between the output value of the controlled system and that of the model does not influence the switching intervals too much. This practically only then no longer applies, when the ratio of T_{S2}/T_u becomes too small - the peak of the compensation term in the negative direction (see Figure 5) then becomes very big - and when τ_w assumes very small values.

6. <u>Examples</u>

In Figure 7 several command transient functions in a section with the frequency response

$$F_S = \frac{1 - pT_o}{(1+pT_1)\,(1+pT_2)\,(1+pT_3)\,(1+pT_o)} \qquad (15)$$

are depicted. The characteristic values of the regulator were determined in the manner stated above and set on the regulator. In the case of an ideal model of the controlled system, a course should occur for y_S, as it is plotted for $\tau_w/T_1 = 0.3$ as a dotted line in Figure 7. The deviation of the linear regulation area from the one given in Figure 3 by the curve I_2 then expresses itself by the difference of the shaded areas. However, the most important statement of these curves is that the behaviour of the circuit has practically become independent of the amplitude of the input signal.

Naturally the reflections carried out here can be transferred in the same manner to sections without all-passes, which is of particular significance for practical application, as sections with all-pass properties do happen to be relatively rare. In Figure 8 a section with a large time constant T_1 and several time constants smaller by the factor 10 were assumed. The predetermined characteristic values of the regulator supply transitional functions, which deviate from the course in a similar manner as those shown in Figure 7. By means of an alteration of the characteristic values by 20 to 50 per cent, by that one recognizes the small parametric sensitivity of the system, the transitional functions shown here were obtained. For the section of the 1st order the process is strictly in the sense of the optimal time regulation; for the section of the 2nd order the compensation is ideal.

All the examples shown here are representative. Further examples are discussed in[8], where the detailed derivations are also specified.

7. Comparison with Linear Regulators

The regulator shown in Figure 6 has very great similarities with the linear PID regulator, if one counts the integrally operating positioning element as part of the regulator. If one starts from the linear system, then one recognizes that in the regulator developed here actually only the customary feedback of a PID regulator is adapted to the limited positioning speed by the insertion of a non-linear characteristic. On the other hand the linear PID regulator here appears as, limiting case (for $\tau_w \rightarrow 0$) of this non-linear regulator, which could be designated as "optimal time PID regulator". The comparison with the customary linear regulators, for which no limitations whatsoever applied, on a section of the 6th order (T_1=T_3=T_4=T_5=T_6=0.1 T_1) is shown in Figure 9. One perceives that the behaviour of the PID regulator is practically attained for small values of τ_w. (In the central region the PID regulator should not ascend more flatly than the regulator to Figure 6. This is caused by a small parasitic time constant in the regulator.)

8. Behaviour in the Case of Interfering Signals

This regulator was derived under the assumption that only stepped changes of command occur. However, its field of application is not restricted to such cases. Should non-stepped command signals or interfering signals of any type occur, then the behaviour of this regulator is analogous to that of the linear PID regulator. Thus, for instance, if the regulating circuit is optimated for command jumps, then an excess inert behaviour results in the case of stepped disturbances at the input of the section (Figure 10), just as one is also accustomed to in the case of linear regulators. In exactly the same manner as the linear regulators, one can also newly optimate this regulator by adjusting it more sharply.

9. Regulators with a Switching Interval

The expenditure for the regulator to Figure 6 can no longer be justified, especially for very large values of τ_w. The optimal regulation area I_o is then practically identical with the regulating area I_1 in Figure 3, which one can attain by means of a switching interval. For such a process with only one switching interval, the model of the controlled system (see Figure 4) consists of a proportional element with the amplification factor V_S and the element to (11). The two-point switch alone already represents the optimal time regulator of the 1st order. By means of appropriate redrawing of the block wiring diagram, the "optimal time PI regulator" results, which consists of the well-known two-point regulator with delayed feedback and the series connected integral positioning element. By means of these reflections, if the controlled system is approximated by means of T_u and T_S, one attains the following setting values for the delayed feedback.

$$V_r = V_S C_R T_S \, e^{T_u/T_S} , \; T_r = T_S \qquad (16)$$

Of course, for an optimal adjustment these setting values must still be somewhat varied, as their derivation is based on considerations of approximation. However, in every case, just as do the setting values (14), they furnish a process which lies fairly close to the optimum and which is generally somewhat too inert.

10. Summary

The optimal linear regulating area of an optimal time process with n switching intervals is determined. It happens that for many cases a transition, which is only produced by two switching intervals or only by a single one, comes very close to the optimal form. Subsequently, constructions of regulators are specified which approximately produce such a process. These regulators are not more expensive than the linear PI and PID regulators, but they can replace these everywhere, where the control action is impaired by limitations of the positioning speed. As the technical possibilities of these devices are extensively utilized, they can on the other hand lead to deliberately taking such limitations into account to a very much greater extent, which will then result in economically more favourable systems.

Literature

1 Reswick, J.B.: A Dead-time Controller. Automatic and Remote Control (Bericht über den 1. IFAC-Kongreß, Band III), Oldenbourg Verlag, München 1961, S. 329-334

2 P.M.E.M. van der Grinten: Stochastische Prozesse in der Meß- und Regelungstechnik. Oldenbourg-Verlag, München 1965

3 L.S. Pontrjagin, V.G. Boltjanskij, R.V. Gamkrelidze, E.F. Miscenko: Mathematische Theorie optimaler Prozesse. Oldenbourg Verlag, München 1964

4 E. Pavlik: Die Ermittlung optimaler Bedingungen für praktische Regelsysteme mit nicht vernachlässigbaren Stellgeschwindigkeitsbegrenzungen. Regelungstechnik 11 (1963) S. 481-487 und gleichnamige Dissertation, T.H. Hannover 1963

5 A.A. Feldbaum: Rechengeräte in automatischen Systemen. Oldenbourg Verlag, München 1962

6 A. Ja. Lerner: Schnelligkeitsoptimale Regelungen. Oldenbourg Verlag, München 1963

7 A.A. Pavlov: On optimal Processes in Systems whose Transfer Functions contain zeroes. Automation and Remote Control 26 (1965) S. 636-642

8 W. Becker: Entwurf näherungsweise schnelligkeitsoptimaler Regelsysteme. Dissertation T.H. Aachen 1968

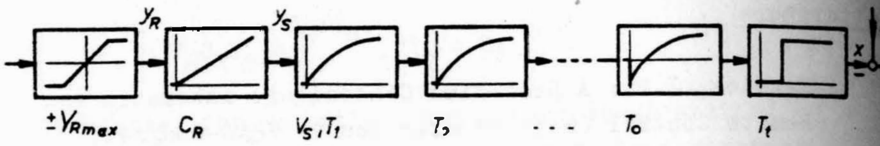

Fig 1

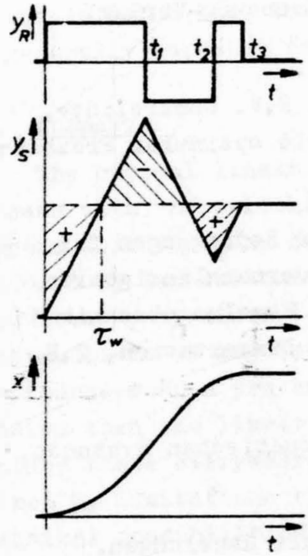

Fig 2

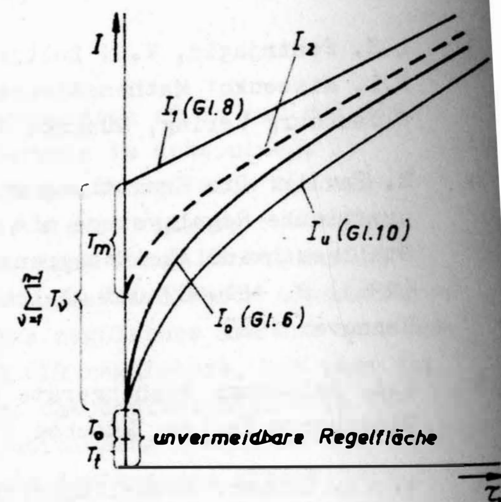

Fig 3

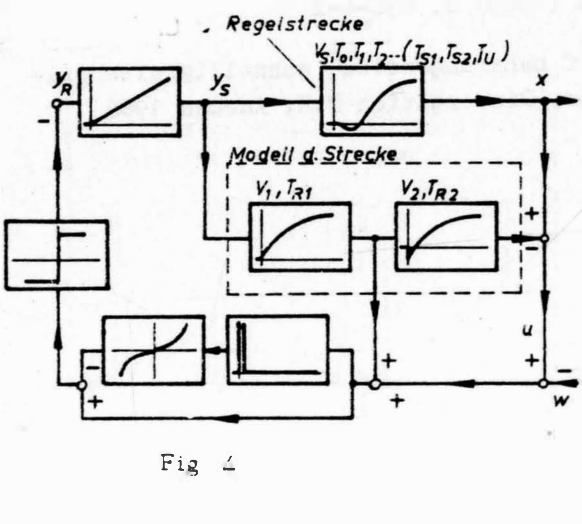

Fig 4

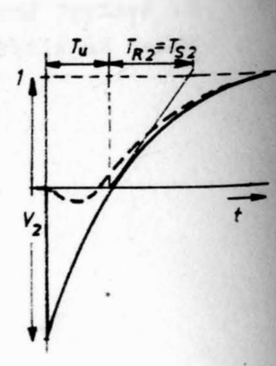

Fig 5

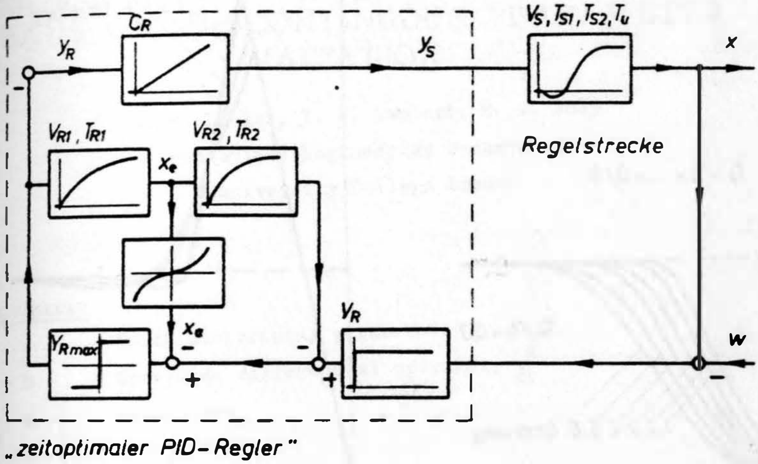
C_R
y_R
y_S
V_S, T_{S1}, T_{S2}, T_u
x
V_{R1}, T_{R1}
V_{R2}, T_{R2}
x_e
Regelstrecke
Y_{Rmax}
x_e
V_R
w
„zeitoptimaler PID-Regler"

Fig 6

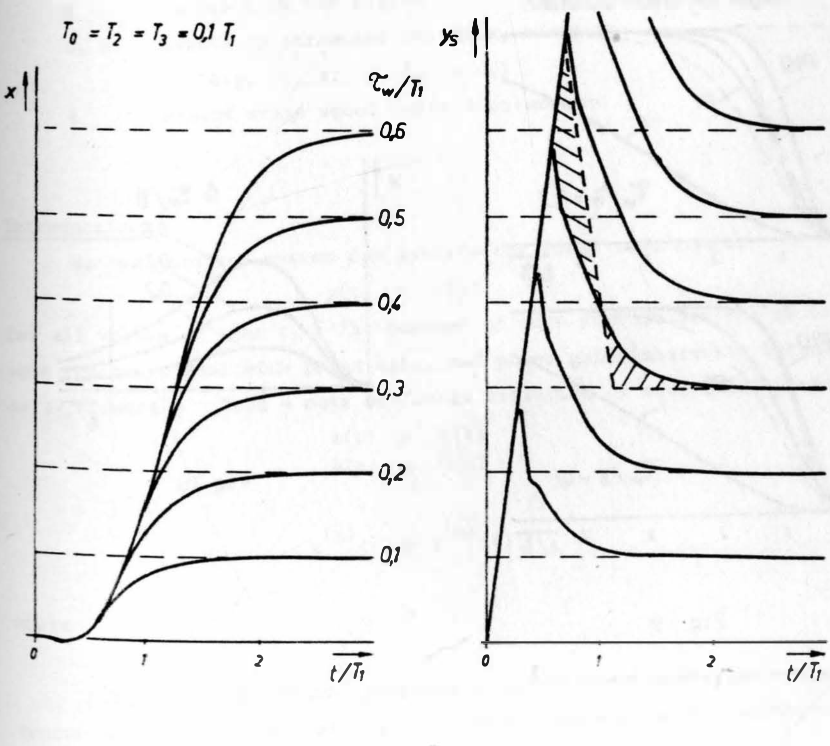
$T_0 = T_2 = T_3 = 0{,}1\ T_1$
x
τ_w/T_1
0,6
0,5
0,4
0,3
0,2
0,1
0
1
2
t/T_1
y_S
0
1
2
t/T_1

Fig 7

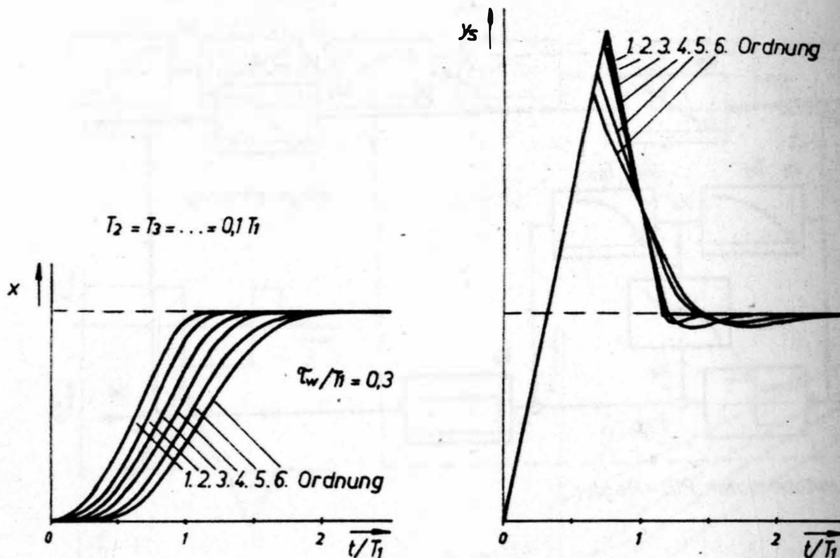

Fig 8

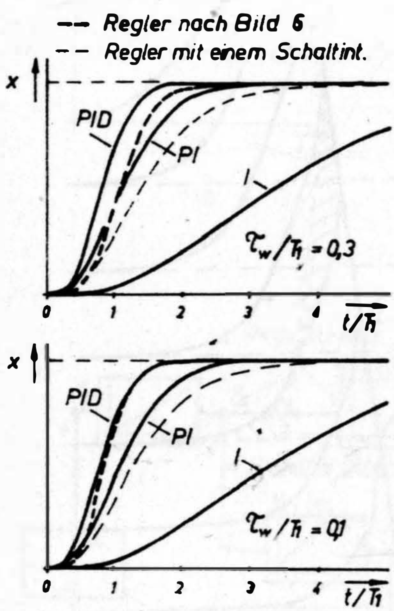

Fig 9

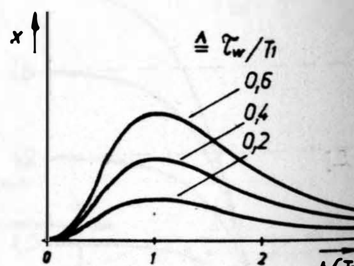

Fig 10

THE REDUCTION OF DYNAMIC ERRORS BY MEANS OF DISCONTINUOUS PARAMETER VARIATION

R. M. Davies, T. H. Lambert, M. J. Joby
Mechanical Engineering Department
University College London

Nomenclature

a	(with subscripts) parameters
D	Heavyside differential operator, $\frac{d}{dt}$
e	error, x-y
k	constant
K	forward gain of summing amplifier
n	order of the derivatives
t	time
V	output voltage from parameter switching circuits
x	input to the system
y	output from the system
α, β	inputs to parameter switching circuits (e.g. y, e; y, $\dot{e}$, etc.)
Φ	second stage spool valve displacement

1. Introduction

No real control system can satisfy the ideal requirement

$$x(t) = y(t) \tag{1}$$

for all values of time t. The purpose of most servomechanisms is to reproduce some control signal with power gain, and power gain inherently introduces time delay effects[1]. Thus a more realistic criterion of near ideal performance is

$$\left.\begin{aligned} x(t) &\approx y(t) \\ \dot{x}(t) &\approx \dot{y}(t) \\ \\ x^{(n)}(t) &\approx y^{(n)}(t) \end{aligned}\right\} \tag{2}$$

where

$$n \geqslant 1 \tag{3}$$

Flügge-Lotz and Wunch[2] proposed a second order nonlinear system which functioned basically by varying the output acceleration discontinuously so as to satisfy the conditions

$$\left.\begin{array}{l} x \approx y \\ \dot{x} \approx \dot{y} \end{array}\right\} \qquad (4)$$

for a range of control signals. The system had an equation of the form

$$(a_2D^2 + a_1D + a_o)\ y = x \qquad (5)$$

with

$$\left.\begin{array}{l} a_o = a_{o1} - a_{o2}\ \mathrm{sgn}\ (y.e) - a_{o3}\ \mathrm{sgn}\ (y\dot{e}) \\ a_1 = a_{11} - a_{12}\ \mathrm{sgn}\ (\dot{y}e) - a_{13}\ \mathrm{sgn}\ (\dot{y}\dot{e}) \end{array}\right\} \qquad (6)$$

The parameter terms of the right hand side of (6) were constants so that the parameters a_o and a_1 could take on a number of discrete values. Analogue studies[3] confirmed that certain combinations of parameters produced a system satisfying (4).

The principle of the system of Flügge-Lotz and Wunch was as follows. The error was maintained small by varying the output acceleration discontinuously so that it was alternately larger or smaller than the input acceleration. When, owing to rapid input changes, this alternating pattern could no longer be sustained, large errors occurred. Fig. 1 indicates the changes occurring in the system of equation (5) following a short segment of the control input. At the points B, C, D, E and F either e or ė change sign, and between these points the system may be regarded as essentially linear. On the sections AB and DF

$$\ddot{y} < \ddot{x} \qquad (7)$$

whilst on BD

$$\ddot{y} > \ddot{x} \qquad (8)$$

The output trends are largely dictated by the variations of the parameters a_o and a_1. On the output sections BC and DE the parameters act so as to prevent excessive overshoot by exercising the maximum corrective action, so that on BC

$$\left.\begin{array}{l} a_o = a_{o1} - a_{o2} - a_{o3} \\ a_1 = a_{11} - a_{12} - a_{13} \end{array}\right\} \qquad (9)$$

which tends to produce an output acceleration

$$\ddot{y} > \ddot{x} \qquad (10)$$

Whereas on DE

$$\begin{array}{l} a_o = a_{o1} + a_{o2} + a_{o3} \\ a_1 = a_{11} + a_{12} + a_{13} \end{array} \qquad (11)$$

so that the output acceleration tends to satisfy the condition

$$\ddot{y} < \ddot{x} \qquad (12)$$

On CD and EF the rate of change of error has changed sign so that the pairs of terms a_{o2} and a_{o3}, a_{12} and a_{13} are opposed in action. The corrective action exercised by the parameters is thus, depending on the relative sizes of parameter terms, either decreased or even reversed. The latter condition is not usually desirable as it can readily cause divergence between input and output. A lessening of the correcting action of the parameters tends to ensure that the succeeding overshoot, when the output crosses the input again, is minimised. The output paths such as BC and DE may be termed 'overshoot' paths, whilst CD and EF are termed 'approach' paths.

The system is equipped to follow input variations so long as

$$|\dot{x}|\ \mathrm{max} < |\dot{y}|\ \mathrm{max} \tag{13}$$

This paper is concerned with the application of discontinuous parameter variation techniques to an inertially loaded electrohydraulic position control system. The advantages and limitations of the technique in a practical situation are examined. Both analogue computer and hydraulic rig studies are an integral part of the experimental programme.

2. System Description

The basic layout of the hydraulic position control used is indicated in Fig. 2. Harmonic response tests were carried out and various parts of the system were excited with constant amplitude signals. The results of these tests indicate that the linear open loop transfer operator of the control system is

$$\frac{y}{e} = \frac{K}{145D(1 + \cdot 0023D)\left(1 + \frac{\cdot 21D}{603} + \frac{D^2}{603^2}\right)\left(1 + \frac{\cdot 52D}{1510} + \frac{D^2}{1510^2}\right)} \tag{14}$$

where K is the forward gain of the summing amplifier.

The factors which comprise the denominator of (14) sensibly arise as follows:

the first is the integrating time constant;

the third is the complex delay associated with the actuator and load including compressibility and leakage effects;

the fourth is the complex delay associated with the torque motor and moving parts of the first stage of the valve;

and the second is the delay associated with the rapid response of the hydraulic second stage of the valve.

It was subsequently found necessary to increase the leakage across the hydraulic ram artificially. The transfer operator then becomes

$$\frac{y}{e} = \frac{K}{\cdot 145D(1 + \cdot 0023D)\left(1 + \frac{\cdot 72D}{565} + \frac{D^2}{565^2}\right)\left(1 + \frac{\cdot 52D}{1510} + \frac{D^2}{1510^2}\right)} \tag{15}$$

These transfer operators were used in the analogue studies which preceded practical tests.

Parameter changing circuits were designed as shown in Fig. 3. The Schmitt trigger and logic circuits provided gating signals for a pair of six-diode gates[4]. When given the input signals $\alpha(t)$ and $\beta(t)$ the circuit output is

$$V_{out} = k\alpha(t) \operatorname{sgn} (\alpha.\beta) \tag{16}$$

The equipment was suitable for use both with the analogue simulation and with the hydraulic rig. Full details of the circuits used are to be found in reference 5.

In this investigation it was found practical to use variable parameter terms dependent upon output, error, and their rates of change only, as in the second order system of reference 2. This limitation was essentially imposed by available transducers, as it can be shown that higher order switched parameter terms can be used to reduce errors in systems of higher than second order[5,6]. The approximate equation of the hydraulic system was thus of the form

$$\left(\frac{1}{KG(D)} + 1\right)y - \{[a_{12}\operatorname{sgn}(\dot{y}e) + a_{13}\operatorname{sgn}(\dot{y}\dot{e})]\dot{y}$$
$$+ [a_{o2}\operatorname{sgn}(ye) + a_{o3}\operatorname{sgn}(y\dot{e})]y\} = x \tag{17}$$

where $KG(D) = \frac{y}{e}$ in equation (14) or (15) as appropriate. The analogue computer flow diagram for the system is shown in Fig.4, and the block diagram of the variable parameter hydraulic system is Fig.5. For the analogue studies, one second computer time was scaled as ten seconds real time.

3. Experimental Procedure

Initial analogue studies were undertaken using the open loop transfer operator of equation (14). The procedure for setting up the system was to set the variable parameters to zero and apply a low frequency harmonic input. The parameter terms were then adjusted sequentially in the order a_{o2}, a_{12}, a_{o3}, a_{13} and so on, until a minimum error was obtained. This process was repeated at a number of other frequencies until a suitable set of parameters was obtained.

It was found that large parameter values, or high forward gain, K, gave rise to an oscillation. The frequency of oscillation was about the same value as the frequency term associated with leakage and compressibility effects on the actual system. Follow up tests carried out on the hydraulic rig confirmed the presence in practice of this condition. Analogue results had indicated that reducing the gain K or the size of the variable parameters, or increasing the damping factor of the term associated with leakage and compressibility effects, suppressed this oscillation. It was decided to use this latter method to suppress oscillations in the hydraulic control as it appeared to be the least restricting of the possible solutions.

All further analogue and practical work carried out was on the increased leakage system, equation (15). Setting up the parameters on the practical system was essentially the same as on the analogue.

4. Results

In the following, the time scaling of the analogue results has been corrected so that direct comparison of analogue and practical results is possible. The parameter sets used in the analogue and rig studies were respectively; for the analogue of the system,

$$\begin{aligned} a_{o2} &= .081 \\ a_{o3} &= .070 \\ a_{12} &= .021 \\ a_{13} &= .015 \\ K &= 3 \end{aligned} \tag{18}$$

and for the hydraulic system,

$$\begin{aligned} a_{o2} &= .19 \\ a_{o3} &= .205 \\ a_{12} &= .031 \\ a_{13} &= .013 \\ K &= 3 \end{aligned} \tag{19}$$

Figs. 6 and 7 show analogue computer harmonic and step response traces.

Figs. 8, 9, 10 and 11 compare the harmonic, step and random responses of the hydraulic system with and without discontinuous parameter variation. The random input was obtained from a signal generator producing band limited noise.

5. <u>Discussion</u>

The discontinuous parameter system, driven harmonically at 1 Hz, shows results which are very similar to its simulation results in Fig. 6. Specifically, the characteristic high frequency oscillations in the error signal have the same form, and the ratios of their amplitudes to the output amplitude is 4.9×10^{-2} peak to peak in both cases. Comparing the discontinuous and the proportional system results of Fig. 8 shows that, even at this frequency, the former has considerable advantages. The phase lag is almost negligible and the flat topping which appears on the proportional trace and attributable to Coulomb friction in the actuator is overcome.

In Fig. 9, similar comparisons can be made for the higher input frequency of 5 Hz. Here the advantages of the discontinuous system, in terms of the faithful following of the command signal, are even more apparent. The phase lag is much smaller and the amplitude ratio is still very nearly unity. As the input frequency was gradually increased, the number of parameter switching occurrences per cycle was reduced, and at 5 Hz there are clearly fewer than at 1 Hz. The trace showing output velocity, $\dot{y}$, shows some saturation, an effect which tends to limit the effectiveness of the performance improvement at higher frequencies. This effect is unidirectional because of unsymmetrical port arrangements in the jack. Delays in switching, which are further discussed below, also contribute to performance deterioration at higher frequencies.

The step responses shown in Fig. 10 show that a faster rise time is achieved by the discontinuous system. This is to be expected since the forward path gains are the same, but in the discontinuous system the presence of amplified parameters in the feedback path increases the loop gain during the rise, resulting in a larger amplitude valve motion. The fourth trace shows the valve motion, Φ, and it is noticeable that after the step there is considerable agitation of the valve because of the continuous switching of parameters. Thus the output, y, shows some deterioration in the presence of a stationary input; and this effect, along with the other characteristics, is evident in the analogue trace for step input, Fig. 7. A modification to avoid this effect is suggested in the next section.

In response to a random input, it is clear that performance of the discontinuous system is superior to that of the proportional system. Errors measured peak to peak are reduced by about $\frac{1}{4}$, and both amplitude and phase results indicate more faithful following of the input without the flat topping which appears in the proportional results. Here it can be seen that the frequency of parameter switching is variable, being higher when the input signal is slowly changing and the accelerations of which the system is capable considerably exceed those demanded. The low frequency switching occurs when the input velocity is near zero, and the agitation is similar to that following a step input. The largest errors occur at points where the output and its velocity are both near zero; resulting in less control because the effects of the parameters are in opposition to one another. This is a result of the particular compromise made in selecting parameter magnitudes. It could be overcome by using other values but other penalties would be incurred.

6. Conclusions

In designing the controller, and obtaining the results reported above, the effects of switching delay imposed constraints on the active components of the controller. These effects were overcome and therefore are not observable in the results above, but can be visualized by reference again to Fig. 1. Clearly large errors will occur if there is delay in switching when the error changes sign - for example at D. Similarly, when the output velocity changes sign, for example at E, a delay will cause the next crossing of y and x to occur at such an angle that unnecessarily large deviations of these variables will follow the crossing. This results from the fact that up to the switching point, E, parameters a_{o2} and a_{o3} are acting together to cause large corrective action; but after this point they are acting in opposition so that the resulting reduced corrective action will effect a less abrupt crossing at zero error.

These delays of course are always present, but in comparison with the response times of the system their magnitudes are important. For this reason, parameter switching by the use of relays incurs delays which are unacceptable for the electrohydraulic system, and a controller using solid state components had to be designed. This controller was initially incorporated in a feedback loop around the electrohydraulic valve but the speed of response of this unit, because of the low inertia of its moving parts, showed the controller to be inadequate. Although there was no deterioration of performance, there was no improvement; and a redesign of the controller would be necessary to meet the higher speed switching requirements.

The overall inertially loaded electrohydraulic system, operated with discontinuous parameters by the controller, shows performance superior to its proportional counterpart with simple feedback for most inputs. Its deterioration when the input is stationary (for example, following a step input) could be eliminated by the introduction of a mode switch for proportional operation at small errors.

Concluding, it can be said that control by the use of discontinuous parameters provides a means of improving the performance of higher order systems as long as frequencies are such that saturation and switching delays do not become excessive. The controller can be considered as an electronic unit which can be inserted in the feedback path, and thus in the low power part of the loop, in order to effect this improvement.

7. References

1. West, J.C., "Analytical Techniques for Non-linear Control Systems" English Universities Press, 1960.
2. Flügge-Lotz, I. and Wunch, W.S., "On a Nonlinear Transfer System" J.App.Phys., 26, No.4, pp 484-488, 1955.
3. Flügge-Lotz, I., Taylor, C., and Lindberg, H., "Investigation of a Nonlinear Control System". N.A.C.A. Report No. 1391, 1958.
4. Millman, J. and Puckett, T.H., "Accurate Linear Bidirectional Diode Gates" Proc.I.R.E., Jan. 1955.
5. Joby, M.J., "Control Systems Subject to Discontinuous Parameter Variation" Ph.D. Thesis, University of London, 1968.
6. Davies, R.M., Lambert, T.H. and Joby, M.J., "The Improved Response of Servomechanisms by Discontinuous Parameter Variation" (to be published)

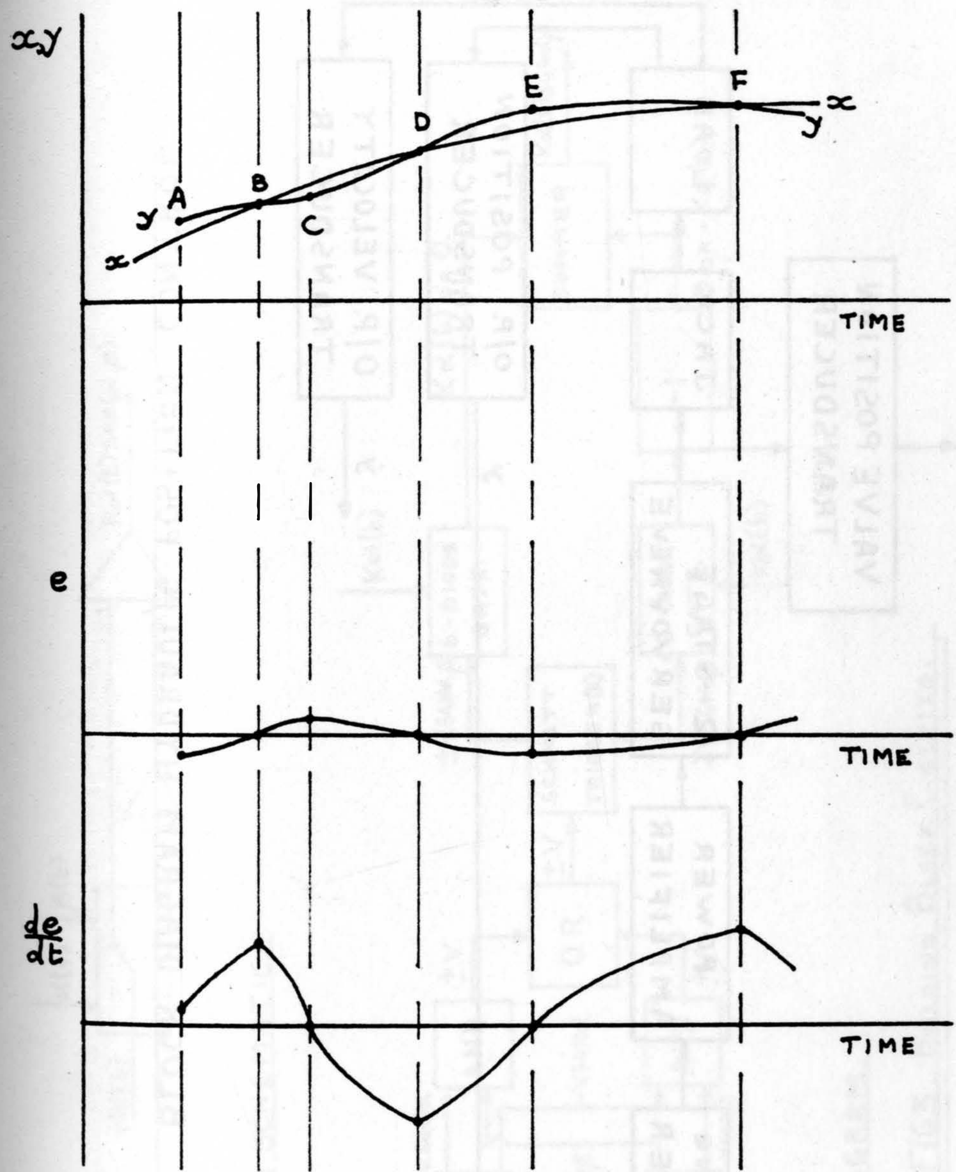

FIG. 1.
TYPICAL SYSTEM VARIABLES.

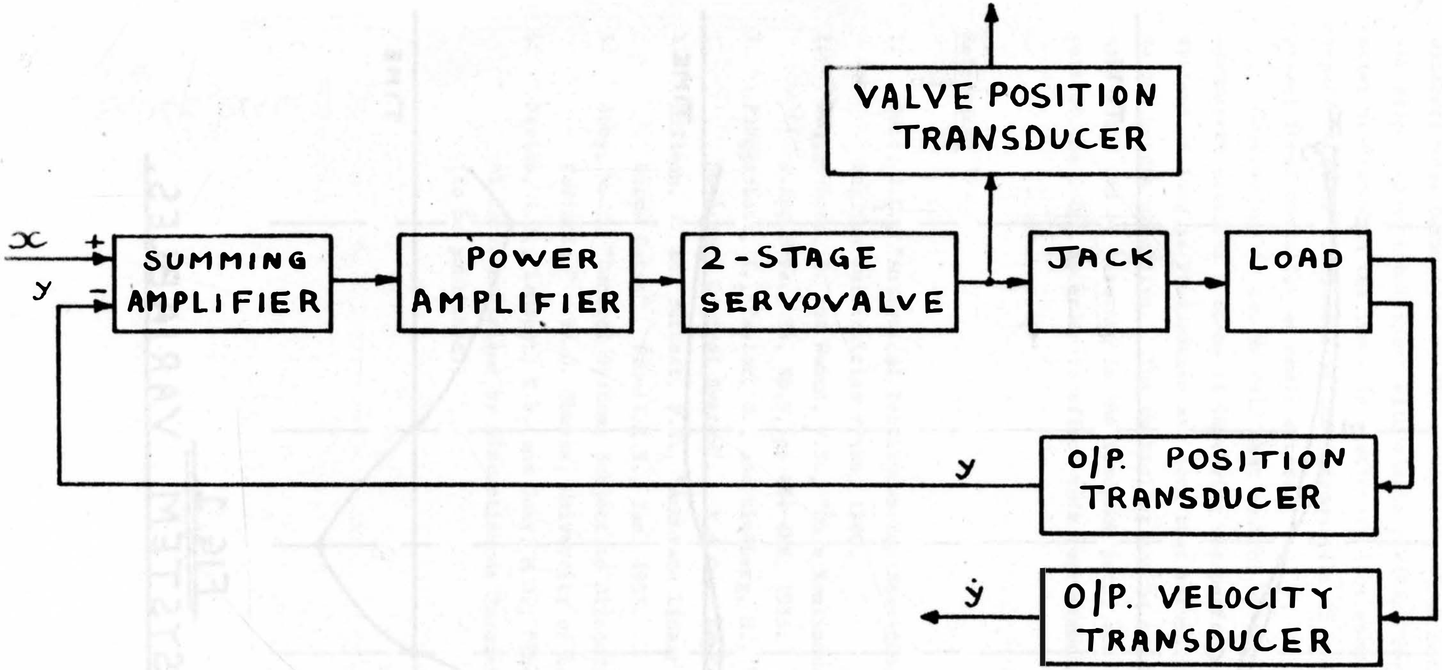

FIG. 2. BLOCK DIAGRAM HYDRAULIC POSITION CONTROL.

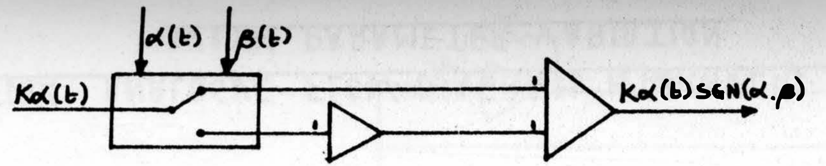

SIMPLIFIED SCHEMATIC.

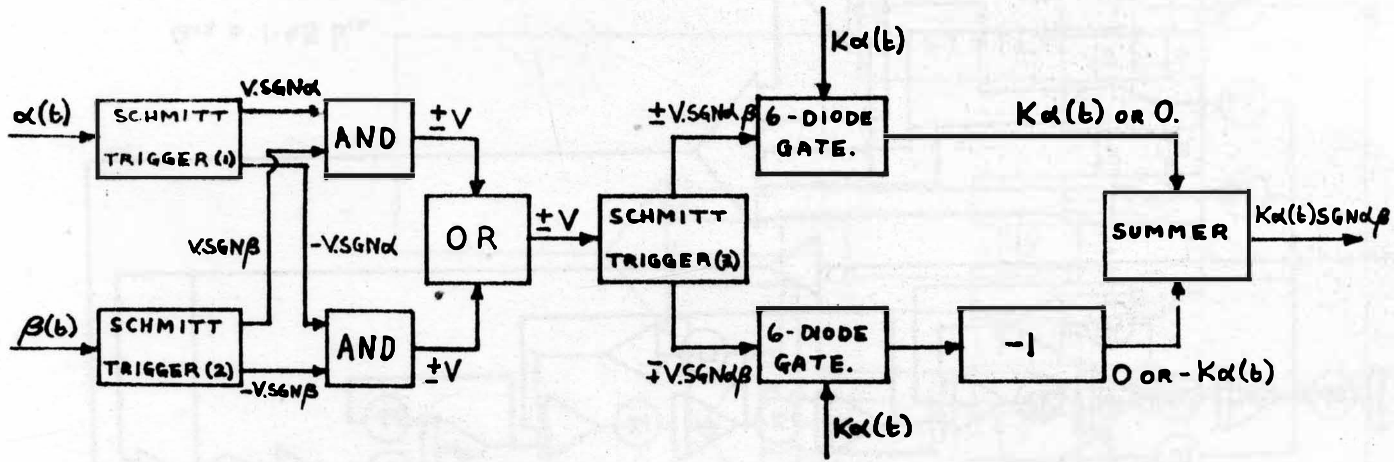

BLOCK DIAGRAM.

FIG3. BUILDING BLOCK CIRCUITS.

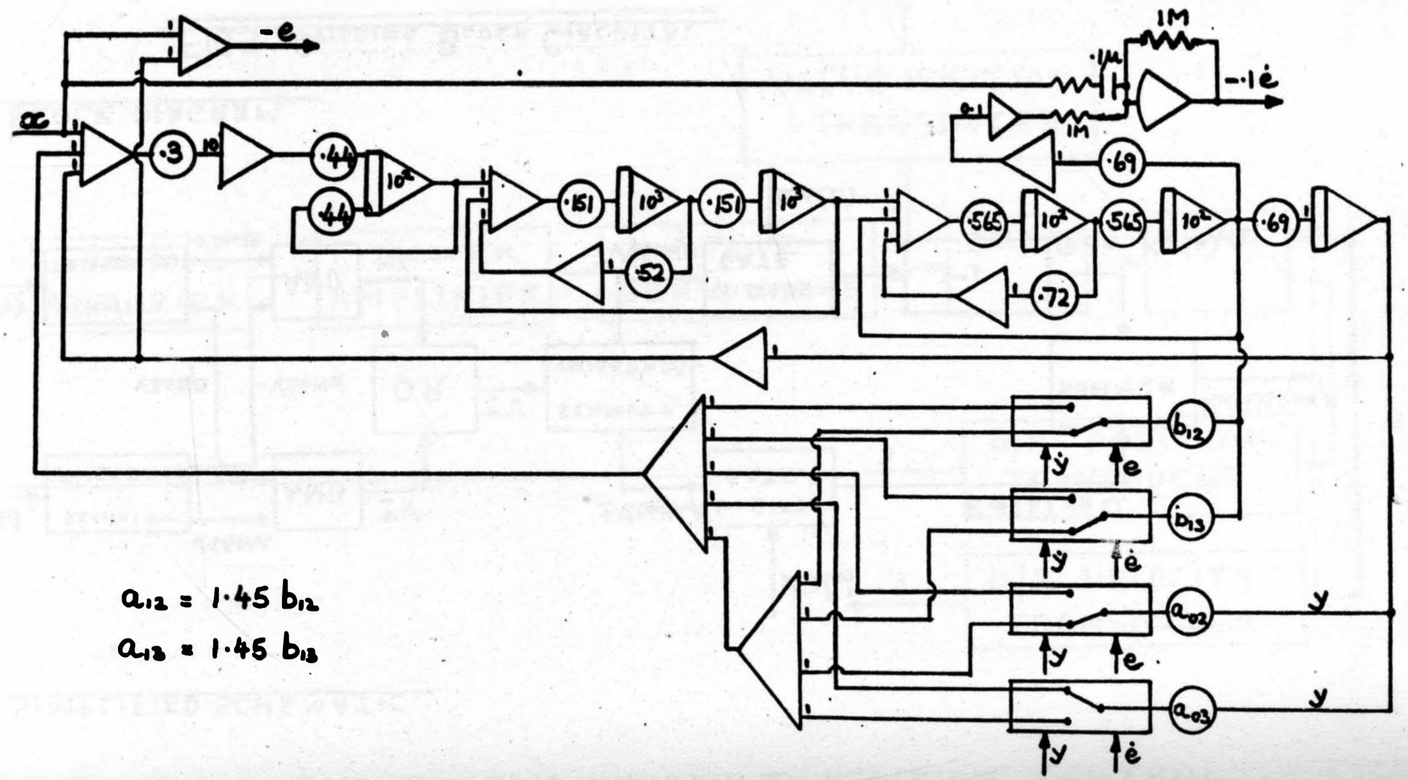

$a_{12} = 1{\cdot}45\, b_{12}$

$a_{13} = 1{\cdot}45\, b_{13}$

FIG.4. ANALOGUE FLOW DIAGRAM HYDRAULIC SYSTEM WITH PARAMETER VARIATION.

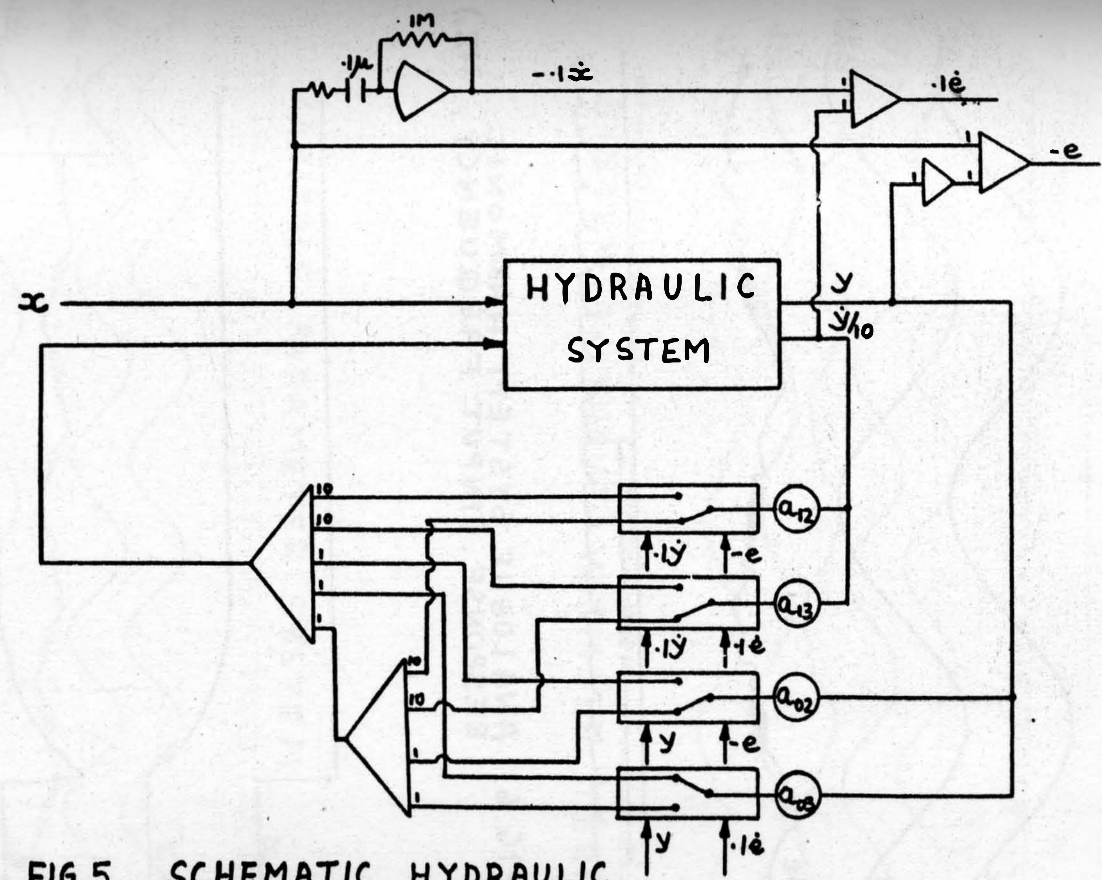

FIG.5. SCHEMATIC HYDRAULIC SYSTEM WITH VARIABLE PARAMETERS

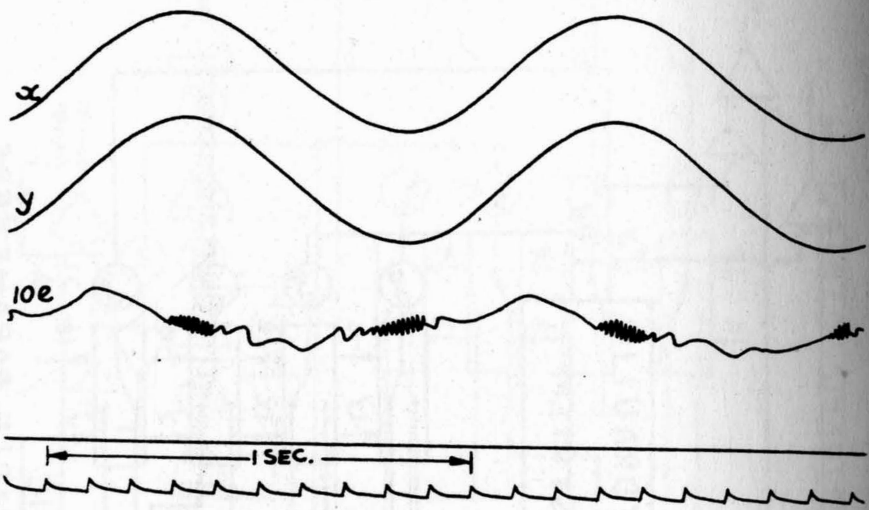

FIG. 6. ANALOGUE SYSTEM HARMONIC RESPONSE. (INPUT FREQUENCY, 1 HZ.)

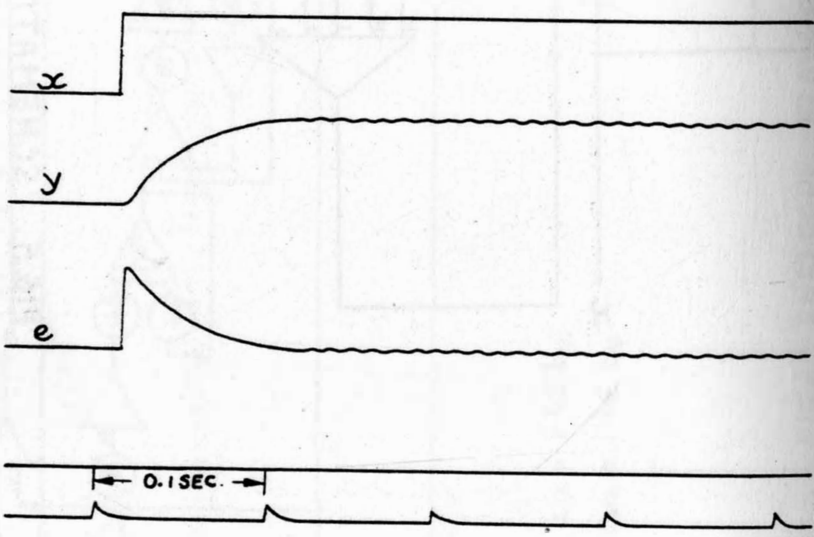

FIG. 7. ANALOGUE SYSTEM, STEP RESPONSE.

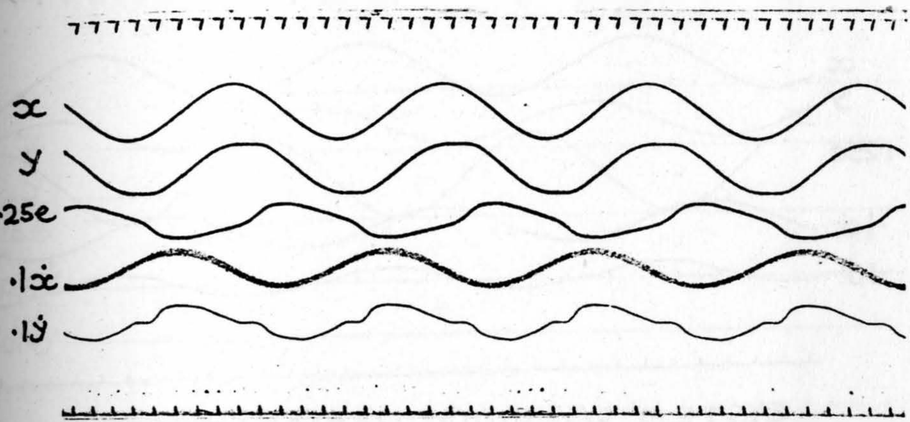

SYSTEM WITHOUT VARIABLE TERMS.

VARIABLE PARAMETER SYSTEM.

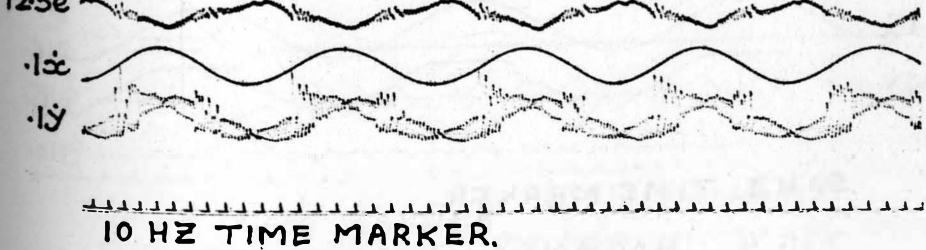

10 HZ TIME MARKER.

FIG. 8. HARMONIC RESPONSE HYDRAULIC SYSTEM. (INPUT FREQUENCY 1HZ.)

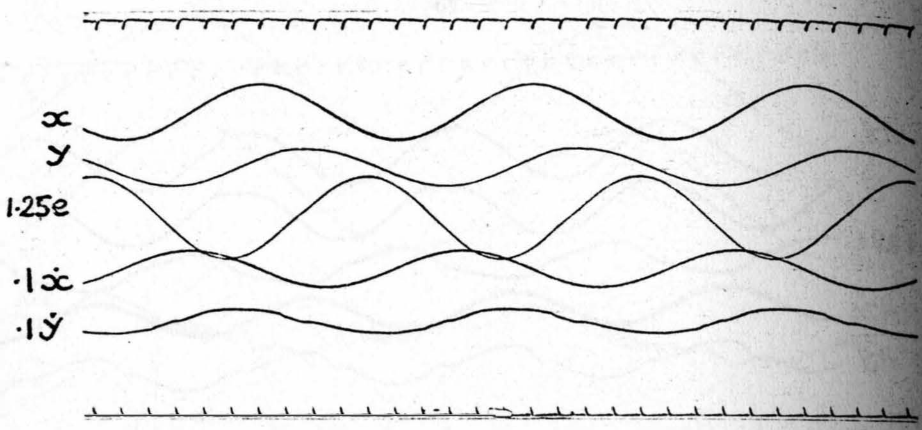

SYSTEM WITHOUT VARIABLE TERMS.

VARIABLE PARAMETER SYSTEM.

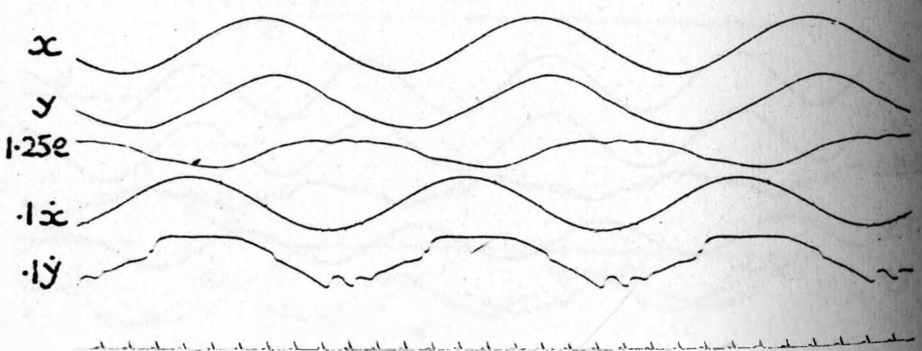

50 HZ. TIME MARKER.

FIG. 9. HARMONIC RESPONSE HYDRAULIC SYSTEM. (INPUT FREQUENCY 5HZ.)

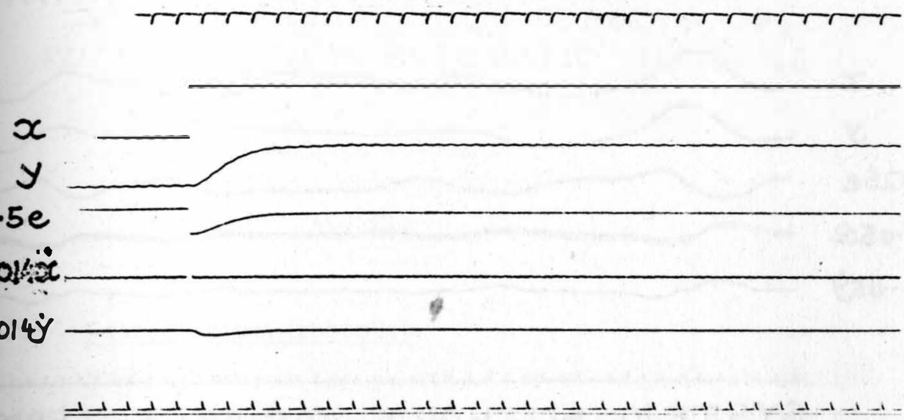

SYSTEM WITHOUT VARIABLE TERMS.

VARIABLE PARAMETER SYSTEM.

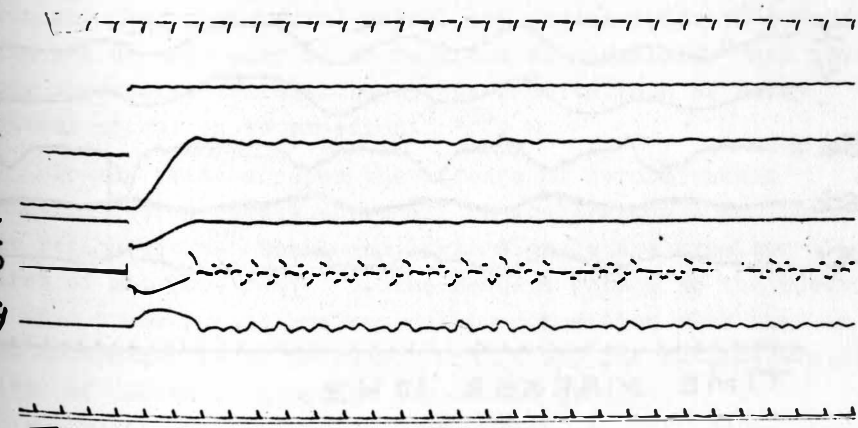

TIME MARKER 50 HZ.

FIG. 10. STEP RESPONSE (1V. STEP)
HYDRAULIC SYSTEM.

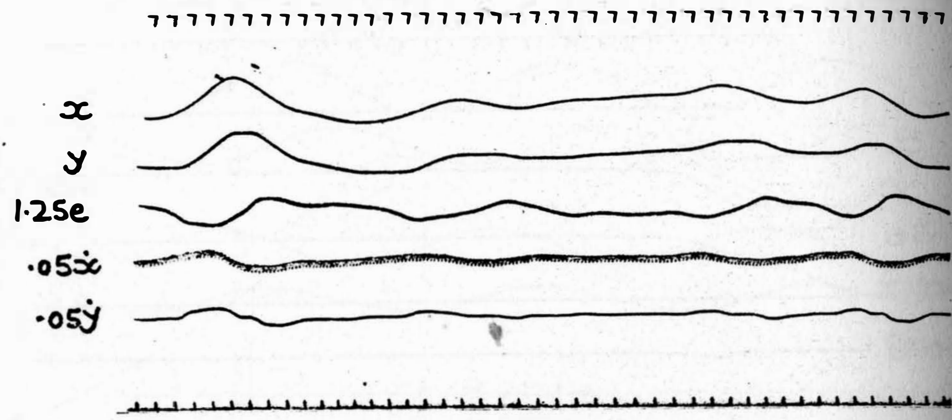

SYSTEM WITHOUT VARIABLE TERMS.

VARIABLE PARAMETER SYSTEM.

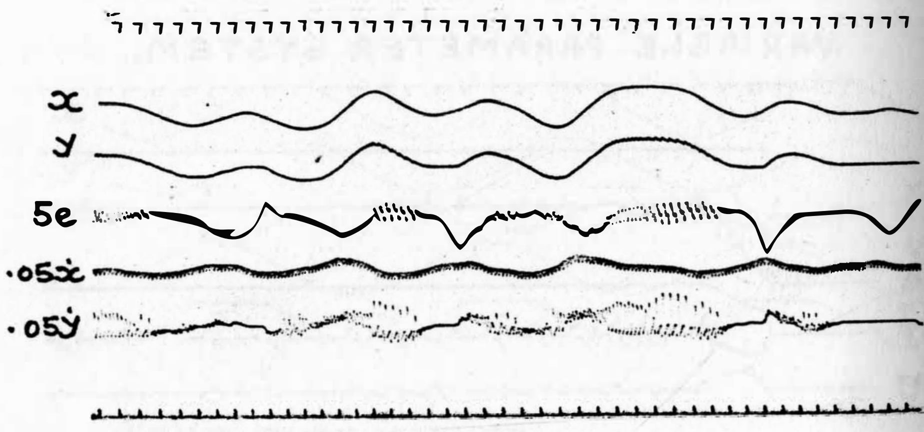

TIME MARKER 10HZ.

FIG. 11. RANDOM RESPONSE
HYDRAULIC SYSTEM.

RECENT RESEARCH ON EFFECTS OF QUANTIZATION IN AUTOMATIC CONTROLS

Alexander Weinmann
Technical College Vienna
Austria

1. Introduction, Abstract

The problem of the quantization of signals in control systems has already frequently been dealt with because of its actuality. Numerous assessments of upper limits for the extent of the effect of quantization by the authors BERTRAM, GRIEG, JOHNSON, MYERS, SLAUGHTER, WIDROW and others have been put forward[4,5,13 to 18,32,40,49,53]; these and other known papers presuppose far-reaching differences of useful signal and qaantization step. In the case of large signals, reference is almost always made to the statistic character of the random noise of quantization (KORN, TABAK, KUO and others [9,12,25,26,42,43]). On the other hand problems are still open, which in the case of small signals mainly result from the fact that useful signal and random noise of quantization are occasionally to be regarded as correlated[8] and therefore appropriate extensions of the examinations of relay systems appear to be expedient[17,36].

In the present paper the effects of deterministic quantization processes above all in small signals and in the region between small and large signals are examined first of all (see JURY [17]). The results relate to the spectra of open transmission systems and in connection with that to the determination of necessary conditions for natural oscillations of closed multi-stage regulation systems.

The results from deterministic considerations are supplemented by results of statistic origin. The suppression of statistic quantization fractions of special distribution density on scanned two-point systems of digital arrangement is also pointed out; for that purpose only a very small amount of filtering or compensation equipment is required.

2. Supplement on the Problem of Deterministic Quantization

In closed functionings, increased occurrence of regulators or other transmission elements is to be found of late, which provide deterministically quantizated output values or others subject to a related signal restriction. Due to this property of signal restrictions, the signal output in closed automatic controls is decisively determined, if the signal amplitude and the respective stage of quantization lie in a comparable order of magnitude.

Several papers have already been written on a similar subject. Thus, for instance, BENNETT[3] points out the spectral dispersion of signals from quantizated elements. In extension of this, the paper in hand offers statements on spectra of signals which result from harmonic input oscillations with only a few steps of quantization, importance being above all attached to the continuous dependence of the spectra on the amplitude of the harmonic input oscillation. In its essential features this applies for any desired gradation of quantization, thus, for instance, also for regulations of optimal distributions of quantization barriers, which were examined by LEWIS, MAX, PEATMAN, HERGLER, TOU and others[6,9,15,28,30,34,35,44].

In order to now show the central problems, leaving away unnecessary difficulties, and to work out the necessity of the calculation process to section 3, only the case of equidistant quantization with regard to the amplitude of a harmonic signal $x(\omega t)$ of the amplitude A is reported on (Figure 1). If the spectrum of $x_2(\omega t)$ is also related to A, then one obtains amplification factors V_2 for the dominant and harmonic waves of the output quantity of quantization. The value V_1 corresponds to the known describing function.

If ε is the constant quantization increment independent of the range then, under the conditions of Figure 1, the following value results for the amplification or exitation factor of the i-th harmonic

$$V_i = \frac{4\varepsilon}{\pi i A} \left[+ \sum_{k=1}^{n} \cos \left(i \arcsin \frac{k\varepsilon}{A}\right) \right] \quad (1)$$

According to Figure 1, i can only accept odd values. The values n or n + 1 represent those integral multiples of , which limit the amplitude value A of the input:

$$n\varepsilon \leq A \leq (n+1)\varepsilon \,. \quad (2)$$

This dependence of the excitation factors V_i on the quotient value ε/A and on the ordinal number i is shown by Figure 2. The fact that the curves display sharp resonance-type sections right into the higher harmonics, for travelling through which only slight changes of the amplitude A of the input are necessary, and the fact that the resonance maxima only decrease slightly with the rising ordinal number i and that the existing controlled systems in many cases exhibit insufficient low-pass characteristics, all underline the necessity of preparing further accurate methods of examination for regulations with the transmission elements mentioned for supplementing estimated methods of the describing function.

Although the example of a possibility of quantization given only represents a special and simple case and numerous other variants also appear to be quite practical for application[13,37], various forms of quantization, however, have the essential common characteristics.

3. Multi-stage Deterministic Relay Systems in Self-contained Regulations

3.1 Multi-stage systems. Natural oscillations

ZYPKIN has specified a widespread process in order to examine relay systems, such as two-point regulators and three-position controllers in their ready state oscillations[55]. The process has undergone various extensions, e.g. by TSCHAUNER[46].

At this point an algorithm is sketched, which formally permits an extension of the above calculation to several optional switching levels, if the quantization or a similar operation takes place in a deterministic manner. To begin with the algorithm is here introduced without statement e.g., of sufficient conditions or of numerical or graphical methods of solution. When occasion arises, this is to be reported on later.

In order to show the nature of the conceptions on which the algorithm is based, simplifications are still selected in the first instance, which are then later discarded.

On the premises of uniform and half-wave symmetrical mode with the fundamental wave angular frequency ω and under the assumption that the amplitude of $x(\omega t)$ of a regulation circuit signal always passes through n switching levels in the ascending and descending branch (Figure 3), per half-wave 2n + 1 switching points result. With the specifications of the switching levels q_k and the still unknown switching phases α_k the time dependence of $x_2(\omega t)$ (Figure 3) can be drawn up, the condition of quantity to the switching points being

$$x(\alpha_K) = x_q(\alpha_K) = q_K \tag{3}$$

In extension of the considerations of ZYPKIN[55], the closing condition of the regulation circuit (at least in the fraction of quantity[11]) can be set up to FOURIER-development of $x_2(\omega t)$.

The formulae for the FOURIER dissociation of the periodic function $f(\omega t)$ with pure alternating portion,

$$b_i = \frac{2}{\pi} \int_0^{\pi} f(\omega t) \sin i\omega t \; d\omega t \tag{4}$$

$$a_i = \frac{2}{\pi} \int_0^{\pi} f(\omega t) \cos i\omega t \; d\omega t, \tag{5}$$

and the equation for the combination to form a FOURIER series, valid for symmetrical half-waves,

$$f(\omega t) = \sum_{i=1,3,5..}^{\infty} \left[b_i \sin i\omega t + a_i \cos i\omega t \right], \tag{6}$$

in this case of application results in

$$\begin{matrix} a_i \\ b_i \end{matrix} = \frac{2}{\pi} \sum_{k=0}^{2n} \int_{\alpha_K}^{\alpha_{K+1}} \varrho_K \begin{matrix} \cos \\ \sin \end{matrix} i\omega t \; d\omega t. \tag{7}$$

The individual harmonics can be superimposed in the remaining regulation part $G(j\omega)$ assumed to be linear. In the thus resulting summation function the switching times α_K and the corresponding switching levels ϱ_K are entered in order to fulfil the closing condition:

$$x_{\varrho}(\alpha_K) = \sum_{i=1,3,5..}^{\infty} \Big\{ (i\omega) \left[b_i \sin i\alpha_K + a_i \cos i\alpha_K \right] + V(i\omega)$$

$$\left[b_i \cos i\alpha_K - a_i \sin i\alpha_K \right] \Big\} = \varrho_K \tag{8}$$

Therein $U(\omega)$ and $V(\omega)$ are the real or imaginary parts of $G(j\omega)$. From the arrangement (8), for k from zero to 2n a total of 2n + 1 equations result for the unknown values ω and α_1 to α_{2n}. The value α_0 can be freely preselected as origin of the time.

The solution of the problem of the arrangement of necessary conditions for steady state oscillations in a multi-state relay system is attributed to the solution of an equation system (8) with transcendental functions, whereby for numerical evaluations the solution values happen to lie within estimable narrow ranges.

Generally, one will only obtain the points of solution after trying out several values of A or n.

It should be pointed out that the method of solution is not restricted to quantized signals with constant course of the signal in the individual periods of time. The method of solution is only bound to a relatively clearly arranged calculation of the FOURIER-coefficients a_i and b_i. This applies as soon as $x_q(\omega t)$ can be built up as $f(wt)$ in such a manner that (4) and (5) can be completely integrated, even in the case of general preselection. Then a system of general equations remains in (8) and not by any means a sequence of integral relations. These prerequisites for integrability are also fulfilled then if, from the point of view a momentary observer of the signal, at the points of time α_k the signal for the subsequent interval α_k to α_{k+1} can be predicted. Among these trains of thoughts the generalizations could be postulated that e.g., the representation of the signal in the interval α_k to α_{k+1} is carried out from q_K and the given equation $\dot{q}_k = \frac{\partial}{\partial \omega t} x(\omega t)\big|$. Hereby the threshold of these processes only seems to be limited by the extent of the numerical calculations or numerical-graphical determinations.

The aforementioned equations of the general arrangement of non-linear feedback systems still allow for manifold extensions, such as expansions of the transcendental functions in the vicinity of the switching point, binding of the switching times α_k to a temporal raster, such as generalized sampling etc.[2,33,56,57], control of the ZYPKIN switching direction conditions, stability of the natural oscillation etc.

The greater the number of switching points per half-wave, the sooner the accurate determination of the wave shape becomes superfluous, as the calculation is already very expensive anyway.

3.2 Two-point regulators with sampling

For small signal changes a two-point response of the regulator or of other transmission elements applies for many cases of application of quantizing systems[1,17].

If the two-point decisions are bound to temporal stroke rasters, as in the case of digital regulators, then the ZYPKIN method for relay systems[55] can be simply extended by the following algorithm. According to the phase position of the sampling times for the own movement of the system, there will be sampling times with and without two-point positioning magnitude changeover switching. At all events sampling here causes decelerated natural oscillations, for the two-point changeover switching can always first be carried out in the sampling time following on a decision.

How the algorithm for the determination of straightforward natural oscillations of sampling two-point regulators without dead zone would have to run off, is specified in the following:

In the hodograph of the continuous two-point system[55] frequency values are plotted, which correspond to integral multiples of the sampling period of the sampling process, namely above all of such values, which lie in the vicinity of the intersection with the straight-line curve, which runs parallel to the abscissa at a distance of $\varkappa_0$, the hysteresis width of the two-point system.

These points would, however, belong to natural oscillations, which require various values $\varkappa_1$ instead of the given $\varkappa_0$ for steady state natural oscillation. For these values $\varkappa_1$ the wave shape of the natural oscillation can be determined in the well-known manner.

It is now to be checked whether, if $\varkappa_0$ should actually be on hand, the vibration amplitude $\varkappa_1$ could be attained by means of sampling to a certain phase and supporting with the corresponding support element. If this should be the case, then a natural oscillation is possible at the examined frequency and phase. There can also be cases, in which one does not find suchlike conformity for any value of $\varkappa_1$, which means that presumably more complicated modes are present.

The consideration can also be carried out in such a manner that for the values $\varkappa_1$ one seeks classes of exterior excitations, which are able to maintain a forced oscillation in the case of the actual hysteresis. These classes are relatively easy to be found as time-dependent area units. They specify within which thresholds the exterior excitation would have to lie, so that an oscillation is also made possible at $\varkappa_0$. It is then possible to judge, whether by means of sampling and support an exterior excitation for the satisfaction of the actual switching condition at $\varkappa_1$ could be built up from the wave shape belonging to $\varkappa_0$, which lies in the aforementioned classes. The discrimination signal of the sampled and unsampled quantity is to be regarded as exterior excitation, although it originates in the internal signal processing of the regulation.

4. Regulation Circuits with Stochastic Multi-stage Quantization Processes

In numerous and frequently cited papers the statistical influences of the quantization processes are dealt with theoretically. The publications range from GAUSS-type and similar distribution of the signals to be quantized[36,38,39,41,53,54,58] over general arrangements of distribution[10,26,31,32,59] up to the binary noise occuring as output of relay components in the case of two-point regulating circuits[14,27,29,39,41,45]. These essays are partially also valid for subsequent representations, in which the practical setting of tasks for the utilization of a special density of probability distribution for the increase worth mentioning of the steady state accuracy of regulations and the reactive effect on the synthesis of digital regulators are also shown in the dynamic respect.

In the following the statistical origin of the quantization error is first of all dealt with in a two-point system which as decisive relay element contains a digital measuring system with pulse code modulation. In it a pulse train of comparatively high frequency f_L (guidance frequency) is controlled by means of a gate circuit (Figure 4); the latter periodically carries out the opening for the duration of the time interval t_M. There is no statistical combination between the phase of the guidance frequency and the time interval t_M. The phase difference, which originated from two uncorrelated signals, influences, as was shown by precise examinations[50], the size of the number originating in the above manner and decisively influences the two-point decision which can be derived from it. The number attained by means of pulse code modulation in the counter can only accept two integral values R and R - 1 in the steady state condition, which are ambient to the exact theoretical numerical value $f_L t_M$ [50], i.e. the rounded off value belonging to $f_L t_M$ is R or R-1.

The probability that R or R - 1 is attained is all the greater, the closer the product $f_L t_M$ lies to the boundary values R or R - 1. If the form of the pulse f_L is disregarded, then the following density of probability distribution results:

$$p(r) = (-f_L t_M + R)\,\delta(r-R+1) + (f_L t_M - R+1)\,\delta(r-R). \qquad (9)$$

In this r is the statistical variable for the counted in number and $\delta(r)$ is the standard Dirac needle function at the point r = 0.

The probability of attaining the adjacent integral (quantized) value R or R - 1, is thus linearly dependent on the exact value $f_L t_M$ (Figure 5).

The two-point decision and the on or off switching command are derived from R or R - 1 in the counter. Because of the linear connection between the on switching command probability and the exact measured value (Figure 5) or because of the equality of the linear expectation value and the exact measured value, the exact value can very well be concluded from the partition function, just as soon as it is possible to calculate by means of a few quantized measured values. The fact that the partition function exhibits characteristic maximum values in dependence on the signal variables also makes it possible, by means of searching methods, to draw conclusions from the quantized measured value to the exact value to be measured.

These two trains of thoughts can advantageously be made use of for control engineering. The proportionality of frequency of the on switching commands and of the value $f_L t_M$ or of a t_M input deviation leads to a control deviation remaining finite. This can be almost nullified by a positive feedback arrangement with low-gain amplification, as it is known in principle for deterministic systems (Figure 6). The searching process in conformity with Figure 7 also brings about very good results.

The positive feedback arrangement is marked by very small requirements[51]. Only a linear element with first order delay is necessary. The linearity confirms the theoretical assumption on the probability distribution function and furthermore also proves the validity of the considerations of being able to go over to dynamic conditions in the steady state condition, e.g., in consequence of working movement of the two-point regulator.

The positive feedback or the searching process in the form of a further regulation loop considerably improve the steady state accuracy, namely to the same extent, in which their own accuracy lies. The overall accuracy of the cascade results from the product of the accuracy values of the partial systems basic regulation and positive feedback or searching process.

The measuring results on digital computers of the non-conventional design just described cited in conjunction with this and the measured values from digital computers of the conventional form cited for comparison, show the essential improvements as regards steady state accuracy, which can be attained at the same counting frequency (bandwidth) and frequency of measurement (repetition frequency).

Hereby, it is even possible at the same bandwidth of the counting elements to reduce the measuring accuracy of each individual measurement (by shortening the counter), in order to increase the frequency of measurement[52], because, after all, the accuracy can be reconstructed by means of the measures mentioned. This measure is similar to the theoretical arrangements for solution of KATZENELSON[19], VIDAL, KARPLUS[48], VELTMAN[47], KNOWLES, EDWARDS[20 to 24] and MONROE[31].

Consequently, the systems described decisively contribute to the improvement of the compromise solutions from rapidity and accuracy of regulations.

The considerations mentioned are not only restricted to two-point systems, but allow for an equivalent extension to multi-stage switching systems; proportionally operating digital computers are to be regarded as such. By means of the positive feedback or searching processes the proportional behaviour caused by the quantization instructions can be increased up to an integral behaviour.

The examinations of two-point systems were emphasized for the simple reason that, among comparable digital systems, these possess the highest amplification and that in the steady state condition even multi-point systems almost always exhibit two-point behaviour.

In further Figures the quantitative effects of the positive feedback on a digital two-point regulator are contrasted with a regulator of the conventional structure:

In Figure 8 the relative accuracy G of a coarse-staged digital regulation without an additional measure is compared with a positive feedback loop. Hereby the curves, which are distinguished by the type of line, apply for different repetition frequencies. Even if the influence of the latter is left out of consideration, the improvement of accuracy by 30 to 40 dB is very striking. Hereby, the higher expenditure for instrument technology for the positive feedback amount to less than 10 per cent.

In the mean switching rate of the regulator output signal, only small deviations with a maximum of ± 30 per cent result when employing the positive feedback.

Figure 9 gives information for the measured discrete statistical distribution density of the regulator output signal for the same form of application.

Hereby, the abscissa determines the integral multiples of the period of the measuring or repetition frequency, the ordinate shows the measured distribution density. The curves are valid for the intervals of the on and off state, as well as for the period of the switching movement.

Further practical experiments on various controlled systems, e.g., on drive speed controls have also furnished proof that by means of positive feedbacks of the form described not only the diminuition of the effects of known-distributed quantization errors is possible, but that statistical quantities with only estimable distribution can also be compensated, as, for instance, the periodical and statistical errors in the employment of speed recorders.

The task aimed at by the employment of positive feedback or searching process could also be approached by means of integrators, which are connected at the output of the two-point measuring systems. As compared with systems with positive feedback, however, the systems with integrators would operate more unfavourably as regards error balance, stability, and starting. This has been confirmed by measurements on actual systems.

5. Summary

The strong resonance-like dependence of the spectral excitation factors on the signal amplitude if the signals are present only quantized with a few stages, shows the requirement for working out a draft of a complete representation for multi-point systems from the common process of the describing function and the well-known ZYPKIN process for two-point systems.

Taking specific distribution densities and their dependence on signals as a basis, extensions worth mentioning, but nevertheless inexpensive, can also be specified for stochastic multi-point systems which have numerous practical advantages.

Acknowledgements

We would thankfully like to point out that the laboratory structures and examinations described were supported by the Federal Ministry for Transport and State Enterprises (Section IV) of the Republic of Austria. Thanks are also be expressed to Herr P. Würleitner for numerous series of measurements.

L I T E R A T U R E

1 ASELTINE,J.A.: Non-linear sampled-data system analysis by the incremental phase-plane method. Proceedings of the 1. IFAC-Congress (Moskau 1960), Band 1, S. 295-304. London, München: Verlag Butterworths and R. Oldenbourg 1961.

2 ASTARDJIAN,G.B., PETROV,P.A. and HRISTOV,H.R.: One a principle of sampled-data control systems with pulse-width modulation and variable signal-dependent sampling. 3. IFAC-Kongreß (London, Juni 1966) Session 34. Paper 34.A.

3 BENETT,W.R.: Spectra of quantized signals. Bell System Technical Journal 27 (1948), S. 446-472.

4 BERTRAM,J.E.: The effect of quantization in sampled-feedback systems. Trans. AIEE 77 (1958), Part II, S. 177-182.

5 BIONDI,E., DEBENEDETTI,A. and ROTOLONI,P.: Error determination in quantized sampled-data systems. 3. IFAC-Kongreß (London, Juni 1966) Session 34, Paper 34.D.

6 BLUESTEIN,L.I.: Asymptotically optimum quantizers and optimum analog to digital converters for continuous signals. IEEE Trans. IT-10 (July 1964), H. 3, S.242-246.

7 BLUESTEIN,L.I. and SCHWARZ,R.J.: Optimum zero memory filters. IRE-Trans. IT-8 (Oct. 1962). H.6, S.337-342.

8 CHARKEWITSCH,A.A.: Signale und Störungen. München und Wien: R. Oldenbourg-Verlag 1968.

9 CLAVIER,A.G., PANTER,P.F. and GRIEG,D.D.: PCM-distortion analysis. Electrical Engineering 66 (Nov. 1947), S. 1110-1122.

10 DRENICK,R.F.: Die Optimierung linearer Regelsysteme. München-Wien: R. Oldenbourg-Verlag, 1967.

11 FASOL,K.H. and SPRINGER,H.: Ein Beitrag zur Vereinfachung der Analyse von Relais-Regelungssystemen. Regelungstechnik 16 (1968), H.3, S. 97 - 104.

12 FELDMAN,C.B. and BENETT,W.R.: Band width and transmission performance. Bell Syst. techn. J. 28 (1949), S.490-595.

13 GRIEG,D.D.: Pulse-count modulation. Electrical Communication 24 (Sept. 1947), S. 287-296.

14 HENNE,W.: Ein Generator für reproduzierbares Präzisionsrauschen. ATM-Blatt Z 423-6 und Z 423-7 (Feb. bzw. März 1968).

15 HÖLZLER,E. and HOLZWARTH,H.: Theorie und Technik der Pulsmodulation. Berlin-Göttingen-Heidelberg: Springer-Verlag 1957.

16 JOHNSON,G.W.: Upper bound on dynamic quantization error in digital control systems via the direct of Ljapunov. IEEE Trans. AC-10 (1965), S. 439-448.

17 JURY,E.I.: Recent advances in the field of sampled-data and digital control systems. Proceedings of the first Internat. Congress of the IFAC (Moskau 1960), Band 1, S. 262-269. London und München: Verlag Butterworths and R. Oldenbourg 1961.

18 KADEN,H.: Impulse und Schaltvorgänge in der Nachrichtentechnik. München: Oldenbourg-Verlag 1957.

19 KATZENELSON,J.: On errors introduced by combined sampling and quantization. IRE-Transactions AC-7 (1962), H. 3, S. 58-68.

20 KNOWLES,J.B. and EDWARDS,R.: Effect of a finite-word-length computer in a sampled-data feedback system. Proc. IEE 112 (1965), H. 6, S. 1197-1207.

21 KNOWLES,J.B. and EDWARDS,R.: Aspects of subrate digital control systems. Proc. IEE 113 (Nov. 1966), H. 11, S. 1893-1901.

22 KNOWLES,J.B. and EDWARDS,R.: Finite word-length effects in multirate direct digital control systems. Proc. IEE 112 (1965), H. 12, S. 2376-2384.

23 KNOWLES,J.B. and EDWARDS,R.: Computational error effects in a direct digital control system. Automatica 4 (1966), S. 7-29.

24 KNOWLES,J.B. and EDWARDS,R.: Ripple performance and choice of sampling frequency for a direct digital control system. Proc. IEE 113 (Nov. 1966), H. 11, S. 1885-1892.

25 KORN,G.A.: Hybrid-computer techniques for measuring statistics from quantized data. Simulation 4 (April, 1965) S. 229-239.

26 KORN,G.A.: Random-process simulation and measurements. New York-Toronto-London-Sydney: Mc Graw Hill 1966.

27 KREPLER,K. and WERNER,G.W.: Korrelatoren mit Amplitudenquantisierung. Messen, Steuern, Regeln 7 (1964), H. 4, S. 172-175.

28 LEWIS,J.B. and TOU,J.T.: Optimum sampled-data systems with quantized control signals. Trans AIEE 82 (July, 1963), Part II, S. 229-233.

29 MACFARLANE,G.G.: On the energy-spectrum of an almost periodic succession of pulses. Proc. IRE 37 (1949), H. 10, S. 1139-1143.

30 MAX,J.: Quantizing for minimum distortion. IRE-Trans. IT-6 (März 1960), S. 7-12.

31 MONROE,A.J.: Digital processes for sampled data systems. New York-London: John Wiley 1962.

32 MYERS,G.H.: Quantization of a signal plus random noise. IRE-Trans. on Instrumentation (June 1956), S. 181-186.

33 OPPELT,W.: Über die Anwendung der Beschreibungsfunktion zur Prüfung der Stabilität von Abtastregelungen. Regelungstechnik 8 (1960), H. 1, S. 15-18.

34 PANTER,P.F. and DITE,W.: Quantization distortion in pulsecount modulation with nonuniform spacing of levels. Proc. IRE 39 (1951), S. 44-48.

35 PEATMAN,J.B. and MERGLER,H.W.: Direct digital control with truncated logarithmic quantization. 3. IFAC-Kongreß (London, Juni 1966), Session 34, Paper 34.B.

36 PERVOZVANSKII,A.A.: Random processes in nonlinear control systems. New York-London; Academic Press 1965.

37 SANCHEZ,M. and POPERT,F.: Über die Berechnung der Spektren modulierter Impulsfolgen. Archiv f. elektr. Übertragung 9 (1955), S. 441-452.

38 SCHLITT,H.: Systemtheorie für regellose Vorgänge. Berlin-Göttingen-Heidelberg: Springer-Verlag. 1960

39 SCHLITT, H.: Stochastische Vorgänge in linearen und nichtlinearen Regelkreisen. Braunschweig: Vieweg-Verlag, 1968.

40 SLAUGHTER,J.B.: Quantization errors in digital control systems. IEEE Transactions on Automatic Control AC-9, (Jan. 1964), S. 70-74.

41 SOLODOWNIKOW,W.W.: Einführung in die statistische Dynamik linearer Regelungssysteme. München-Wien: R. Oldenbourg-Verlag und Berlin: VEB Verlag Technik, 1963.

42 TABAK,D. and KUO,B.C.: Determination of the output statistics of a sampled-data system with a nonlinearity. IEEE Int. Con. Rec. 14 (1966), Part 6, S. 173-178.

43 TOU,J.T.: Digital and sampled-data control systems. New York-Toronto-London: Mc Graw-Hill. 1959.

44 TOU,J.T.: Optimum design of digital control systems New York-London: Academic Press. 1963.

45 TRUXAL,J.G.: Entwurf automatischer Regelsysteme. Wien und München: R. Oldenbourg Verlag. 1960.

46 TSCHAUNER,J.: Zur Berechnung der Frequenzcharacteristiken von Relaissystemen. Regelungstechnik 9 (1961), H. 5, S. 200-203.

47 VELTMAN,B.P.Th.: Quantisierung, Abtastfrequenz und statist. Streuung bei Korrelationsmessungen. Regelungstechnik 14 (1966), H. 4, S. 151-158.

48 VIDAL,J. and KARPLUS,W.J.: Characterization and compensation of quantization errors in hybrid computer systems. IEEE Internat. Convention Record 13 (1965), Part 3, S. 236-241.

49 WEBER,H.: Grundlegende Eigenschaften der Pulscodemodulation. Bull. SEV 57 (1966), H. 2, S. 58-63.

50 WEINMANN,A.: Wahrscheinlichkeitsverteilung von Quantisierungsfehlern und im Stationärzustand wirksame Kompoundierung bei Proportional- und Differentialmessungen durch Zählvorgänge in unstetigen und stetigähnlichen Regelungen. Zeitschrift Mathematik-Technik-Wirtschaft (MTW) 11 (1964), H. 4, S. 166-170.

51 WEINMANN,A.: Regler mit digitaler Messung der Regelgröße. Österreichisches Patent Nr. 242.246 (Anmeldung v.3.4.1962).

52 WEINMANN,A.: Digitale Regelung. Grundlagen, Bauteile, Anwendungen. Schriftenreihe des Arbeitsausschusses für Automatisierung im österreichischen Produktivitätszentrum. 1966. Wien: Verlag des Österr. Produktivitätszentrums, A-1014 Wien, Renngasse 5.

53 WIDROW,B.: A study of rough amplitude quantization by means of Nyquist sampling theory. IRE-Trans CT-3 (Dez. 1956), H. 4, S. 266-276.

54 WIDROW,B.: Statistical analysis of amplitude-quantized sampled-data systems. AIEE-Transactions 79 (1960), erschienen Jan. 1961, Part II, S. 555-568.

55 ZYPKIN,J.S.: Theorie der Relaissysteme der automatischen Regelung. Berlin, München: Verlag Technik, Verlag Oldenbourg. 1958.

56 ZYPKIN,J.S.: Estimating of intervall quantization effect on processes in digital automatic control systems. Avtomatica e telemechanika 21 (1960), S. 281-285.

57 ZYPKIN,J.S.: Theorie der linearen Impulssysteme. München-Wien: R. Oldenbourg Verlag. 1967.

58 ZYPKIN,J.S.: Elements of theory of numerical automatic systems. Proceedings of the 1. IFAC-Congress (Moskau 1960), Band 1, S. 286-294. London-München: Verlag Butterworths und R. Oldenbourg, 1961.

59 VAN LOON,D.: Properties of quantized statistical signals. Research Rept., Department of Technical Physics. Techn. University Delft, Netherlands, Oct. 1963.

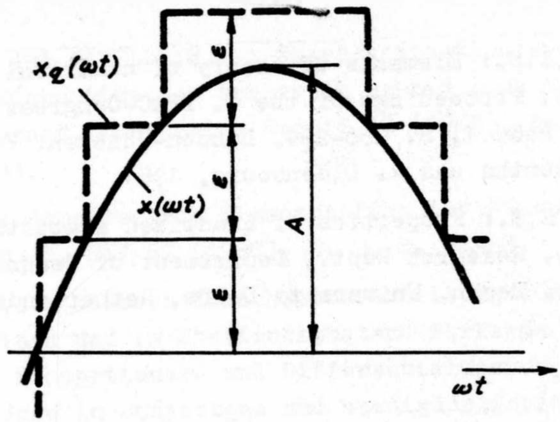

Figure 1. Equidistant quantization of a harmonic signal

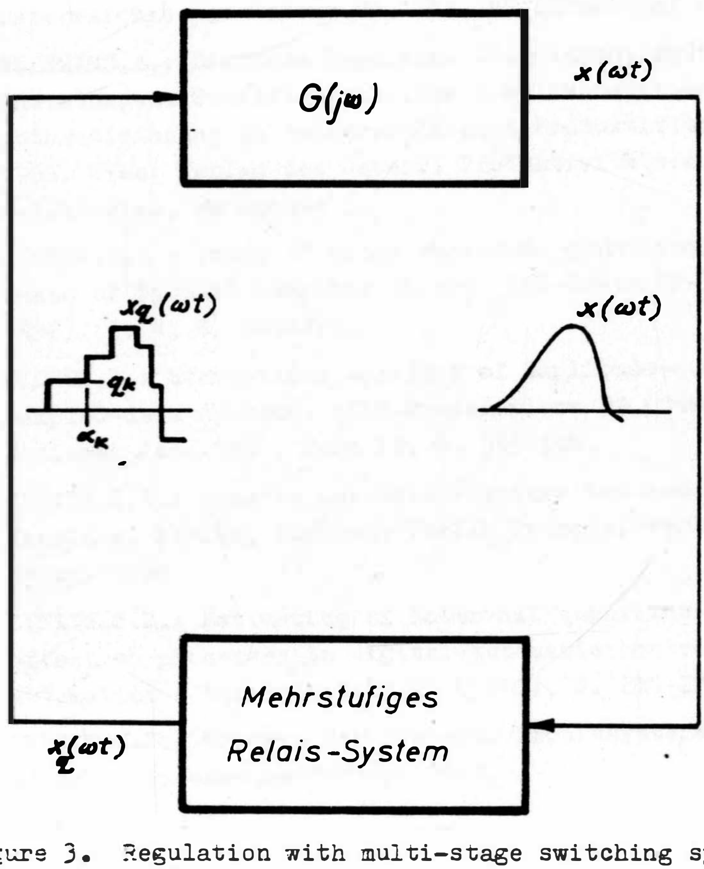

Figure 3. Regulation with multi-stage switching system

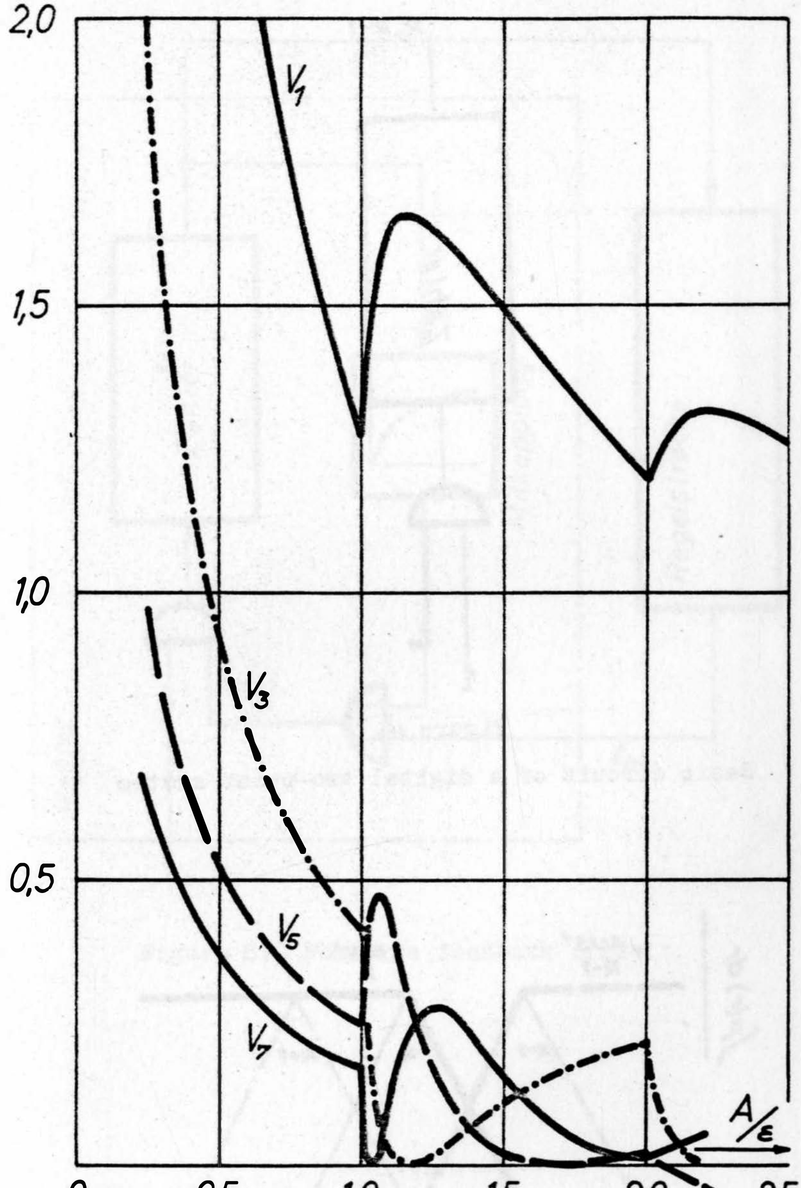

Figure 2. Dependence of the excitation factors V_i on the relative amplitude $A/_E$

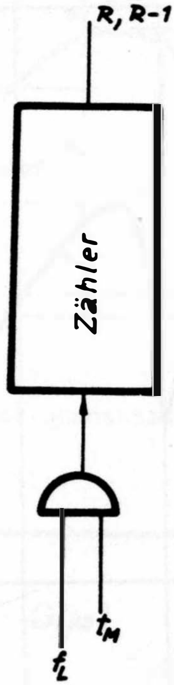

Figure 4.

Basic circuit of a digital two-point system

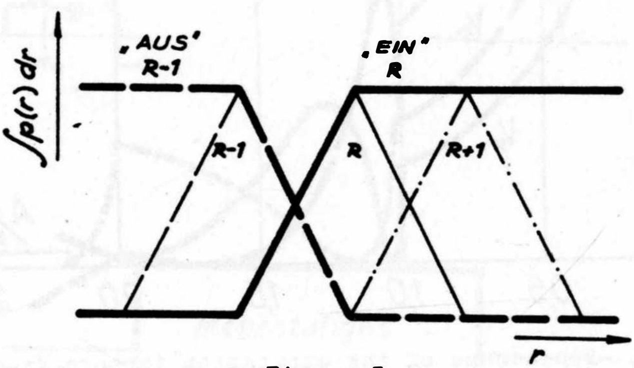

Figure 5.

Probability distribution for the quantization with pulse code modulation

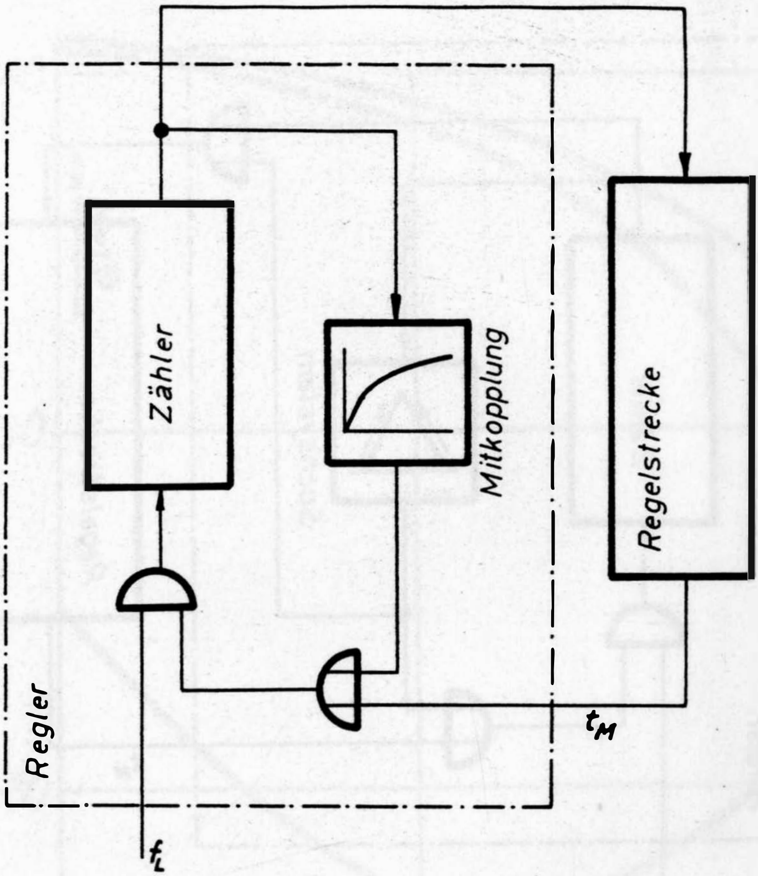

Figure 6. Positive feedback circuit

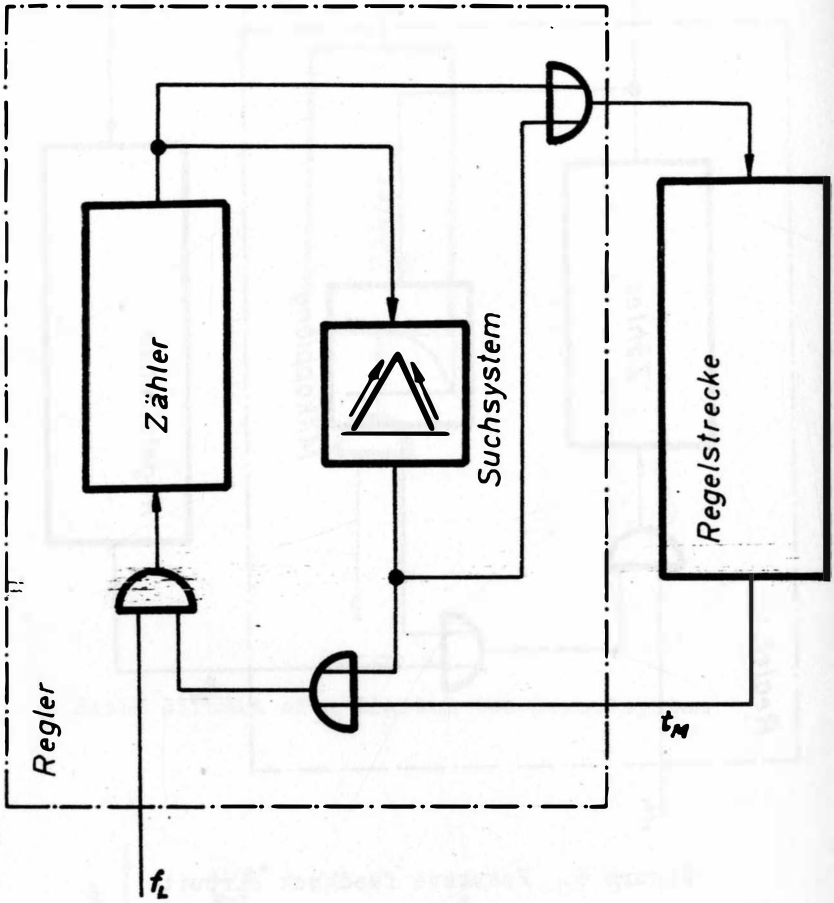

Figure 7. Circuit for the searching process for the maximum value of the probability distribution

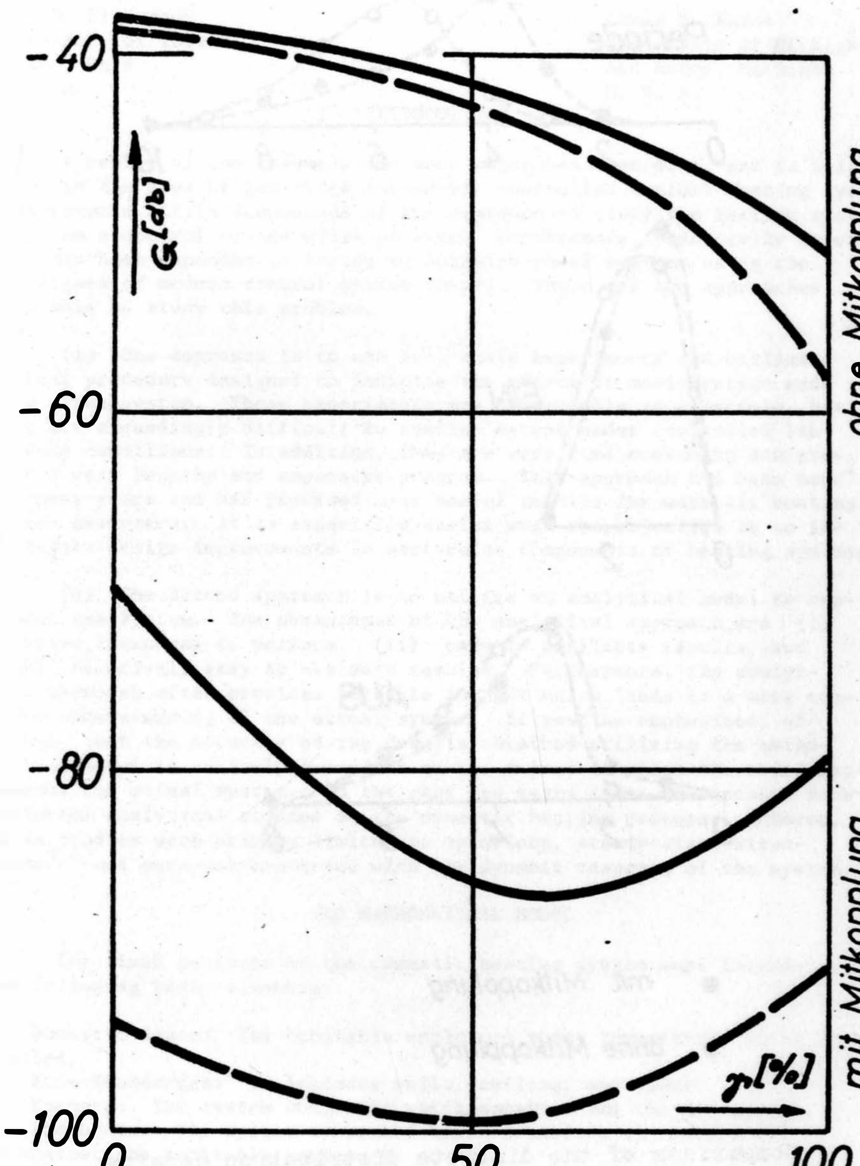

Figure 8. Comparison of the accuracy attained

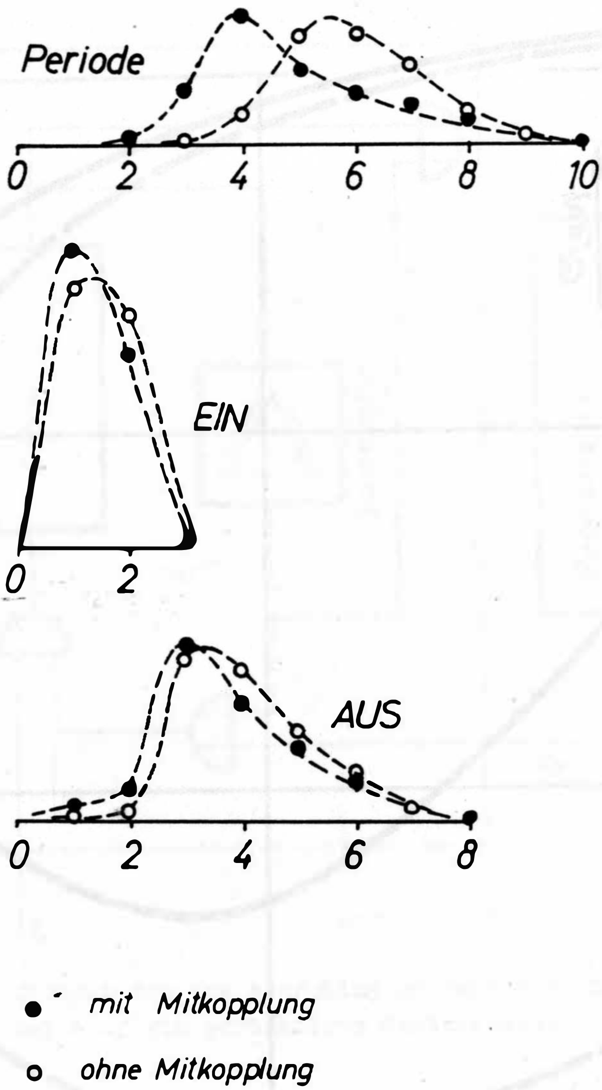

Figure 9.

Comparison of the discrete distribution density of the on and off intervals as well as the period of the switching movement

AN OPTIMAL HEATING SYSTEM

Adel H. Eltimsahy
University of Toledo
Toledo, Ohio
U. S. A.

Louis F. Kazda
University of Michigan
Ann Arbor, Michigan
U. S. A.

I. INTRODUCTION

A review of the research and work which has been done, and is being done, in the area of gas-fired forced-air controlled comfort heating systems reveals little documented effort expended to study the heating system from a control system point of view. Furthermore, practically no effort has been expended in trying to optimize these systems using the techniques of modern control system theory. There are two approaches available to study this problem.

(a) One approach is to use full scale experiments and utilize a testing procedure designed to indicate the effect of modification made on a given system. These experiments are practicable in principle, but they are exceedingly difficult to realize except under controlled laboratory conditions. In addition, they are very time consuming and present a very lengthy and expensive program. This approach has been used[2] for many years and has provided many useful results for warm air heating system designers. It is especially useful when the objective is to investigate design improvements in particular components of heating systems.

(b) The second approach is to utilize an analytical model to represent the system. The advantages of the analytical approach are (i) relative inexpense to perform, (ii) easy to duplicate results, and (iii) relatively easy to evaluate results. Furthermore, the analytical approach often provides valuable insight which leads to a more complete understanding of the actual system. It must be emphasized, of course, that the accuracy of the results obtained utilizing the mathematical model is entirely dependent on the degree to which the model represents the actual system. In the past few years other researchers have performed analytical studies on the domestic heating process. However, these studies were primary limited to open loop, steady-state situations[3,4] and were not concerned with the dynamic response of the system.

II. THE MATHEMATICAL MODEL

The fixed portions of the domestic heating system must include the following basic elements:

1. Domestic Space: The habitable enclosure whose temperature is to be controlled.
2. Room Boundaries: It includes walls, ceiling, and floor.
3. Furnace: The system component which supplies the thermal energy.
4. Air Ducts: The system component which transfers the heated air throughout the habitable enclosure.
5. Gas Control Valve: The system component which releases combustible gas to the furnace heat exchanger on signal from the controller unit.

In general all of the above elements affect the dynamic performance of the system; effects of some of the components, however, are negligible[1].

The above listed components are integrated into a schematic block diagram indicating their relationship to the overall system. Such a diagram is shown in Figure 1.

An approximate mathematical model for the fixed components of the system has been established[1] and is expressed by the following single vector linear differential equation:

$$\dot{x} = Ax + u + m \tag{1}$$

where: $x = \begin{bmatrix} T_R \\ T_W \\ T_e \end{bmatrix}$, $u = \begin{bmatrix} 0 \\ 0 \\ u_3 \end{bmatrix}$, $m = \begin{bmatrix} 0 \\ m_2 \\ 0 \end{bmatrix}$, $A = \begin{bmatrix} a_{11} & a_{12} & a_{13} \\ a_{21} & a_{22} & a_{23} \\ a_{31} & 0 & a_{33} \end{bmatrix}$

T_R = average temperature of the space to be heated.
T_W = average temperature of the inside surface of the outside wall.
T_e = average temperature of the heat exchanger wall.
T_f = average temperature of the furnace flame.
T_o = outside atmospheric temperature.
$u_3 = b_3 T_f$, $m_2 = d_2 T_o$

The components a_{ij} of the matrix A, b_3, and d_2 are parameters of the system.

III. FORMULATION OF THE PERTURBATION MODEL

In this section a perturbation model is formulated to represent the heating system as referred to some equilibrium position. First, assume that the controlled input u and the uncontrolled input m are such that the system is operating in an equilibrium condition, in other words $\dot{x} = 0$. In this case any disturbance which occurs in the system, for example an opened door, entering people, additional lighting, etc., causes a deviation in x from its nominal or equilibrium value.

To obtain the equilibrium values, set $\dot{x} = 0$, therefore:

$$Ax_o + u_o + m = 0 \tag{2}$$

The zero subscript here refers to the equilibrium vectors. In order to maintain a desirable room temperature which is a component of the vector x, it is evident that u, the controllable input to the system in the equilibrium state, takes on some value u_o. To determine the value of u_o required, consider Equation (2):

$$\begin{bmatrix} a_{11} & a_{12} & a_{13} \\ a_{21} & a_{22} & a_{23} \\ a_{31} & 0 & a_{33} \end{bmatrix} \begin{bmatrix} T_{R_o} \\ T_{W_o} \\ T_{e_o} \end{bmatrix} = - \begin{bmatrix} 0 \\ 0 \\ u_{3o} \end{bmatrix} - \begin{bmatrix} 0 \\ m_2 \\ 0 \end{bmatrix}.$$

By appropriate manipulations this equation becomes:

$$\begin{bmatrix} a_{12} & a_{13} & 0 \\ a_{22} & a_{23} & 0 \\ 0 & a_{33} & 1 \end{bmatrix} \begin{bmatrix} T_{W_o} \\ T_{e_o} \\ u_{3o} \end{bmatrix} = - \begin{bmatrix} a_{11} \\ a_{21} \\ a_{31} \end{bmatrix} T_{R_o} - \begin{bmatrix} 0 \\ m_2 \\ 0 \end{bmatrix} \tag{3}$$

From Equation (3), it can be seen that knowledge of the desired room temperature T_{R_o} and the outside temperature expressed by m, determines the equilibrium values of the controllable variable T_{f_o}, and the various state temperatures. Let $x = x_o + \delta x$, $\dot{x} = \dot{x}_o + \delta \dot{x}$
and $u = u_o + \delta u$
where δx, δu, and $\delta \dot{x}$ represent deviations from the nominal values of x_o, u_o, and $\dot{x}_o$ respectively, then $\dot{y} = Ay + v$ (6)
where $\delta x = y$, $\delta u = v$

This latter equation is the conventional well-known linear first order matrix differential equation. The components of the vectors in this equation represent variations in the state of the system. It is to be noted that in this case this new perturbation model (6) is valid for large swings from equilibrium since the model of the original dynamic system is linear.

IV. THE OPTIMIZATION CRITERION

The main objective in the optimization of a gas-fired forced-air heating system is to reduce and penalize room temperature variations due to disturbances, and is primarily used here to define the optimization criterion. The square penalizing will discriminate heavily against occasional large room temperature variations. This philosophy is justified as long as the type of control used does not have any significant physical limitations. In a gas-fired heating system. for example, physical limitations are imposed by the heat exchanger[5]. It is mainly due to power limitations. Therefore in order to consider power limitations, a term in the square error criterion is added that is proportional to the square of the control signal. Having these two factors in mind, the optimization criterion for the forced-air heating system can be represented as follows:

$$J(y, v) = \sum_{n=1}^{3} \int_{o}^{T} [q_n^2(\sigma) + v_n^2(\sigma)]\, d\sigma \tag{7}$$

where $J(y,v)$ is the error criterion to be minimized, σ is a dummy time variable, T is the period over which the minimization takes place, $q(\sigma)$ and $v(\sigma)$ are defined as:

$$q(\sigma) = \begin{bmatrix} q_1(\sigma) \\ q_2(\sigma) \\ q_3(\sigma) \end{bmatrix} = \begin{bmatrix} 1 & 0 & 0 \\ 0 & 0 & 0 \\ 0 & 0 & 0 \end{bmatrix} \begin{bmatrix} y_1(\sigma) \\ y_2(\sigma) \\ y_3(\sigma) \end{bmatrix} \quad ; \; v(\sigma) = \begin{bmatrix} v_1(\sigma) \\ v_2(\sigma) \\ v_3(\sigma) \end{bmatrix}$$

The first term in the integrand of the quadratic criterion (7) represents the penality on the room temperature variations, and the second term is introduced for power limitation.

V. THE OPTIMAL CONTROL LAW

The optimization problem at hand is one of starting from some initial temperature disturbance y_o, and driving the system $\dot{y} = Ay + v$ to the equilibrium state while constraining the original system to perform in such a way as to minimize the value of the cost functional $J(y, v)$. Here the perio of optimization is allowed to be very large (i.e., $T \to \infty$), since the heating system has to be optimized over a long period of time.

The method of dynamic programming applied to this linear time invariant heating system is guaranteed to provide a closed loop or feedback control law [6,7] for a given set of heating system parameters, which satisfies the optimization criterion defined in section IV. It does not pose any difficulties such as instability of the resulting equations which could result by applying the calculus of variations to a system to be optimized over a semi-infinite interval (as $T \to \infty$)[6]. For these reasons, the method of dynamic programming is thought to be the most suitable method for the optimization of the heating system under the optimization criterion represented by (7). Bellman's Dynamic programming is basically an optimization process that proceeds backward in time; that is, the solution is computed over the last interval of the process and successive solutions are computed for the remaining intervals of decreasing time until the total solution is obtained for the entire process.

In order to apply the functional equation technique of dynamic programming, this optimization problem is embedded within the wider problem of minimizing:

$$\sum_{n=1}^{3} \int_{t}^{T} [q_n^2(\sigma) + v_n^2(\sigma)]\, d\sigma$$

subject to the heating system Equation (6) and the initial condition $y(o) = y_o$, with t ranging over the interval (0,T). Let the minimum of this cost functional be:

$$E(y,t) = \min_{v} \sum_{n=1}^{3} \int_{t}^{T} [q_n^2(\sigma) + v_n^2(\sigma)] \, d\sigma \tag{8}$$

Invoking the principle of optimality to Equation (8) the functional equation becomes:

$$E(y,t) = \min_{v} \left\{ \sum_{n=1}^{3} \int_{t}^{t+\varepsilon} [q_n^2(\sigma) + v_n^2(\sigma)] \, d\sigma + E(y+\dot{y}\varepsilon, t+\varepsilon) \right\} \tag{9}$$

where ε is an incremental change in the time t. This equation is reduced to the following expression (by integration and Taylor series expansion):

$$E(y,t) = \min_{v} \left\{ \sum_{n=1}^{3} [q_n^2(\sigma) + v_n^2(\sigma)]\varepsilon + E(y,t) + \sum_{n=1}^{3} \dot{y}_n \frac{\partial E}{\partial y_n}\varepsilon + \frac{\partial E}{\partial t}\varepsilon \right\} + \Delta(\varepsilon)$$

Simplifying:

$$\min_{v} \left\{ \sum_{n=1}^{3} [q_n^2(\sigma) + v_n^2(\sigma)] + \sum_{n=1}^{3} \dot{y}_n \frac{\partial E}{\partial y_n} + \frac{\partial E}{\partial t} \right\} + \Delta'(\varepsilon) = 0,$$

where $\Delta'(\varepsilon) \to 0$ as $\varepsilon \to 0$

Therefore

$$\min_{v} \left\{ \sum_{n=1}^{3} [q_n^2(\sigma) + v_n^2(\sigma)] + \sum_{n=1}^{3} \dot{y}_n \frac{\partial E}{\partial y_n} + \frac{\partial E}{\partial t} \right\} = 0 \tag{10}$$

The minimizing control signal vector $v^*(\sigma)$ is obtained by minimizing the sum of terms within the brackets of equation 10 with respect to each signal of the control vector. Minimizing now with respect to $v_3(\sigma)$, the only non zero component of the vector $v(\sigma)$, ...(keeping in mind the relation between the vectors q and y), is therefore: $2v_3^* + \frac{\partial E}{\partial y_3} = 0$,

where v_3^* = optimum control signal.

Consequently, the condition for minimum error is: $v_3^* = -\frac{1}{2}\frac{\partial E}{\partial y_3}$ (11)

In order to determine the optimum signal v_3^*, $\frac{\partial E}{\partial y_3}$ for minimum error must be determined first. Substituting Equation (11) and the value of q in terms of y into the functional Equation (10), the condition for minimum error becomes:

$$y_1^2 + \frac{1}{4}\left(\frac{\partial E}{\partial y_3}\right)^2 + \sum_{n=1}^{3} \dot{y}_n \frac{\partial E}{\partial y_n} + \frac{\partial E}{\partial t} = 0 \tag{12}$$

As seen from Equation (12), the condition for minimum error is in a partial differential form. To solve such an equation a power series solution is assumed, and the coefficients in the series are found by direct substitution.

Since the integrand of the error criterion function is a quadratic expression and the dynamic system is linear, the minimum error function E(y,t) is also quadratic and can be written as:

$$E(y,t) = k(t) + \sum_{m=1}^{3} k_m(t)y_m(t) + \sum_{m=1}^{3}\sum_{k=1}^{3} k_{mk}(t)y_m(t)y_k(t) \tag{13}$$

where $k_{mn}(t) = k_{nm}(t)$, and

where $k(t)$, $k_m(t)$, $k_{mn}(t)$ are the parameters to be determined from Equations (12) and (13). By partial differentiation of Equation (13), $(\partial E(y,t))/(\partial y_n)$ and $(\partial E(y,t))/(\partial t)$ are written as follows:

$$\frac{\partial E(y,t)}{\partial y_n} = k_n(t) + 2\sum_{m=1}^{3} k_{nm}(t)y_m(t) \tag{14}$$

and

$$\frac{\partial E(y,t)}{\partial t} = k'(t) + \sum_{m=1}^{3} k'_m(t)y_m(t) + \sum_{m=1}^{3}\sum_{k=1}^{3} k'_{mk}(t)y_m(t)y_k(t) \qquad (15)$$

If these partial derivatives are substituted into Equation (12) the condition for minimum error becomes:

$$y_1^2 + \frac{1}{4}\left[k_3 + 2\sum_{m=1}^{3} k_{nm}y_m\right]^2 + k' + \sum_{m=1}^{3} k'_m y_m + \sum_{m=1}^{3}\sum_{k=1}^{3} k'_{mk}y_m y_k \qquad (16)$$

$$+ \sum_{n=1}^{3}\left[k_n\dot{y}_n + 2\dot{y}_n \sum_{m=1}^{3} k_{nm}y_m\right] = 0$$

The condition for minimum error expressed by (16) is satisfied for all finite values of $y_n(t)$, assuming the k-parameters are independent of $y_n(t)$, only if each of the coefficients of the constant term, $y_n(t)$, and $y_n(t)y_m(t)$ in Equation (16) vanishes, where n,m = 1,2,3. Therefore by equating the coefficients of the constant term, y_n and $y_n y_m$ each equal to zero, the following simultaneous first order differential equations in the k-parameters result.

$$\begin{aligned} &f_1(k,k_1,k_2,k_3,k_{11},k_{22},k_{33},k_{12},k_{13},k_{23}) = k' \\ &f_2(k,k_1,k_2,k_3,k_{11},k_{22},k_{33},k_{12},k_{13},k_{23}) = k'_1 \\ &f_3(k,k_1,k_2,k_3,k_{11},k_{22},k_{33},k_{12},k_{13},k_{23}) = k'_2 \\ &\vdots \\ &f_{10}(k,k_1,k_2,k_3,k_{11},k_{22},k_{33},k_{12},k_{13},k_{23}) = k'_{23} \end{aligned} \qquad (17)$$

where: f_1, f_2, ...,f_{10} are in general nonlinear functions of the k-parameters, and the primed k's refer to the derivatives of the k-parameters with respect to time.

This method of assuming a solution leads to the reduction of the problem of solving a partial differential equation to the problem of solving a set of first order ordinary differential equations. The boundary condition for the k-parameters are deduced directly from the required boundary condition on the minimum error function. From the expression for minimum error function for t = T, the boundary condition is

$E(y(T),T) = 0$ which means that $k(T) = k_n(T) = k_{nm}(T) = 0$ (18)

The problem becomes now one of finding the optimum control system of a one-point boundary value problem. The parameters of the optimum control system, $k(t)$, $k_{mn}(t)$ where m, n = 1, 2, 3 can be determined from the set of ten differential Equations (17) with boundary conditions given by (18). It is to be noted that the number of parameters are ten and the number of initial conditions expressed by (18) are ten.

The solution of the set of differential Equations (17) as T tends to ∞, must assume steady state. If the k-parameters assume steady state values, then the differential equations given by (17) reduces to a set of algebraic equations. Therefore, when the dynamic system is time invariant, the error function is quadratic, and the optimization process is carried over a semi-infinite time interval, the parameters of the optimal control law become time-invariant.

Since the heating system is to be optimized over a semi-infinite time interval for a quadratic optimization criterion, equations (8) through (15) become

$$E(y) = \min_v \sum_{n=1}^{3} \int_t^{\infty}\left[q_n^2(\sigma) + v_n^2(\sigma)\right] d\sigma \qquad (8')$$

$$E(y) = \min_v \left\{ \sum_{n=1}^{3} \int_t^{t+\varepsilon} \left[q_n^2(\sigma) + v_n^2(\sigma)\right] d\sigma + E(y + \dot{y}\varepsilon) \right\} \qquad (9')$$

$$\min_{v}\left\{\sum_{n=1}^{3}\left[q_n^2(\sigma)+v_n^2(\sigma)\right]+\sum_{n=1}^{3}\dot{y}_n\frac{\partial E}{\partial y_n}\right\}=0 \qquad (10')$$

$$v_3^* = -\frac{1}{2}\frac{\partial E}{\partial y_3} \qquad (11')$$

$$y_1^2+\frac{1}{4}\left(\frac{\partial E}{\partial y_3}\right)^2+\sum_{n=1}^{3}\dot{y}_n\frac{\partial E}{\partial y_n}=0 \qquad (12')$$

$$E(y) = k+\sum_{m=1}^{3}k_m y_m(t)+\sum_{m=1}^{3}\sum_{k=1}^{3}k_{mk}y_m(t)\,y_k(t) \qquad (13')$$

where k, k_m, and k_{mn} where m, n = 1, 2, 3 are fixed constants.

$$\frac{\partial E}{\partial y_n} = k_n + 2\sum_{m=1}^{3}k_{nm}y_m(t) \qquad (14')$$

$$\frac{\partial E}{\partial t} = 0 \qquad (15')$$

also
$$\frac{\partial E}{\partial y_3} = k_3 + 2\left[k_{31}y_1+k_{32}y_2+k_{33}y_3\right] \qquad (19)$$

By substituting $(\partial E)/(\partial y_3)$ from (19) into (11') gives:

$$v_3^* = -\frac{k_3}{2}-k_{31}y_1-k_{32}y_2-k_{33}y_3 \qquad (20)$$

Therefore it is necessary to determine the parameters k_3, k_{31}, k_{32}, and k_{33} to determine the optimum control signal.

Substituting now from Equations (14') and (19) into the condition for minimum error (12'), and also using the vector matrix differential equation $\dot{y} = Ay + v$, the following is obtained:

$$y_1^2-\frac{1}{4}\left[k_3^2+4k_3\sum_{m=1}^{3}k_{m3}y_m+4\left(\sum_{m=1}^{3}k_{m3}y_m\right)^2\right]+\sum_{n=1}^{3}\left(\sum_{m=1}^{3}a_{mn}y_m\right)\left[k_n+2\sum_{s=1}^{3}k_{sn}y_s\right]=0$$

Since equation (21) is satisfied for all values of $y_n(t)$, by equating the constant term in this equation to zero, the following is obtained:

$$k_3 = 0 \qquad (22)$$

Similarly for the coefficient of y_m: $-k_3k_{m1}+\sum_{n=1}^{3}a_{mn}k_n = 0$ (m=1,2,3) and since this is true for all finite values of a_{mn}, therefore

$k_1 = k_2 = k_3 = 0.$

For the coefficient of y_1^2: $1-k_{13}^2+4\sum_{n=1}^{3}a_{1n}k_n = 0$ (23)

For the coefficient of y_2^2:

$$-k_{23}^2+4\sum_{n=1}^{3}a_{2n}k_{2n} = 0 \qquad (24)$$

For the coefficient of y_2^3: $-k_{33}^2+4\sum_{n=1}^{3}a_{3n}k_{3n} = 0$ (25)

For the coefficient of y_1y_2: $-k_{13}k_{23}+\sum_{n=1}^{3}(a_{1n}k_{2n}+a_{2n}k_{1n}) = 0$ (26)

For the coefficient of y_1y_3: $-k_{13}k_{33}+\sum_{n=1}^{3}(a_{1n}k_{3n}+a_{3n}k_{1n}) = 0$ (27)

For the coefficient of y_2y_3: $-k_{23}k_{33}+\sum_{n=1}^{3}(a_{2n}k_{3n}+a_{3n}k_{2n}) = 0$ (28)

Equations (23) to (28) are in general nonlinear algebraic equations in the parameters k_{mn}, m, n = 1, 2, 3 and require a digital computer for solution. In the next section a solution of these parameters for a particular heating system on the digital computer will be shown.

Equation (20) now becomes: $v_3^* = -\left[k_{31}y_1 + k_{32}y_2 + k_{33}y_3\right]$ (29)
The control function v_3^*, derived here is referred to as the optimum control law.

This optimal control scheme for the variational system may be combined with the equilibrium system developed in Section III to obtain an optimal feedback system for the heating process. In block diagram form the system may be schematically represented as shown in Figure (2). In this diagram a controller is provided which compares the values of the environmental state and the desired state and commands the appropriate equilibrium input. It should be noted that the number of feedback loops is equal to the order of the heating system; it is noted also that the feedback signals are measurable state variables.

Thus, an optimal heating system for a defined quadratic cost function has been developed which has the desirable property of providing feedback loops to account for distrubances in the system. This optimum law will be applied to a particular heating system in the next section to develop an optimum controller. The optimal heating system is then simulated on an analog computer to study its behavior.

VI. EXAMPLE

Consider a domestic forced-air gas-fired heating system defined by[1]:

$$A = \begin{bmatrix} -0.191 & 0.0422 & 0.097 \\ 0.2278 & -0.0974 & -0.09 \\ 0.25 & 0 & -0.489 \end{bmatrix}, \quad u = \begin{bmatrix} 0 \\ 0 \\ 0.239 \end{bmatrix} T_f, \quad m = \begin{bmatrix} 0 \\ 0.0184 \\ 0 \end{bmatrix} T_o$$

The variational vector matrix differential equation as derived in section III now becomes: $\dot{y} = Ay + v$
where $v^T = (v_1, v_2, v_3) = (0, 0, 0.239\delta T_f)$
and $y^T = (y_1, y_2, y_3) = (\delta T_R, \delta T_w, \delta T_e)$ where $y_1 = \delta T_R$, $y_2 = \delta T_w$, $y_3 = \delta T_e$

The square matrix A determines the system under consideration, and therefore the k parameters of the system as defined by Equations (23) to (28) may be written as follows:

$$1 - k_{31}^2 + 0.388\,k_{31} - 0.764\,k_{11} + 0.1688\,k_{12} = 0$$
$$-k_{32}^2 - 0.388\,k_{32} + 1.112\,k_{12} - 0.3896\,k_{22} = 0$$
$$-k_{33}^2 - 1.956\,k_{33} + k_{31} = 0$$
$$-k_{31}k_{32} - 0.2884\,k_{12} + 0.0422\,k_{22} + 0.097\,k_{32} + 0.2278\,k_{11} - 0.097\,k_{31} = 0$$
$$-k_{31}k_{33} - 0.68\,k_{31} + 0.0422\,k_{32} + 0.097\,k_{33} + 0.25\,k_{11} = 0$$
$$-k_{32}k_{33} + 0.2278\,k_{31} - 0.5864\,k_{32} - 0.097\,k_{33} + 0.25\,k_{12} = 0$$

The University of Michigan Control System Algorithm Program employing a 7090 digital computer was used to solve for the k-parameters. This program was basically obtained from IBM, with some modifications added. The modified program is entitled CSAP and is currently available at the University of Michigan Computing Center Library. This program appears as a subroutine on the system disc and may be entered simply by calling CSAP. Once the program has been called, it will function exactly as described in the user's manual.[9] The solution for this particular system is:
$k_{11} = 1.4449$, $k_{22} = 1.3273$, $k_{33} = 0.2065$, $k_{12} = 0.805$, $k_{31} = 0.4467$, $k_{32} = 0.36$. The optimal control signal becomes: $v_3^* = -(0.4467\,y_1 + 0.36\,y_2 + 0.2065\,y_3)$, or $0.239\,\delta T_f = -(0.4467\,\delta T_R + 0.36\,\delta T_w + 0.2065\,\delta T_e)$
Hence, the block diagram of the optimum heating system using this control law follows as shown in Figure 3. It is to be noted that δT_f, δT_R, δT_w, and δT_e are the variations of temperatures from equilibrium values, and are defined as follows: $\delta T_f = T_f - T_{f_o}$, $\delta T_R = T_R - T_{R_o}$,
$\delta T_w = T_w - T_{w_o}$, $\delta T_e = T_e - T_{e_o}$.

Therefore, to generate v_3^*, the variational signal, it is necessary to first generate the equilibrium values of the temperatures, T_{f_o}, T_{R_o}, T_{w_o}, and T_{e_o}.

For equilibrium conditions: $\dot{T}_R = \dot{T}_w = \dot{T}_e = 0$,
then: $T_{f_o} = -1.045\, T_{R_o} + 2.05\, T_{e_o}$, $T_{e_o} = 0.43\, T_{w_o} + 1.97\, T_{R_o}$,
$T_{w_o} = 2.37\, T_{R_o} - T_{e_o} + 0.19\, T_o$

From these latter equations it follows that having T_{R_o}, and T_o as set inputs, the equilibrium values T_{f_o}, T_{e_o}, and T_{w_o} may be generated.

Having established the equilibrium values, they may be now combined with the fixed portion of the heating system and the optimum controller to provide the optimum control system.

1. First Case: The room temperature T_R is set at 70°F, and the outside temperature is initially set at 20°F. The system is therefore initially in the equilibrium state of:
$x_o^T = (70, 52.9, 115)$ °F , $T_{f_o} = 163.8$°F
The outside temperature T_o is then suddenly changed from 20°F to 0°F. For these conditions the room temperature T_R, the surface wall temperature T_w, the heat exchanger wall temperature T_e, and the control signal temperature T_f were recorded. These temperature responses are shown in Figures 4, 5, 6, and 7 respectively.

From Figure 4, it is evident that the room temperature T_R decreases gradually from the time the disturbance occurs until the time when the variation δT_R becomes -0.15°F; a total of 16 minutes. After this, it begins to increase at a slower rate back toward its original value. In 40 minutes, the room temperature attains the value of 69.9°F. This is expected, since the optimization criterion was considered over a semi-infinite time interval. The optimum control signal T_f as seen in Figure 7 increases gradually from the time of the drop in the outside temperature. This effect occurs to compensate for the heat loss caused by sudden disturbance. In Figure 5, it is noted that the surface temperature of the wall initially falls rapidly to 45.37°F, then it gradually begins increasing until it reaches 49°F. Figure 6 indicates the effect of the disturbance on the heat exchanger temperature T_e. This temperature initially drops to about 109°F because of both the decrease in room temperature and the decrease in surface wall temperature. It then begins to gradually increase until it reaches within 2.4°F of its original value. This is caused by the increase in the flame temperature.

2. Second Case: For this case the room temperature is set at 70°F and the outside temperature is initially at 0°F. The equilibrium values are: $x_o^T = (70, 49, 117)$ °F, $T_{f_o} = 182.8$°F. The outside temperature then rises suddenly to 40°F. Figures 8 to 11 show the state variables and control signal responses to this disturbance. The room temperature response is shown in Figure 8. This temperature increases gradually to 70.15°F then falls to 70.05°F. The wall surface temperature shown in Figure 9 rises as a result of the disturbance and then it decreases until it reaches 63°F. The heat exchanger temperature also rises by 6°F and then will decrease gradually to 110°F. This result is illustrated in Figure 10. Figure 11 shows the optimal control signal. It is apparent that the flame temperature changes gradually to 153.5°F, which implies that the disturbance caused by an outside temperature rise from 0°F to 40°F, decreases the flame temperature by 29.3°F to keep the room temperature to within 0.1°F of 70°F.

<u>Comparison</u>: If the conventional heating system is to be compared with the optimal system, the basis of comparison must be the defined performance criterion. It is true by definition that the optimal system developed is the best with respect to this criterion; however, interesting points can be made by analyzing the systems in general.

For a conventional heating system the main properties are: (a) An on-off controller is used. (b) Only the average room temperature T_R is controlled. For analysis purposes [1], the heat output of the furnace is adjusted so that the temperature of the air circulating in the heating system is 120°F when it is leaving the furnace during the on-period. During the off-period the temperature of the air is considered to be 70°F. The outside temperature T_o is held fixed at 20°F, and then allowed to drop suddenly to zero. Computer runs were made for the conventional heating system for different values of thermostat (controller) time constant τ_T minutes and hysterisis q °F. The peak to peak room temperature variation is measured and is called the cycling amplitude. Also the time for one complete cycle of the room temperature is recorded, and is called the cycling period.

If the conventional heating system is analyzed and compared to the optimum heating system it is found that:

(i) the peak to peak variations of the room temperature are much greater for the conventional heating system, when compared to the maximum deviation of the optimal system.

(ii) For an outside temperature disturbance the response and adjustment of the optimum heating system is superior to the corresponding response of the conventional heating system. In the optimum system, the temperature begins to fall gradually (due to an outside temperature drop) until it deviates to -0.15°F. Then within about 5 minutes it tends to remain to within 0.1°F or less from the original value. The conventional heating system, on the other hand, begins to oscillate. The rates of increase and decrease in the room temperature depend on the thermostat time constant, and thermostat hysteresis. They also depend on the nature of the disturbance. This is shown in Figures 12, 13, 14, and 15.

(iii) The rate of change in the room temperature is greater when using the conventional controller thus causing the conventional heating system to be less comfortable.

VII. CONCLUSION

An optimal heating system for a defined integral quadratic cost function has been developed which incorporates the main objective of minimizing room temperature variations. The optimal control was shown to have the desirable property of providing additional feedback loops to account for disturbances in the system. The feedback portions of the optimum control heating system were also shown to be time-invariant, a characteristic which is advantageous in practice. Parameters of the optimum controller were determined through the use of the Control System Algorithm Program (CSAP) on the 7090 digital computer at the University of Michigan. The optimum heating system represents an optimum from the theoretical point of view for the configuration and cost function selected. Therefore it represents an upper bound or standard with which conventional or sub-optimal systems may be compared. However, for some specialized installations possessing rigid performance standards, it may be feasible to utilize a system such as the optimal.

Analog computer results showed a significant degree of improvement could be obtained using the optimum controller rather than a conventional controller.

REFERENCES

1. "The Optimization of Domestic Heating Systems," Adel H. Eltimsahy, Ph.D. Dissertation, April 1967, University of Michigan.

2. "Distribution of Air Within a Room for Year-Round Air Conditioning," Parts I and II, Harold E. Straub, Stanly F. Gilman, Seichi Konzo, and Michael Ming Chen. University of Illinois Engineering experiment Station Bulletin Nos. 435 and 442.

3. "Room Temperature Response to a Sudden Heat Disturbance Input," by R. O. Zermuehlen, H. L. Harrison, ASHRAE 1965.

4. "Dynamic Characteristics of Water to Air Cross Flow Heat Exchanger," by J. R. Gartner, H. L. Harrison, ASHRAE 1965.

5. "Fundamentals of Heat Transfer in Domestic Gas Furnaces," Research Bulletin 63, American Gas Association Laboratories.

6. Optimization Theory and the Design of Feedback Control Systems, C. W. Merriam III, McGraw-Hill, 1964.

7. Modern Control Theory, J. Tou, McGraw-Hill, 1964.

8. "Control Systems Analysis Program II," (CSAP II), User's Manual.

9. "The Optimal Control of Gas-Fired Warm Air Heating Systems," by L. F. Kazda, G. Casserly, A. Eltimsahy and R. Spooner. AGA Final Report Contract DO-14-GU, University of Michigan.

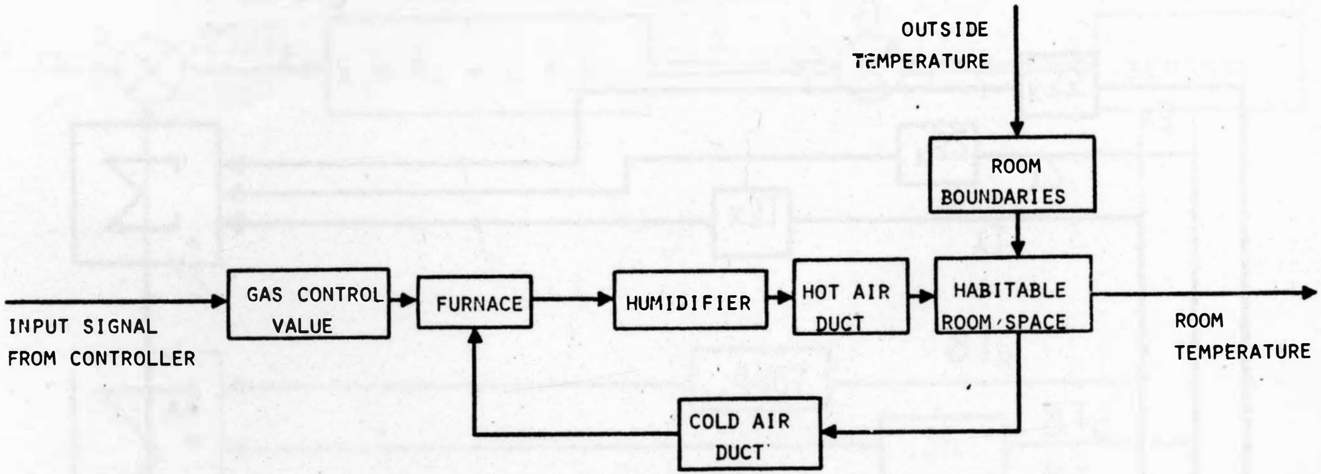

FIGURE 1. COMPONENTS OF THE HEATING SYSTEM.

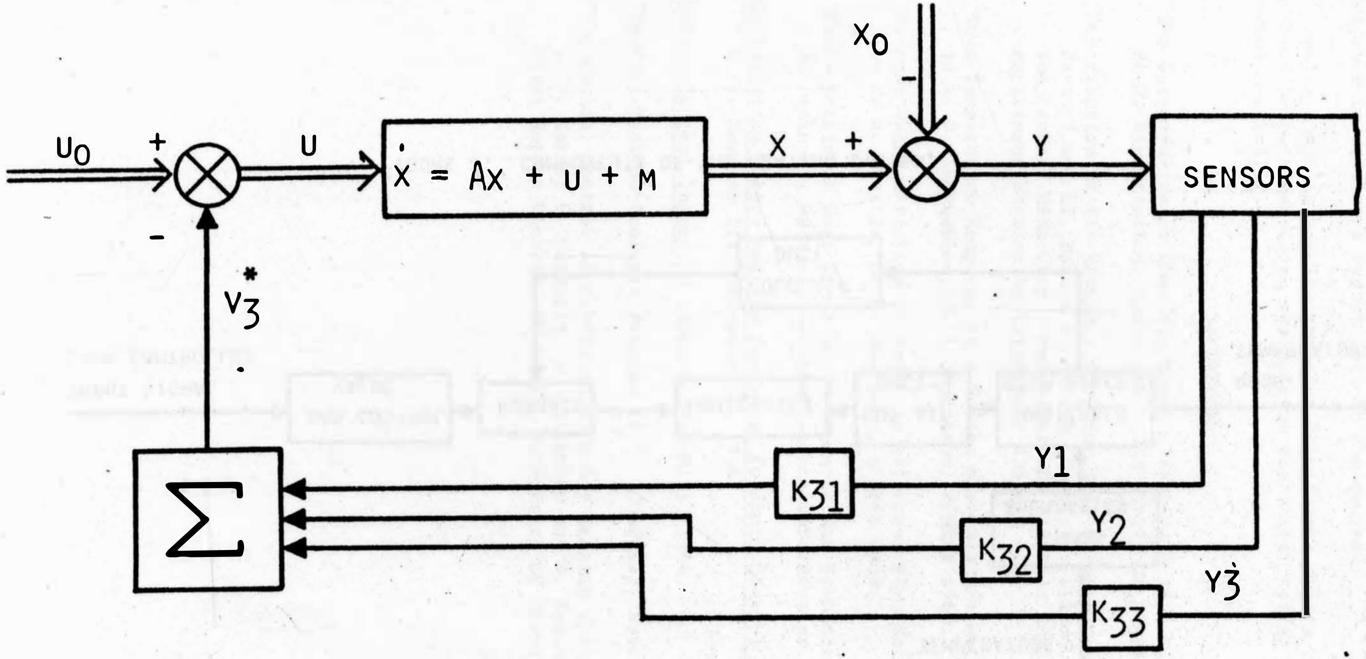

FIGURE 2. BLOCK DIAGRAM OF THE OPTIMUM HEATING SYSTEM.

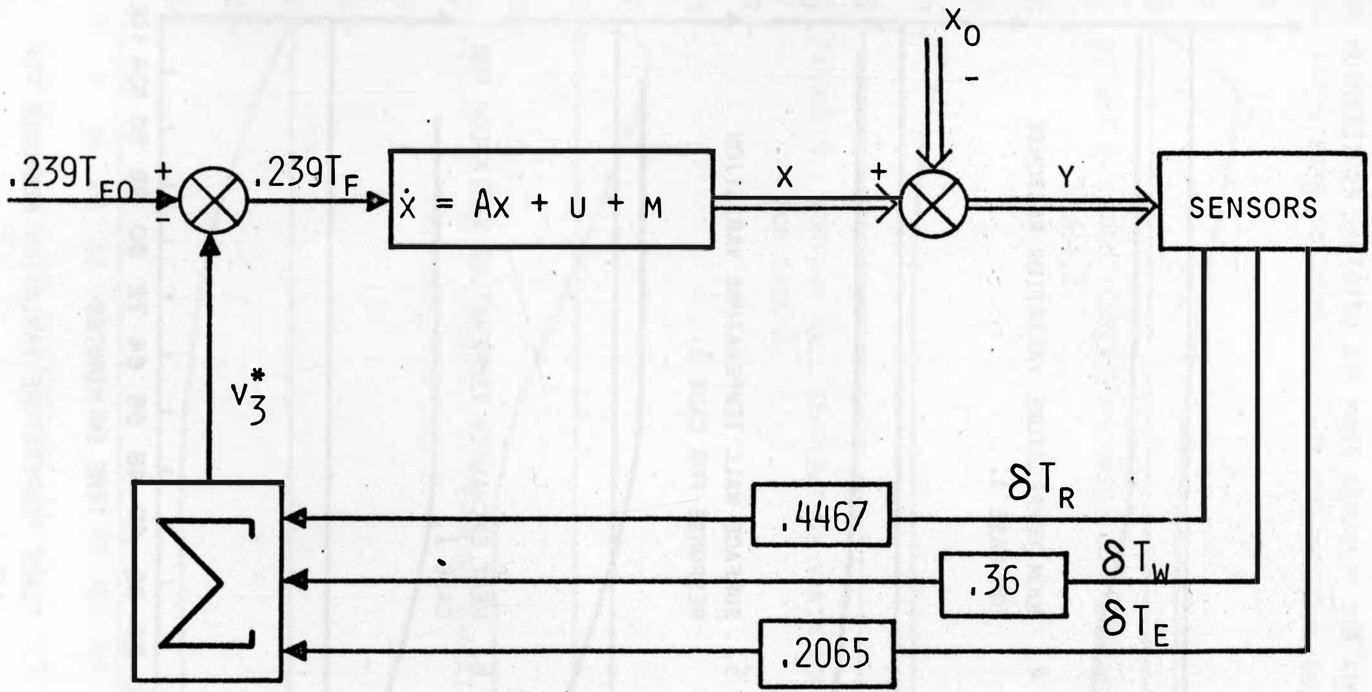

FIGURE 3. BLOCK DIAGRAM OF THE OPTIMUM HEATING SYSTEM.

ALL VARIATIONS ARE MEASURED FROM THE ORIGINAL EQUILIBRIUM VALUES.

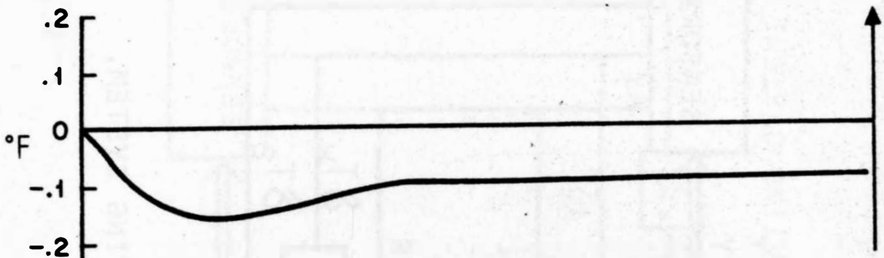

FIGURE 4. ROOM TEMPERATURE VARIATION RESPONSE FOR CASE 1.

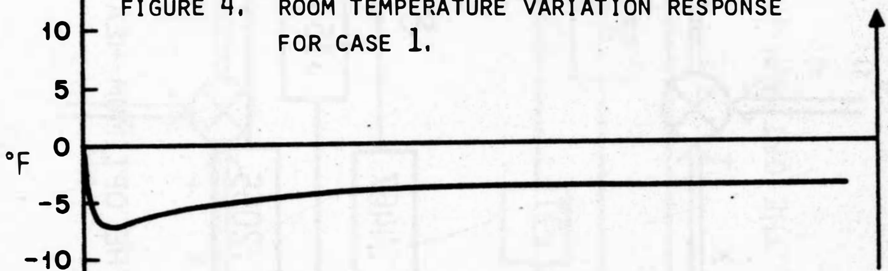

FIGURE 5. SURFACE WALL TEMPERATURE VARIATION RESPONSE FOR CASE 1.

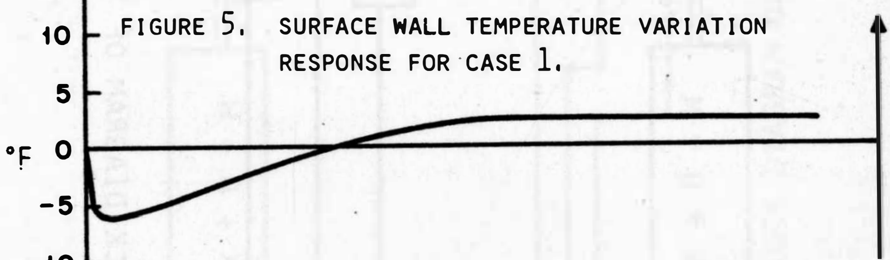

FIGURE 6. HEAT EXCHANGER TEMPERATURE VARIATION FOR CASE 1.

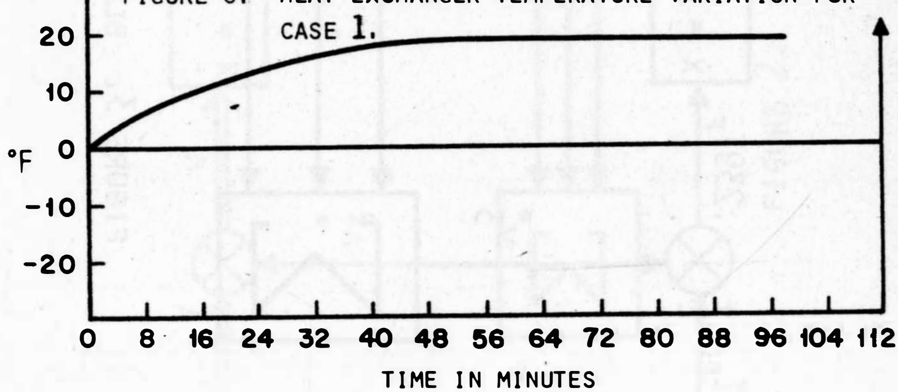

FIGURE 7. FLAME TEMPERATURE VARIATION RESPONSE FOR CASE 1.

ALL VARIATIONS ARE MEASURED FROM THE ORIGINAL EQUILIBRIUM VALUES.

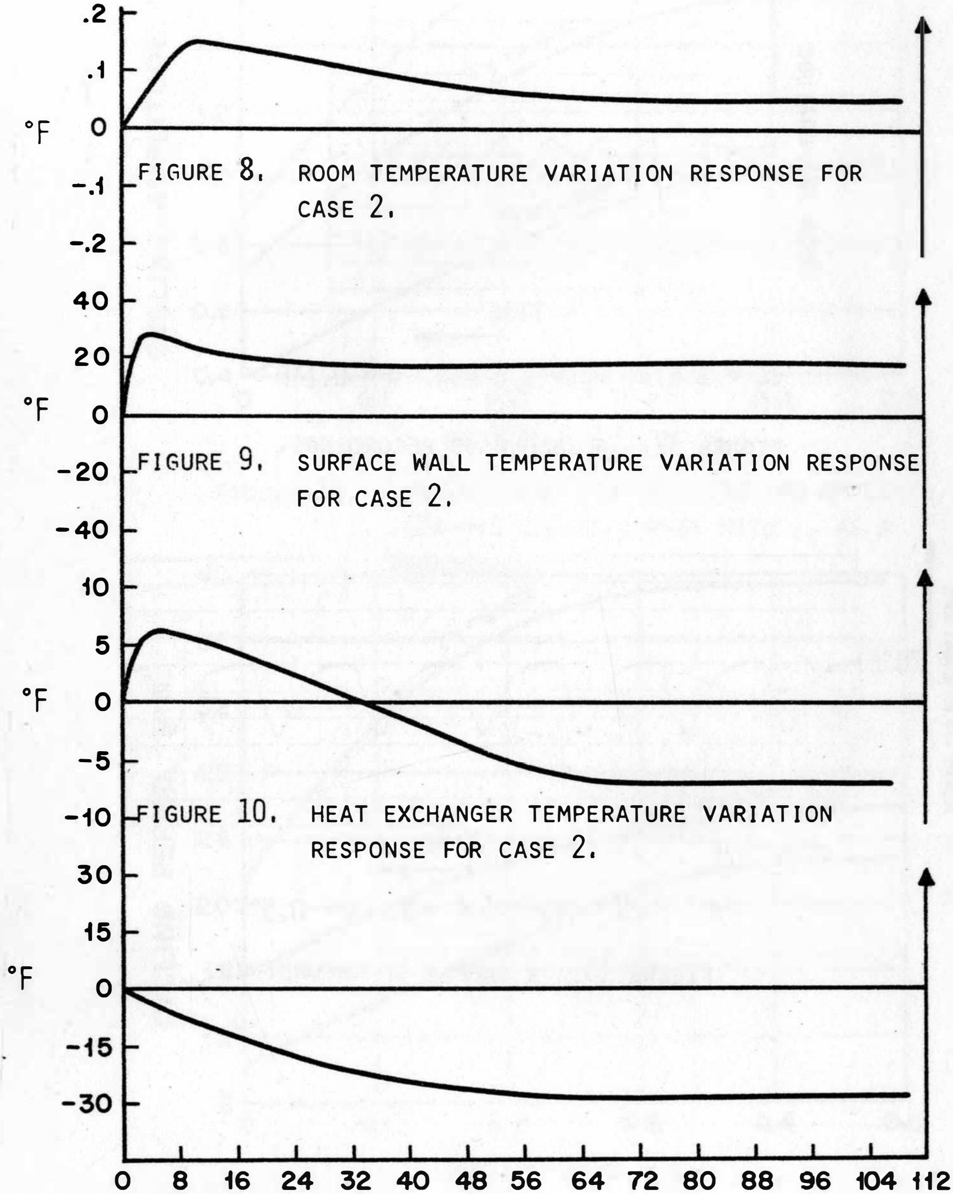

FIGURE 8. ROOM TEMPERATURE VARIATION RESPONSE FOR CASE 2.

FIGURE 9. SURFACE WALL TEMPERATURE VARIATION RESPONSE FOR CASE 2.

FIGURE 10. HEAT EXCHANGER TEMPERATURE VARIATION RESPONSE FOR CASE 2.

FIGURE 11. FLAME TEMPERATURE VARIATION RESPONSE FOR CASE 2.

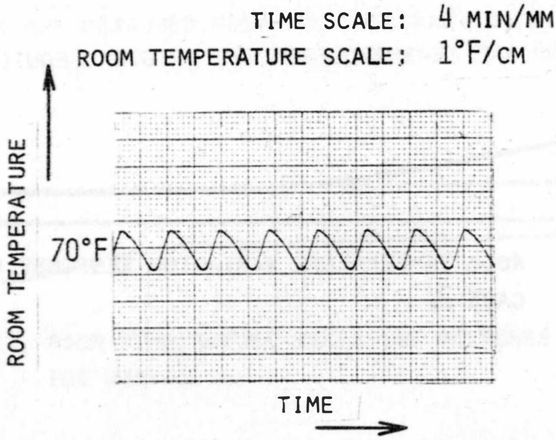

τ_T = 1 MIN, τ_F = 1.6 MIN, q = 0.1°F

FIGURE 12. A SAMPLE OF RECORDINGS.

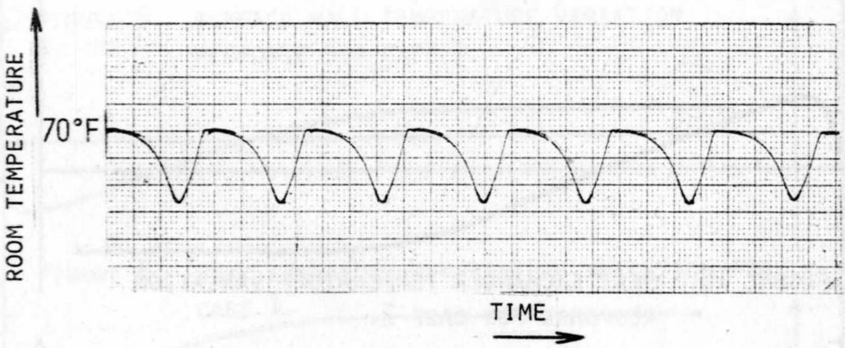

τ_T = 1 MIN, τ_F = 1.6 MIN, q = 0.3°F

FIGURE 13. A SAMPLE OF RECORDINGS.

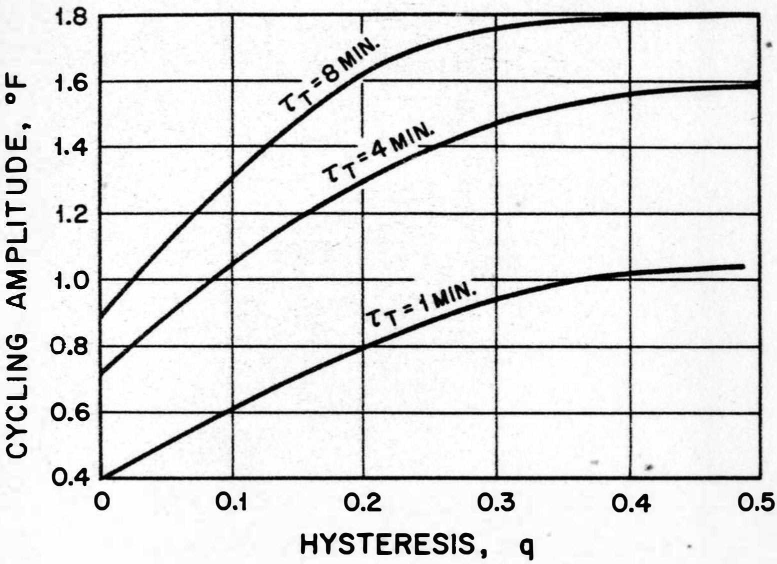

FIGURE 14. CONVENTIONAL SYSTEM'S CYCLING AMPLITUDE-HYSTERESIS CURVES WITH τ_T AS A PARAMETER.

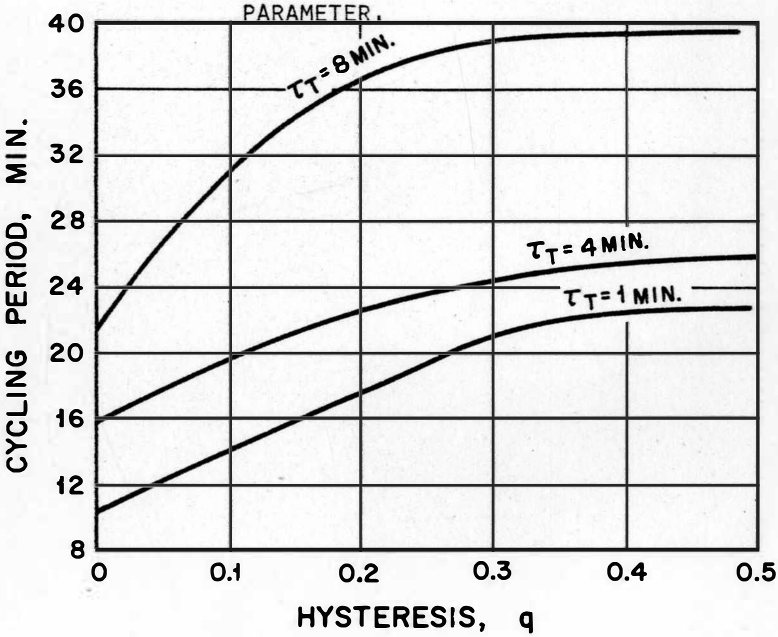

FIGURE 15. CONVENTIONAL SYSTEM'S CYCLING-PERIOD-HYSTERESIS CURVES WITH τ_T AS A PARAMETER.